USING NITROGEN-14 NUCLEAR QUADRUPOLE RESONANCE AND ELECTRIC FIELD GRADIENT INFORMATION FOR THE STUDY OF RADIATION EFFECTS

By

LOUIS HENRY ISELIN

A DISSERTATION PRESENTED TO THE GRADUATE SCHOOL
OF THE UNIVERSITY OF FLORIDA IN PARTIAL FULFILLMENT
OF THE REQUIREMENTS FOR THE DEGREE OF
DOCTOR OF PHILOSOPHY

UNIVERSITY OF FLORIDA

1995

This dissertation is presented in faith for the glory of God the Father, Son and Holy Spirit, for the mystery of life and what we will become.

This work is dedicated to my loving wife, Huong, and our darling daughter, Megan Rochelle. The time and effort put in graduate school are only early steps along the way towards the future. It is also dedicated to the memory of the two men for whom I was named, my grandfathers: Louis Max Iselin, whom I never knew, and Henry August Trinkaus, who was a great inspiration to me. He taught me that the worth of a man was not determined by how much education he had but in what he did and what he stood for.

My continuing professional career is dedicated to the many teachers in the public schools in Jonesboro, Arkansas, who encouraged me and pushed me to excel, especially G. Frazier, E. Frazier, D. Hammett, R. Patterson, and K. Bridger.

ACKNOWLEDGEMENTS

I am pleased to acknowledge the support and guidance of my graduate research advisor, Dr. David E. Hintenlang, and the rest of my committee. Thanks are extended to Dr. Samim Anghaie and Dr. E. Raymond Andrew for representing the Department of Nuclear Engineering Sciences. I extend my gratitude to Dr. Ulrich H. Kurzweg and Dr. Michael T. Olexa for representing the College of Engineering and the University of Florida *at large*, respectively. A special debt is acknowledged to Dr. Robert A. Marino of Hunter College of the City University of New York for providing specialized guidance on the theoretical and experimental aspects of NQR. The gracious assistance of Drs. Dirk van Ormondt and Ron de Beer of the Technical University of Delft is acknowledged. They sent me a copy of HSVD and helped me get it up and running. Thanks to the advice of Dr. Alexander Koukoulas of Paprican I was able to get the NQR equipment functioning reliably. I would be remiss if I did not acknowledge the many times that Mr. James M. Ogles assisted me with computer problems and provided stimulating conversation.

This research was partially supported by the Department of Energy Office of Energy Research under contract DE-FG07-89ER12890. Research also partially performed under appointment to the Nuclear Engineering and Health Physics Fellowship program administered by the Oak Ridge Institute for Science and

Education for the U.S. Department of Energy. Research assistantships were provided at the end of my fellowship period by Dr. David E. Hintenlang and Dr. Genevieve S. Roessler under projects that were part of the Florida Radon Research Program funded by the Florida Department of Community Affairs with assistance from the U.S. Environmental Protection Agency.

TABLE OF CONTENTS

Abstract of Dissertation Presented to the Graduate School
of the University of Florida in Partial Fulfillment of the
Requirements for the Degree of Doctor of Philosophy

USING NITROGEN-14 NUCLEAR QUADRUPOLE RESONANCE
AND ELECTRIC FIELD GRADIENT INFORMATION
FOR THE STUDY OF RADIATION EFFECTS

By

Louis Henry Iselin

December, 1995

Chairman: David E. Hintenlang
Major Department: Nuclear Engineering Sciences

Nitrogen-14 nuclear quadrupole resonance (NQR) was used in an attempt to detect the effects of ionizing radiation on organic material. Previously reported resonances for urea were detected at 2913.32 $\pm$ 0.01 kHz and 2347.88 $\pm$ 0.08 kHz with associated T_2^* values 780 $\pm$ 20 μs and 523 $\pm$ 24 μs, respectively. The previously unreported ν_- line for urea-d_4 was detected at 2381 $\pm$ 0.04 Khz and used to determine accurately for the first time the values for the nuclear quadrupole coupling constant χ (3548.74 $\pm$ 0.03 kHz) and the asymmetry parameter η (0.31571 $\pm$ 0.00007) for urea-d_4. The inverse linewidth parameter T_2^* for ν_+ was measured at 928 $\pm$ 23 μs and for ν_- at 721 $\pm$ 12 μs. Townes and Dailey analysis was performed and urea-d_4 exhibits a 0.004 increase in lone pair electronic density and a slight

decrease in N-H bond electronic density, as compared to urea, probably due to the mass difference.

A relationship is proposed, referred to as NQR linewidth analysis, between the dynamic spin relaxation times T_2 and T_2^* and the widths of the distributions of the NQR parameters. This is the NQR version of the well known nuclear magnetic resonance (NMR) relationship that relates the linewidth to a function of the spin-spin relaxation time and the magnetic field inhomogeneity. The electric field gradient inhomogeneity in NQR is substituted for the magnetic field inhomogeneity in NMR. Linewidth analysis is presented as a tool for possible use in future NQR work in all areas, not just radiation effects. This relationship is tested using sodium nitrite T_2 and T_2^* values for ν_+ and ν_- as a function of temperature; a most rigorous test for ^{14}N NQR as the T_2 and T_2^* values for ν_d are unavailable for any nitrogen-14 containing compound. Linewidth analysis successfully meets its own requirement that the ν_+ and ν_- resonance lines yield the same results for the difference of the inverted time constants T_2 and T_2^* for each line. By assuming that the ν_- resonance line would yield results similar to the other two lines, the natural width of χ for sodium nitrite is estimated to be 150-950 Hz in the temperature range from 77 to 470 K.

Urea recrystallized in the presence of water was observed to have a T_2^* decreased from the dry, polycrystalline form value of 780 μs to 550 $\pm$ 50 μs, regardless of gamma ray exposure up to 900 Gy. Urea:water ratios were tested in the range of 0.1 to 1.3 by molar weight. Observations of previous studies on urea-water

conducted in this laboratory by Higgins and Hintenlang were not able to be replicated and are not supported by this work.

CHAPTER 1
INTRODUCTION

There is a need for more understanding of the interaction between ionizing radiation and biological systems and the chemical processes by which that interaction takes place. In health physics, the final measure of interest for ionizing radiation is the damage done to a biological system, usually a person. Current radiation protection standards and practices rely on a correlation between the radiation dosimetry parameters at high doses and high dose rates (extrapolated down from 250 mGy to the smallest measurable dose) and any observed biological effects. As the doses and dose rates are lowered, the observed correlation weakens. The sequence of interaction is known to be

$$\textit{PHYSICAL} \rightarrow \textit{CHEMICAL} \rightarrow \textit{BIOLOGICAL}. \qquad [1\text{-}1]$$

While researchers actively pursue radiation dosimetry (physics) and radiation biology, the intermediate chemical effects in this sequence are studied to a much lesser degree. More information is needed in the area from physical energy deposition to chemical change. While an absorbed dose can be measured very accurately and precisely in some special cases, the biological effects due to that dose cannot be known with any reasonable certainty except in the high dose and high dose rate limit. The conversion factor for radiation protection, quality factor (Q), is a gross approximation to a

varying factor of biological damage for different radiations, relative biological effectiveness (RBE). Even though the RBE can be experimentally determined for a given radiation and a given biological effect in the biological system in question, the amount of natural biological variation in the given biological system demonstrates that RBE is still a crude measure of radiation effect on a biological system. This work focuses on the concept of a relative chemical effect by ionizing radiation on the chemical structure of an organic system by investigating changes in the bonding configuration surrounding nitrogen-14 atoms. The chosen system is a simple complex of an organic and water. The complex is chosen so that the indirect effects of the radiation-water interaction will be present on the organic and the organic is still in the solid phase and not in solution.

Although most radiation chemistry research is in aqueous solution, some work has been done in the area of chemical radiation effects on solids [Swallow 1960]. Magnetic resonance techniques are able to measure relatively small changes in chemical structures. The technique used most often to detect the presence of radiolytic products in solids is electron spin resonance (ESR).[1] In most cases, single crystal studies are emphasized so that the structure of the radical can be determined [Box 1977; Rogers and Kispert 1968; Tolkachev 1972]. The primary advantage to the use of ESR is that only the products contribute to the signal. The primary disadvantage is that only paramagnetic products can be detected with this method. It

[1] ESR is also know as electron paramagnetic resonance (EPR) and recently as electron magnetic resonance (EMR).

has been generally assumed, however, that the paramagnetic products are those primarily responsible for biological interactions. Electron nuclear double resonance (ENDOR) has also been used [Box 1977] to study radiation effects on some organics.

Nuclear magnetic resonance (NMR) has been used by a few researchers [Panin 1985; Panin et al. 1987; Thomasson 1990] to explore radiation effects at the chemical level, but all have focused on solutions, usually Fricke dosimetry or polymers. Nuclear quadrupole resonance (NQR) has been used to study the effects of radiation on ^{35}Cl containing compounds [Duchesne et al. 1955, 1956; Milia and Hadjoudis 1968; Vargas et al. 1978] and, since 1989 at the University of Florida, to study the effects of radiation on ^{14}N containing compounds [Iselin and Hintenlang 1990, 1991, 1992; Higgins 1990; Hintenlang and Higgins 1992; Jamil and Hintenlang 1993; Hintenlang, et al. 1992; Jamil 1992]. NQR does not require magnets which can degrade the signal due to inhomogeneities in the applied magnetic field; the internal fields created by the physical makeup of the ^{14}N containing compound is exploited instead.

Background

It is generally believed that the indirect effects of ionizing radiation are the primary causes of biological damage. These indirect effects are the result of free radicals, radical ions, and ions reacting with biological materials to cause breaks in existing molecules or to form new compounds which the organism may not be able to repair or isolate. Since biological organisms are primarily composed of water, the

radiolysis of water has always been the theoretical starting point in discussions of radiation effects on biological systems.

Radiolysis of Water

The interactions of ionizing radiations with water either lead to the water being ionized or left in an excited state. Since excitations have never been shown unequivocally to play a significant role in the radiation chemistry of aqueous solutions [Buxton 1987], they will be disregarded. On a time scale of 10^{-16} seconds, an electron can be separated from a water molecule. In the presence of other water molecules, the ionized water molecule becomes a hydronium ion and a hydroxyl ion in the 10^{-14} second time scale. The free electron will be solvated in 10^{-12} seconds and the three products will begin to diffuse away from the radiation track. By 10^{-7} seconds, the primary products will be formed: hydrated electrons, hydrogen radicals, hydroxyl radicals, hydrogen gas, hydrogen peroxide and hydronium ions. Primary cellular damage is believed to be caused by hydrogen peroxide, hydroperoxide and superoxide [Ewing 1983] which are part of the secondary (or steady-state) product yield.

As long as the ionizing radiation is photons or electrons, the energy of the incoming radiation has not been shown to make a difference in the yields of radiolytic products. All photons and electrons are considered equal at the level of energy deposited in the material by interactions which involve energy transfer to the electrons

in the medium being irradiated. This equivalence does not hold for other radiations which interact with the target material by other mechanisms.

Radiation Chemistry of Solids

The primary differences between the radiation chemistry of liquids and solids are due to the increased density of solids and the accompanying forces of interaction between the constituent atoms. About 85% of interaction electrons recombine for a G-value[2] for escape from the parent cation of ~0.3. The G-value for electron trapping is ~3.0 for most solids, but trapping in crystalline organics does not normally occur [Willard 1987].

The radicals formed in a solid can be stable over a period of months or more. There is much evidence that new compounds are formed upon dissolving an irradiated organic solid in water [Swallow 1960]. Certain radiolytic products may be more stable in crystals with water of hydration than in anhydrous crystals, and such products may be favored in crystals where hydrogen bonding is important in determining the crystalline structure [Rogers and Kispert 1968].

Material of Choice

Of all available compounds containing nitrogen, urea is one of the most studied by ^{14}N NQR. Not only has pure polycrystalline urea been studied, but also

---

[2] G-values are a measure of yield or removal defined as the number of a chemical species created or destroyed for each 100 eV of energy absorbed in the material or solution.

urea complexes, substituted ureas, and structurally related guanidine compounds. In spite of all of this work, the ν_- line of urea-d_4 has not been previously reported. Urea's crystalline structure has been investigated since 1902. The current lattice parameters are due to Swaminathan et al. [1984]. The crystal is held together by hydrogen bonding between the oxygen atoms and neighboring hydrogen atoms.

The spontaneous hydrolysis of urea occurs via the elimination reaction:

$$(NH_2)_2C{=}O + H_2O(\alpha) \rightarrow H{-}N{=}C{=}O + NH_3 + H_2O(\beta)\,. \qquad [1\text{-}2]$$

The Greek letters denote that the water molecules on each side of the reaction have different constituent atoms [Blakeley et al. 1982]. The unimolecular decomposition reaction

$$(NH_2)_2C{=}O \rightarrow H{-}N{=}C{=}O + NH_3 \qquad [1\text{-}3]$$

as studied by theoretical means has a large energy of activation (72.0 kcal mol^{-1}) which precludes this reaction in favor of the hydrolysis reaction given in Eqn. [1-2] with a smaller energy of activation (35 kcal mol^{-1}) [Koizumi et al. 1988].

Method of Choice

The resonance method of NQR was first reported by Dehmelt and Krüger in 1950 and ^{14}N NQR was first reported by Watkins and Pound in 1952. Since that time, it has been used by physicists and chemists and has developed mostly in the shadow of NMR. The ease with which experimenters in the former Soviet Union could build NQR spectrometers in-house led to NQR being the method of choice for

taking and confirming crystallographic measurements [Kitigorodskii 1960]. General descriptions of NQR have been given by many experts in the field. Most theoretical descriptions of the dynamic spin interactions in NQR have borrowed heavily from NMR.

Radiation Effects

Vargas and co-workers [1978] reported linear shifts in ^{35}Cl resonance frequencies and relaxation times in chlorates with ^{60}Co gamma irradiation. It is believed that the NQR spectral parameters of ^{14}N containing biologically significant organics should similarly change upon irradiation in an observable way. One paper [Hintenlang and Higgins 1992] demonstrates that effects are observable in at least one such compound, hydrated urea. Observing these changes will require the development of a systematic analytical method since biologically significant organic chemicals frequently have a complex structure and therefore complex NQR resonance spectra.

Currently published work on using ^{14}N NQR techniques to study radiation effects is limited to the reports of this laboratory. The basic knowledge on how to carry out NQR experiments is detailed in one document [Iselin 1992] and well characterized methods for analysis of the resulting magnetic resonance spectra have reached publication [de Beer and van Ormondt 1992, Iselin 1992].

Objectives

The goal of this work is to directly measure and quantify the effects of ionizing photons on an original, biologically significant substance, using ^{14}N NQR as the measuring tool and urea-water as the subject material. The specific objectives in this work are as follows:

1) Propose and test a method for quantifying changes in NQR signals.

2) Demonstrate the validity of NQR measurements taken on the Ritec spectrometer system by detecting and quantifying one or more unreported resonances as well as resonances previously described in the literature.

3) Follow up the work of Higgins and Hintenlang by replicating their measurements of the ^{14}N NQR spin-spin relaxation times for urea-water and extending the range of ^{60}Co gamma ray absorbed doses above 300 Gy.

4) Compare and correlate changes in the NQR experimentally derived quantities of urea-water to gamma ray dose to quantify the broadening of the electric field gradient at the nitrogen sites.

5) Make recommendations for further study in this area.

The following chapters will expand on the theory and experiments used in NQR. Chapter 2 gives the derivation of the NQR energy levels and resulting transition frequencies and also explores the relationship between theoretical and experimental quantities. Chapter 3 overviews and then details the different parts of the NQR spectrometer system, the experimental techniques, and several data analysis

techniques. Chapter 4 gives the results of the theoretical and experimental work while Chapter 5 provides the discussion. Conclusions and recommendations are given in Chapter 6. The four appendices expand on details in the text: Appendix A is a listing of the FORTRAN programs used, Appendix B gives parts of sample data and analysis files, Appendix C reports the Petersen data used, and Appendix D details Higgins' original work.

CHAPTER 2
THEORETICAL BACKGROUND

Theory of NQR

Nuclear quadrupole resonance is the branch of radiofrequency (RF) resonance spectroscopy which investigates the interaction between the nuclear electric quadrupole moment and the electric field gradient (EFG) produced by the electronic charge distribution about the nucleus of interest in a solid state material. This chapter will discuss the various theoretical components of NQR and their relationship to experiment, both for the static secular equations for transition energies and the dynamic spin systems which are excited by the RF interaction. Townes and Dailey theory, a static model for NQR, is also presented.

Nuclear Electric Quadrupole Moment

The traditional semi-classical definition of the nuclear electric quadrupole moment, Q, is

$$eQ = \iiint (3z^2 - r^2)\, \varrho_{m_I = I}(\vec{x})\, d^3x \qquad [2\text{-}1]$$

where e is the fundamental charge, $\varrho_{m_I = I}(\vec{x})$ is the nuclear charge density when it is in the $m_I = I$ state, and the triple integral is taken over the nuclear volume. Note that I

is the spin quantum number, m_I is the magnetic spin quantum number, and the z axis is the axis along which m_I is the projection of I. This form for the quadrupole moment is usually based on the Taylor series expansion about the nucleus for a charge distribution on an external electric field or on the multipole expansion in Cartesian coordinates of the electric potential $V(\vec{x})$ [for example, see Jackson 1975].

A simple quantum mechanical derivation has be given [Wong 1990] using the correspondence principle. The quadrupole operator is defined as

$$e\hat{Q} = e(3\hat{z}^2 - \hat{r}^2) \tag{2-2}$$

so that the quantum mechanical operator has the same form as the classical definition. The quadrupole moments are then the expectation values of the appropriate nuclear wavefunctions

$$<e\hat{Q}_{m_I}> = \langle I m_I | e\hat{Q} | I m_I \rangle \tag{2-3}$$

for each m_I and the primary quadrupole moment is when $m_I = I$.

$$<e\hat{Q}_I> = \langle II | e\hat{Q} | II \rangle \tag{2-4}$$

Equation [2-4] in Dirac notation is the quantum mechanical equivalent to the classical expression given in Eq. [2-1].

<u>Electric Field Gradient</u>

Any electric field, $\vec{E}$, can be written as the negative gradient of a scalar potential, V,

$$\vec{E} = -\nabla V. \qquad [2\text{-}5]$$

Component by component this means that

$$E_x = -\frac{\partial V}{\partial x} \quad E_y = -\frac{\partial V}{\partial y} \quad E_z = -\frac{\partial V}{\partial z}. \qquad [2\text{-}6]$$

The electric field gradient is then, in general,

$$\frac{\partial E_i}{\partial x_j} = -\frac{\partial^2 V}{\partial x_i \partial x_j}. \qquad [2\text{-}7]$$

It is important to note that since there is no preferred direction in space, an EFG tensor is symmetric about the main diagonal

$$V_{ij} \equiv \frac{\partial^2 V}{\partial x_i \partial x_j} = \frac{\partial^2 V}{\partial x_j \partial x_i} \equiv V_{ji} \qquad [2\text{-}8]$$

and the orientation of the axes is arbitrary, but defined by convention such that

$$\left|\frac{\partial^2 V}{\partial x^2}\right| \leq \left|\frac{\partial^2 V}{\partial y^2}\right| \leq \left|\frac{\partial^2 V}{\partial z^2}\right| \qquad [2\text{-}9]$$

in the principal axes representation where the terms not on the main diagonal are all identically zero. The component of the EFG in the z direction is then renamed eq.

$$eq \equiv \frac{\partial^2 V}{\partial z^2} \qquad [2\text{-}10]$$

Of interest to NQR is the EFG at the nucleus due to the bonding structure of the surrounding electrons. Each different electronic configuration, including non-bonded, has a unique structure associated with it. The various charge distributions

created by the electrons lead to different electric fields and therefore different electric field gradients at the nuclear site.

Since the electronic charge density at the nucleus is zero in the classical limit, the electric potential obeys Laplace's equation.

$$\frac{\partial^2 V}{\partial x^2} + \frac{\partial^2 V}{\partial y^2} + \frac{\partial^2 V}{\partial z^2} = \nabla^2 V = 0 \qquad [2\text{-}11]$$

Deviations from axial symmetry are measured by the asymmetry parameter, η, which is defined by

$$\eta = \frac{\dfrac{\partial^2 V}{\partial x^2} - \dfrac{\partial^2 V}{\partial y^2}}{\dfrac{\partial^2 V}{\partial z^2}}. \qquad [2\text{-}12]$$

Equation [2-9] and Eq. [2-12] limit the possible values of the asymmetry parameter to

$$0 \leq \eta \leq 1. \qquad [2\text{-}13]$$

Quadrupole Hamiltonian and Associated Energy Levels

The strength of the interaction between the nuclear quadrupole moment and the principal EFG for a particular substance is given in the literature by χ, the Nuclear Quadrupole Coupling Constant (NQCC).

$$\chi = \frac{e^2qQ}{h} \qquad [2\text{-}14]$$

The NQCC is usually reported in units of megahertz (Mhz). This NQCC represents the constant term of the NQR interaction for a given nucleus, as will be seen below.

The traditional Hamiltonian for NQR is

$$\hat{\mathcal{H}}_Q = \frac{e^2qQ}{4I(2I-1)}\left[3\hat{I}_z^2 - I(I+1) + \eta(\hat{I}_x^2 - \hat{I}_y^2)\right] \qquad [2\text{-}15]$$

where I is the spin of the nucleus in question and $\hat{I}_i$ is the spin operator for the ith direction. Substituting the spin raising and lowering operators,

$$\hat{I}_\pm = \hat{I}_x \pm i\hat{I}_y \qquad [2\text{-}16]$$

the Hamiltonian is

$$\hat{\mathcal{H}}_Q = \frac{e^2qQ}{4I(2I-1)}\left[3\hat{I}_z^2 - I(I+1) + \frac{\eta}{2}(\hat{I}_+^2 + \hat{I}_-^2)\right]. \qquad [2\text{-}17]$$

This form of the Hamiltonian can be constructed by starting at the operator form

$$\mathcal{H}_Q = \vec{I}\,\vec{\vec{Q}}\,\vec{I} \qquad [2\text{-}18]$$

where $\vec{I}$ is the nuclear spin tensor and $\vec{\vec{Q}}$ is the quadrupole energy tensor (QET). After expanding the matrix form in the principal axes representation in the same orientation as the EFG components (Eq. [2-9]) and noting that the components of the

QET Q_{ij} are proportional to the EFG components V_{ij}, the results lead to the complete Hamiltonian down to an arbitrary constant.

$$\mathcal{H}_Q = A\left[3I_z^2 - I(I+1) + \eta\left(\hat{I}_x^2 - \hat{I}_y^2\right)\right] \qquad [2\text{-}19]$$

This constant, A, will now be further examined.

Hamiltonian Constant

The classical definition of an arbitrary quadrupole moment is

$$Q_{i,j} = \iiint (3x_i x_j - \delta_{ij} r^2)\, \rho(\vec{x})\, d^3x \qquad [2\text{-}20]$$

where i,j,k cycle through x,y,z, δ_{ij} is the Kronecker delta, $\rho(\vec{x})$ is a density function, and the triple integral is taken over the appropriate volume. Note that Eq. [2-20] becomes Eq. [2-1] when $i=j=k$ and the density ρ is the nuclear charge density in the appropriate state. The energy associated with a classical quadrupole moment of charge in an electric potential has been given by Slichter [1990].

The classical Hamiltonian has the form

$$\mathcal{H} = \frac{1}{6}\sum_{i,j} V_{ij}\hat{Q}_{ij} \qquad [2\text{-}21]$$

with the quadrupole operator as

$$\hat{Q}_{ij} = e\sum_{p}^{Z} (3x_{ip}x_{jp} - \delta_{ij} r_p^2) \qquad [2\text{-}22]$$

The sum in Eq. [2-22] is over the protons and r_p is the distance from the center of the nucleus to the proton. Since this operator can be shown to be a linear combination of

irreducible tensor operators, the Wigner-Eckart Theorem can be used to demonstrate that

$$\langle Im_I|\hat{Q}_{ij}|Im_I'\rangle = A\langle Im_I|\frac{3}{2}(I_iI_j+I_jI_i)-\delta_{ij}I^2|Im_I\rangle \qquad [2\text{-}23]$$

which becomes

$$\begin{aligned} <e\hat{Q}_I> &= A\langle 3I_z^2-I^2\rangle \\ &= AI(2I-1) \end{aligned}. \qquad [2\text{-}24]$$

This means that the constant has the form, incorporating the *eq* term,

$$A = \frac{e^2qQ}{4I(2I-1)}. \qquad [2\text{-}25]$$

This equates Eq. [2-19] with Eq. [2-15]. Note that the derivation of the constant used classical arguments. These classical arguments were necessary since a quantum mechanical operator is only defined to within an arbitrary constant.

<u>Energy Levels</u>

To get the energy levels from the Hamiltonian, we will solve Schrödinger's equation for the energy eigenvalues.

$$\mathcal{H}|Im_I\rangle = E_m|Im_I\rangle \qquad [2\text{-}26]$$

In matrix form, Eq. [2-15] becomes, for the case I=1,

$$\hat{\mathcal{H}}_Q = \begin{bmatrix} A & 0 & \eta A \\ 0 & -2A & 0 \\ \eta A & 0 & A \end{bmatrix}. \qquad [2\text{-}27]$$

The secular equations are found from

$$\det[\hat{\mathcal{H}}_Q - EI] = 0 \qquad [2\text{-}28]$$

or

$$\begin{vmatrix} A-E & 0 & \eta A \\ 0 & -2A-E & 0 \\ \eta A & 0 & A-E \end{vmatrix} = 0. \qquad [2\text{-}29]$$

The eigenvalues are

$$E = (1+\eta)A,\ -2A,\ (1-\eta)A \qquad [2\text{-}30]$$

and the energy levels are

$$\begin{aligned} E_0 &= -2A \\ E_{\pm 1} &= (1 \pm \eta)A. \end{aligned} \qquad [2\text{-}31]$$

The three possible transitions are

$$\nu_+ = \frac{(3+\eta)A}{2\pi\hbar} \qquad \nu_- = \frac{(3-\eta)A}{2\pi\hbar} \qquad \nu_d = \frac{2\eta A}{2\pi\hbar} \qquad [2\text{-}32]$$

or

$$\nu_+ = \frac{(3+\eta)e^2qQ}{4h} \qquad \nu_- = \frac{(3-\eta)e^2qQ}{4h} \qquad \nu_d = \frac{e^2qQ\eta}{2h}. \qquad [2\text{-}33]$$

These can be rearranged to give NQCC and the asymmetry parameter when any two of the three transitions are known. In terms of ν_+ and ν_-, they are

$$\chi = \frac{2}{3}(\nu_+ + \nu_-) \qquad [2\text{-}34]$$

and

$$\eta = 3\frac{(\nu_+ - \nu_-)}{(\nu_+ + \nu_-)}. \qquad [2\text{-}35]$$

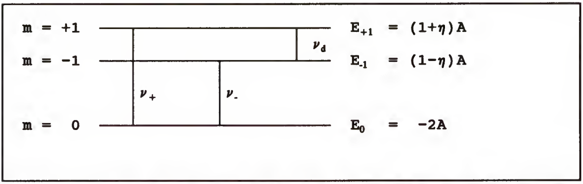

Figure 2-1 Energy level diagram for spin $I = 1$ showing the three possible transitions.

In a pulsed NQR experiment, a burst of RF energy is added to the sample at the proper frequency to stimulate one or more of the three transitions, ν_+, ν_-, or ν_d. As the system relaxes it radiates energy at the resonance frequency. The NQCC and asymmetry parameter can be determined using Eq. [2-34] and Eq. [2-35] after measuring the correct values of ν_+ and ν_- for the sample.

Townes and Dailey Theory

Two parameters are obtained from NQR experiments: χ and η. These two parameters can be related to the electronic densities around the target nucleus through an idea suggested by Townes in 1948 and elaborated upon by Townes and Dailey in 1949. While more complete quantum chemical pictures of the electronic structure are available at the current time, this simplified model provides acceptable accuracy for a model that only has two free parameters, especially if a series of compounds with a bonding trend are compared. This discussion will follow the outline of the various workers from Bray's group at Brown University [Marino 1969, Subbarrao 1978].

In an NQR experiment, a given target nucleus is surrounded by its own electrons, other nuclei, and their electrons. Each of these charged particles contributes to the EFG at the target nucleus. This is shown symbolically in Eq. [2-36] with T representing the target nucleus and N representing the neighboring nuclei.

$$q^{T} = q_{e^-}^{T} + q_{p^+}^{N} + q_{e^-}^{N} \qquad [2\text{-}36]$$

The electronic terms must be dealt with quantum mechanically but the nuclear term can be treated classically.

The main approximation in the theory is to ignore contributions to the EFG except those from the electrons of the target nucleus itself. The majority contribution is from the valence electrons since the s orbitals and any other closed orbital will be spherically symmetrical or nearly so. The exception to this spherical symmetry would be if there are polarization effects in the closed shell and they are ignored due to their

small size, although they could be compensated for with the Sternheimer shielding factor, if necessary. The ignored terms are the contributions to the EFG from other nuclei, the electrons of other nuclei, the overlap electronic densities, and any electrons of the target nuclei besides the valence electrons.

To determine the contribution from each electron, recall that classically a charge of $-e$ a distance of r from the nucleus produces a potential of

$$V(r) = -\frac{e}{r}. \tag{2-37}$$

The EFG component in the principal z direction, V_{zz} (see Eq. [2-10]) is

$$V_{zz}(r) = -e\frac{(3\cos^2\theta - 1)}{r^3} \tag{2-38}$$

where θ is the angle between the z axis and r. Quantum mechanically, the correct value is the expectation value given by

$$eq = \langle V_{zz}\rangle = -e\left\langle\frac{3\cos^2\theta - 1}{r^3}\right\rangle. \tag{2-39}$$

The approximations by Townes and Dailey are justified to a great extent by the r^{-3} relationship between the distance to the electron and the corresponding small contribution to the EFG.

The second major approximation is to treat the molecular wave functions of the electrons as linear combinations of atomic orbitals (LCAO) with the form

$$|\psi\rangle = \sum_j a_j \phi_j . \qquad [2\text{-}40]$$

In general, atomic orbitals are separable into a function of r and the spherical harmonics Y_m^l.

$$\phi = f(r)\ Y_m^l(\theta,\phi) \qquad [2\text{-}41]$$

Calculation of q_{zz} thus becomes

$$q_{zz} = \frac{3m^2-l(l+1)}{2l-1}\frac{2}{2l+3}\left\langle\frac{1}{r^3}\right\rangle . \qquad [2\text{-}42]$$

The only important case for nuclei like ^2H or ^{14}N is $l = 1$ for the p electrons. The p_z electrons with $m = 0$ contribute the most to q_{zz} with

$$q_{zz}\big|_{p_z} = -\frac{4}{5}\left\langle\frac{1}{r^3}\right\rangle \equiv q_p . \qquad [2\text{-}43]$$

The p_x and p_y electrons with m $= \pm 1$ yield a value of

$$q_{zz}\big|_{p_x} = q_{zz}\big|_{p_y} = \frac{2}{5}\left\langle\frac{1}{r^3}\right\rangle \equiv -\frac{1}{2}q_p . \qquad [2\text{-}44]$$

Notice that Laplace's equation (Eq. [2-11]) is satisfied with

$$q_{xx} = q_{yy} = -\frac{1}{2}q_{zz} . \qquad [2\text{-}45]$$

Using n_x, n_y, and n_z to represent the orbital occupation numbers for the corresponding p electrons, the following relationships can be written for each molecular orbital (MO):

$$q_{zz} = [n_z - \frac{1}{2}(n_x + n_y)]\,q_p \qquad [2\text{-}46]$$

$$q_{yy} = [n_y - \frac{1}{2}(n_z + n_x)]\,q_p \qquad [2\text{-}47]$$

$$q_{xx} = [n_x - \frac{1}{2}(n_y + n_z)]\,q_p\,. \qquad [2\text{-}48]$$

By summing over all present MOs, the general relationship for the NQCC can be obtained.

$$e^2qQ = \sum_i \; [n_{zi} - \frac{1}{2}(n_{xi} + n_{yi})]\,e^2q_pQ \qquad [2\text{-}49]$$

Following the usual convention, this is rearranged to give

$$\frac{e^2qQ}{e^2q_pQ} \equiv \alpha = n_z - \frac{1}{2}(n_x + n_y) \qquad [2\text{-}50]$$

and

$$\frac{[e^2q_{xx}Q - e^2q_{yy}Q]}{e^2q_pQ} = \alpha\eta = \frac{3}{2}(n_x - n_y)\,. \qquad [2\text{-}51]$$

The quantity e^2q_pQ is the NQCC for a single *2p* electron and it cannot be measured experimentally in nitrogen due to Hund's Rule on the filling order of orbitals. Since each of the three *2p* orbitals in atomic nitrogen has one electron, the total wave function is spherically symmetric. Spherical symmetry means that there is no quadrupole interaction since there is no energy level splitting. Different authors

have assumed different values for e^2q_pQ, always in the range suggested by other measurement methods. These values have been in the range of 8 MHz to 14 MHz. Popular values are 8.4 MHz [Subbarao 1978] and 10 MHz [Oja 1973, Hintenlang and Higgins 1992]. For this work, a value of 10 MHz will be used. It is noted that this arbitrariness in the value of e^2q_pQ means that the resultant occupation numbers derived from the Townes and Dailey analysis are themselves somewhat arbitrary. Trends in the occupation number values will have greater validity than their actual numerical values.

As an example of how Townes and Dailey theory can be used, consider the compound urea. Values for NQR parameters of urea have been known since 1959 [Chiba et al., Minematsu]; current values [this work] are

$$\chi = 3507.47 \pm 0.006 \text{ kHz} \quad \text{and} \quad \eta = 0.32242 \pm 0.00015 . \qquad [2\text{-}52]$$

To apply the Townes and Dailey theory, first examine the symmetry of the molecule. Urea is known to be planar with the nitrogen lone pair electrons out of the plane and the amide groups relatively symmetrical about the C-N bond. Assign the x-y plane to the molecule with the carbon atom along the y axis. The bonding in urea is known to correspond closely to sp^2 hybridization. A set of sp^2 orbitals that match the given geometry with each bond angle set to 120° are as follows

$$\psi_{NC} = \frac{1}{\sqrt{3}}s + \sqrt{\frac{2}{3}}p_y, \text{ and} \qquad [2\text{-}53]$$

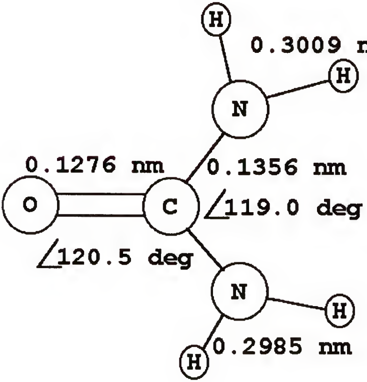

Figure 2-2 Crystal structure of Urea [Values from Caron and Donohue 1964]

$$\Psi_{NH} = \frac{1}{\sqrt{3}}s \pm \frac{1}{\sqrt{2}}p_x - \frac{1}{\sqrt{2}}p_y \qquad [2\text{-}54]$$

where Ψ_{NH} gives the two wavefunctions for the two N-H bonds. The needed occupation numbers for these orbitals are σ_π, σ_{NC}, and σ_{NH1} ($= \sigma_{NH2}$). These will be shortened to π, σ_C, and σ_H for convenience. The occupation numbers for the p_x, p_y and p_z orbitals of nitrogen, labelled n_x, n_y and n_z, respectively, are given as

$$n_x = \frac{2}{3}\sigma_C + \frac{1}{3}\sigma_H,\ n_y = \sigma_H,\ \text{and}\ n_z = \pi\,. \qquad [2\text{-}55]$$

We know from Eq. [2-43] and Eq. [2-44] that each p_z electron adds q_p to the EFG and each $p_{x,y}$ electron adds $-½q_p$ to the EFG. Equation [2-50] for the case of urea becomes

$$\alpha = \pi - \bar{\sigma} = \pi - \frac{2}{3}\sigma_H - \frac{1}{3}\sigma_C \qquad [2\text{-}56]$$

and Eq. [2-51] becomes

$$\alpha\eta = \sigma_H - \sigma_C\,. \qquad [2\text{-}57]$$

Before using these relationships, one must check to see if they are reasonable. Checking the convention given in Eq. [2-9], it is reasonable that the lone pair π has the largest contribution to the EFG. Since we have three unknown parameters and only two knowns, it has been customary to assign to one of the parameters the known value for that parameter in a related compound. For urea, the assigned value is $\sigma_H \equiv 1.33$, the value for ammonia. Using the three known values, the orbital occupation numbers for urea are

$$\sigma_C = \sigma_H - \frac{\chi}{\chi_p}\eta = 1.33 - \frac{3507.47}{10000}0.32242 = 1.217 \qquad [2\text{-}58]$$

and

$$\pi = \alpha + \bar{\sigma} = \sigma_H + \frac{\chi}{\chi_p}\left(1 - \frac{\eta}{3}\right) = 1.643\,. \qquad [2\text{-}59]$$

These values are for comparison to ammonia and related compounds only since the value of σ_H was set to the value for ammonia.

The exact values for χ and η may be difficult to calculate if the values for the transition frequencies are uncertain. One source of uncertainty is where the center frequency of the resonance occurs. Since NQR can be performed on a polycrystalline sample as well as a single crystal, there may be (and usually are) some resonance sites which have slightly different resonance frequencies. The shape of the resonance distribution is usually Lorentzian, Gaussian, or some combination of the two. As RF energy is added to the system in pulses, the nonideal pulse shape distribution is folded into the resonance distribution. That means that some of the resonance sites are at different frequencies and some at the same frequency are not affected by the pulse. These differences for each site combine to give a complex resonance picture. The pulses are controlled by their voltage (height), a measure of how much energy is transferred to the system by each pulse, and their width, a measure of how long the pulse lasts. For a pulse of a given height, the longer the pulse the more the nuclear spin vector is forced to rotate in response to the pulse. A pulse which gives the

maximum FID amplitude during an NQR experiment is called an *effective* 90° pulse.[1] An *effective* 180° pulse therefore yields no output signal (or gives a minimum) yet does interact with the spin system. This section has been done by analogy to NMR due to the complex mathematics involved that do not add to this work and cannot be explicitly calculated for the cases presented here. These subjects are additionally dealt with in more detail in the following sections.

Spin Relaxation Times

The population distributions of spins in NQR obey Boltzmann's distribution

$$\frac{N_1}{N_0} = e^{-\frac{\Delta E}{kT}} \qquad [2\text{-}60]$$

where ΔE is the difference in the energy levels, E_1 - E_0, k is Boltzmann's constant, and T is the absolute temperature. At a transition frequency of 3 MHz at the temperature of liquid nitrogen (LN_2), 77 K, the ratio of N_0 to N_1 becomes

$$N_0{:}N_1 \approx e^{-1.870x10^{-6}} \approx 0.99999813\,. \qquad [2\text{-}61]$$

Thus the two energy levels are almost equal in population when the system is at thermal equilibrium. If we take a model spin system with $\sim 10^8$ spins (much smaller than the typical spin system encountered in ^{14}N NQR), then the excess number of spins in the lower energy level, N_0 - N_1, would be ~ 100. We can represent the net

---

[1] This definition is used to provide an analogy to the NMR experiment. The actual spin system dynamics are more complex in NQR than in NMR. The Bloch equations used for NMR do not apply to I=1 NQR or any other system which has more than one transition energy [Sanctuary and Krishnan 1993].

behavior of this spin system at thermal equilibrium at the temperature of LN_2 with no spins in the upper level and 100 in the lower level.

We can excite this spin system and then model the time dependent relaxation of the system by $g_1(t)$. The exact form of $g_1(t)$ depends on the way the spin system couples to the lattice for the removal of the excess energy. For excited spins to de-excite to the lower level, they must give up their excess energy to the lattice. The time in which the function $g_1(t)$ decays from $g_1(0)$ to $g_1(0)/e$ (where e is the base of the natural logarithm) is represented by a characteristic time constant, T_1, the spin-lattice relaxation time, such that

$$g_1(T_1) = \frac{g_1(0)}{e}. \qquad [2\text{-}62]$$

The spin-lattice relaxation time can be measured by the two pulse method of inversion-recovery which uses an *effective* 180° pulse followed by an *effective* 90° pulse after a time delay of duration τ. The spin-lattice relaxation time is determined from a fit of the echo amplitude as a function of τ.

Another way for an individual spin to give up its excess energy is to transfer the excess energy to another spin. This does not change the total energy of the spin system. The excited spin system's ability to transfer energy between spins can be modeled by a function $g_2(t)$, which has a characteristic time constant T_2, referred to as the spin-spin relaxation time. The spin-spin relaxation time is defined in an analogous manner to the spin-lattice relaxation time in Eq. [2-60]. Note that the physical relationship between $g_1(t)$ and $g_2(t)$ requires that

$$T_2 \leq T_1 . \qquad [2\text{-}63]$$

This is because a T_2 longer than T_1 would be meaningless since T_2 is defined only when the system is in an excited state.

The other vital spin relaxation time is the effective spin-spin relaxation time T_2^* also known as the inverse linewidth parameter because it is inversely proportional to the full width at half maximum (FWHM) of the resonance line. The inverse linewidth parameter is the easiest dynamic NQR parameter to determine as it is the characteristic time constant of a free induction decay (FID) produced by a single *effective* 90° pulse.

Lineshapes

Fourier analysis is often used for the analysis of real linear systems where the basis set consists of any combination of sinusoids. These sinusoids can be of the form $\cos(2\pi ft + \phi)$ or $e^{i2\pi ft}$, where i is $\sqrt{-1}$. When the lineshapes are Lorentzian [refer to $g_2(t)$ in the previous section], magnetic resonance spectra can be fit to the following model:

$$v(t) = \sum_{i=1}^{N} A_i \cos(2\pi f_{d_i} t + \phi_i)\, e^{-\frac{t}{T_{2i}^*}} \qquad [2\text{-}64]$$

where $v(t)$ is the data signal, N is the number of resonance sites, A_i is the amplitude of the i th site, f_d is the measured difference frequency between the resonance

frequency and the applied reference frequency, ϕ_i is the phase angle, and T_{2i}^* is the inverse linewidth parameter. This implies a Fourier transform (FT) of a sum of Lorentzian lineshapes.

When the FT has been calculated, the magnetic resonance parameters can be identified from the location of the resonance peaks and the associated linewidths. In the absorption spectrum (cosine part of the transform), the centroid of a peak is the difference frequency identified in Eq. [2-62]. The inverse linewidth parameter is inversely proportional to the full width at half of the maximum value (FWHM). The exact relationship is determined by the precise lineshape. For a Lorentzian line, the relationship is

$$T_2^* = \frac{2}{FWHM(\omega)} = \frac{1}{\pi \, FWHM(\nu)} . \qquad [2\text{-}65]$$

In taking magnetic resonance data, the phase information is often lost. Phase here has two different meanings. First, the model given in Eq. [2-62] has a phase ϕ_i for each individual site. These values are often distorted in the electronic detection of the resonance signals. The presence of this physical phase leads to a second phase and this is from the imaginary part of the resulting Fourier transform. When the FT is complex, the real part is the amplitude transform and the imaginary part gives the phase. With all phase information lost in the NQR spectrometer, the FT becomes not corrected for phase distortion. This distortion can cause shifts in line positioning and line widths when the FT absorption spectrum is estimated.

CHAPTER 3
EQUIPMENT, EXPERIMENT, AND PROCEDURES

A ^{14}N NQR radiation effects study involves comparing the ^{14}N NQR spectral parameters from unirradiated samples to those of irradiated samples. This chapter starts with a summary of the experiment. That is followed by a short description of the primary components in the pulsed NQR spectrometer system [Oja and Petersen 1973, Petersen and Oja 1974]. After the irradiation technique is detailed, a description is also given of the experimental NQR techniques used.

Summary Description of Equipment

Approximately 15 g of the polycrystalline solid to be studied is placed in a sample vial. The sample vial is put inside a primary sample coil wound from magnet wire in such a way as to maximize the response of the coil in the desired frequency range. A secondary coil is wound with twice the inductance of the primary coil to be put in the impedance matching network to allow for fine tuning of the frequency response of the equipment. The primary coil and sample are placed in an aluminum can for shielding from undesired RF interference and then submerged in a dewar of liquid nitrogen (LN_2). The dewar, matching network, and preamplifier are placed in a glove bag filled with dry nitrogen gas to purge the water vapor from around the dewar. Ice buildup on the cables and dewar is known to cause arcing and is avoided

by using the dry nitrogen. Although the glove bag is not "air tight" it still keeps the humidity level around the dewar down to an acceptable level.

The RF source is a continuous wave (CW) high resolution frequency source. The output of the CW source is fed to a gated amplifier while being monitored with a universal counter in frequency mode. The gated amplifier allows either single or dual pulse sequences to be applied to the sample coil through the impedance matching network. The gated amplifier is capable of providing variable pulse widths, delay times, and sequence intervals. The gated amplifier is phase locked to a broadband receiver. The resonance signal from the sample coil is first amplified in a charge-sensitive, high-impedance pre-amp. When the pulses from the gated amplifier are being sent to the coil, the receiver is locked off by diode switching. After the pulse is sent, the receiver is turned on again by diode switching to accept any signal from the sample. This switching is necessary to avoid damaging the receiver or losing the < 100 mV return signal because the pulses are ~ 1400 V. The receiver uses phase sensitive detection to discriminate between the return signal and electronic noise. The output from the receiver is sent to a digital oscilloscope for signal averaging and storage. The digital waveforms can be transferred to a personal computer for analysis. A diagram of the experimental setup is shown in Fig. 3-1.

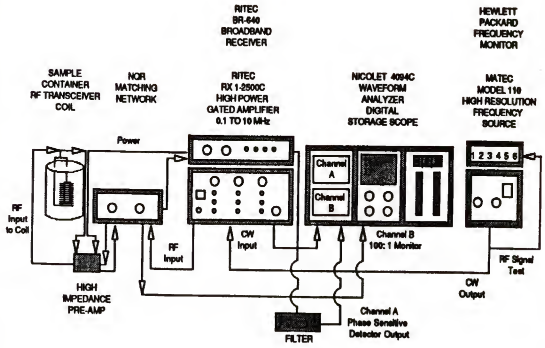

Figure 3-1 Diagram of experimental setup [Higgins 1990, Iselin 1992]

Equipment Specifications

Continuous Wave Frequency Source and Monitor

The CW RF source is a Matec[1] Model 110 High Resolution Frequency Source with an output range of 0.5 Hz to 5 MHz. According to the manufacturer,[2] the stability of the square wave output is better than 6 significant figures. The short term stability of the oscillator is rated at 2 parts in 10^7, with a temperature dependence of 1 part in 10^6 per °C change in ambient room temperature. The RF source has been left on continually according to the manufacturer's suggestion for maximum stability. The observed stability is ± 3 Hz over a 4 hr period if the frequency source has had >24 hrs to stabilize at the reference frequency. If the frequency has been changed in the last 12 hours, the frequency source has a tendency to drift back towards its previous setting and is stable to only ± 30 Hz for a 4 hr period.

The output of the CW source is monitored using a Hewlett-Packard[3] Model 5314A Universal Counter. The maximum frequency resolution[4] for this counter is 0.1 Hz in the frequency range from 10 Hz to 10 MHz. The mode used for data collection had a frequency resolution of ± 10 Hz, which is about 3 parts in 10^7 at 3 MHz.

---

[1] Matec Instruments, Inc., Hopkinton, MA 01748.

[2] Matec High Resolution Frequency Source Model 110 Operation and Service Manual, Matec Instruments, Inc.

[3] Hewlett-Packard, Santa Clara, CA 95051.

[4] Hewlett-Packard Operating and Service Manual 5314A Universal Counter.

Gated Amplifier

The gated amplifier is a RITEC[5] High Power Gated RF Amplifier Model RX 1-2500C. The amplifier[6] requires a positive trigger mechanism and a CW signal of 1 V rms as input and outputs 2.5 kW RF pulses at the CW input frequency into a 50 Ω load. Standard operating frequency range is from 100 kHz to 5 MHz. Maximum rated pulse widths are $\sim$550 μs with a 0.1% duty cycle. The RF signal is output in either single or dual pulses of $\sim$0.2 μs to $\sim$550 μs in width with a time delay between pulses of from 0.01 ms to 200 ms. The pulse sequences can be automatically repeated at intervals of from 0.1 x 10^0 to 1 x 10^7 ms.

The controls of the pulse sequence interval are a knob, which ranges from 0.1 to 1 by increments of 0.1, and a wheel counter, which controls the power of ten exponent. The knob control is marked for intervals larger than the actual intervals. Calibration values are posted on the amplifier next to the controls and are given in Table 3-1. The time required for 1000 pulses is timed and the result is the calibrated value for each setting. External triggers and gates can be optionally applied if desired. The amplifier has an RF pulse output monitor for the user to view the shape and amplitude of the pulses on channel two of the oscilloscope during setup without effecting the signal to the load. The pulse width and pulse separation controls have demonstrated a tendency to drift if the top multiple settings are used. This makes two

[5] RITEC, Inc., Warwick, RI 02886.

[6] RITEC Manual for the N.Q.R. spectrometer system.

Table 3-1 Pulse sequence interval calibration

C.W. Level Multiplier Knob Marking	Actual Value
0.1	0.061
0.2	0.118
0.3	0.203
0.4	0.293
0.5	0.353
0.6	0.422
0.7	0.510
0.8	0.598
0.9	0.693
1	0.772

pulse experiments tricky at best and unreliable if pulse widths of >40 μs or pulse delays of >20 ms are needed.

Coils and the Impedance Matching Network

The sample coils were made in the laboratory from coated 16 gauge magnet wire wrapped around an empty sample vial to ensure that the coil is of the proper size. The coils were then coated in epoxy to retain their shape. Details of the coil design are given in Iselin [1992] with formulas taken from Wheeler [1928], Smith [1941], and Fukushima and Roeder [1981]. With a particular set of sample vial size, spectrometer system, and applied frequency, the only unconstrained variable is the Q of the coil. The higher the Q value, the more sensitive the coil to the resonance signal, but a higher Q value also means that the coil will require a longer time to recover from a pulse and will have a narrower resonance frequency range. A

workable solution is to have a low Q value that is still high enough for successful experimentation. For a given wire size, the only independent variable is the number of turns in the coil due to the way our coils were wound without a spacing wire.

In addition to the sample coil, a secondary coil was wound to go in the impedance matching network. This secondary coil should have approximately twice the inductance of the primary coil. Multiple sample coils were wound with the highest Q coils being kept for actual work. The secondary coils are not required to have as high a Q as the sample coils.

Broadband Receiver with Phase Sensitive Detector

The RITEC model BR-640 broadband receiver[7] was designed for a linear response over its entire operating range from 100 kHz to 50 MHz. The receiver is capable of signal amplification of from -12 dB to 64 dB in 4 dB steps. The receiver digitizes the resonance signal at the frequency of the applied RF and then amplifies the signal. The noise is mostly out of phase with the RF and will be filtered. Any in-phase signal will be passed through the filtering at the beat frequency between the reference frequency (applied RF) and the resonance frequency. These beat frequencies are seen in the subsequent Fourier transform of the output signal and not the original resonance frequencies. The following filters are built into the receiver: 100 kHz, 500 kHz, and 1 MHz high pass filters and 3 MHz or 12 MHz low pass

[7] RITEC Manual for the N.Q.R. spectrometer system.

filters. Any high/low combination of filters is available for use. The settings used in this work were low pass at 1 MHz and high pass at 12 MHz.

Digital Oscilloscope and Personal Computer

Multiple sweeps are averaged to further increase the signal-to-noise ratio by minimizing the effects of random noise. The averaged spectra are viewed on a Nicolet[8] Digital Oscilloscope Model 4094C with model 4180 storage control plug-in module and an F-43 dual floppy diskette data storage plug-in module. The Nicolet is externally triggered by the gated amplifier, is capable of averaging up to 32767 sweeps, and can digitize the data at dwell times from 5 ns per point up to 10 s per point for up to 15767 different points. The final spectra are saved to 5¼" DSDD floppy disks in a proprietary format which can store up to 20 spectra of 15767 points on a single floppy disk. The spectra can also be exported to a personal computer via HENRY,[9] a data transfer software package supplied by Nicolet. The transfer is via a null modem board installed on the Nicolet to a serial port on the computer. The usual settings on the oscilloscope were 10 μS per point at 100 mV full scale.

[8] Nicolet Instrument Corp., Madison, WI 53711-0288.

[9] HENRY - 4094, version 1.2, Part # 177-001600.

Experimental Technique

Sample Preparation

The sample vials[10] to be filled were first numbered and weighed while empty on an electronic balance.[11] Fifteen grams (± 0.5 g) of the sample material were placed in each vial. If a solvent was added, it was measured with a disposable pipette. Deionized ultrafiltered water[12] was the only solvent used in this work. The vial lids were replaced tightly and sealed with plastic tape.[13] This tape eventually cracks under the repeated thermal stress of cooling to LN_2 temperature and warming back up to room temperature and must be replaced routinely.

Irradiation of Samples

The irradiator used was built by the J. L. Sheppard Company and reported by Hanrahan . The only modifications from the article were an added safety interlock on the irradiator door to prevent accidental exposures and additional external shielding. The source was originally a nominal 400 Ci (15 TBq) of ^{60}Co. With the encapsulated source in the shielded position, the shield door can be opened. For irradiation, the source is lowered to the center of the irradiation chamber and touches the chamber

---

[10] Kimble Opticlear® (23 x 85 mm) vials with screw cap, available from Fisher Scientific, Orlando, FL 32809.

[11] Ohaus Model GA200D, Ohaus Corp., Florham, NJ 07832.

[12] FisherChemical W2-4 Lot No. 903294, Fisher Scientific, Fair Lawn, NJ 07410.

[13] Scotch® brand tape series 23-2087-9 by 3M, St. Paul, MN 55144.

floor. Samples can be placed in the chamber at any location except directly under the source, to prevent sample breakage. The baseline calibration of the irradiator was by Fricke dosimeter in 1989[14] and was 0.52 Gy s^{-1} @ 5 cm (3100 rad min^{-1} @ 2"). A more recent calibration was reported by Jamil [1992] as 0.25 Gy s^{-1} @ 5 cm (1500 rad min^{-1} @ 2"). The irradiator was originally under the control of Dr. P. M. Achey in the Microbiology and Cell Science department and is presently under the control of Prof. J. S. Tulenko in the Department of Nuclear Engineering Sciences at the University of Florida.

The samples were placed in a circle on a wooden board marked with the distance from the source position. The samples were placed on the outer edge of the circle marked as 2 inches from the source. The samples were turned 180° after the first half of the irradiation time, starting with all vial labels in and finishing with all labels facing away from the source. This was done to provide uniform energy deposition by minimizing self-shielding effects in the sample. Active dosimetry for data runs was performed by adding a sample vial with a radiachromic imaging film[15] inside. The reading from the film, containing an aminotriphenylmethane derivative radiation sensitive dye, was used as a check on the irradiation levels as compared to Jamil's calibration with a decay correction. All radiachromic film results, consistent

---

[14] Notes from Dr. P. M. Achey, Department of Microbiology and Cell Science, University of Florida.

[15] GAFCHROMIC™ dosimetry media D-200, FWT radiachromic radiation measurements, Far West Technology, Goleta, CA 93017.

with Jamil after correcting for radioactive decay of the source strength, yielded 0.20 Gy s^{-1} @ 5 cm (1200 rad min^{-1} @ 2").

Pulse Selection

The selection of pulse height and width for a set of experimental runs is based on the fact that the a shorter pulse width can be used with a higher voltage (height) to achieve the desired spin system interaction. A large pulse height is desirable as it allows for a shorter pulse width to provide a pulse with the desired spin system interaction, usually an *effective* 90° pulse. With the coils in place and tuned according to the manufacturer's instructions, the maximum voltage that can be applied without arcing at either the coil or the matching network is found by slowly increasing the voltage. With the pulse height set, the amplitude of the FID is monitored as the pulse width is increased. The first maximum value for the FID is the *effective* 90° pulse and the first zero or minimum is the *effective* 180° pulse.

Data Collection

With the equipment set up as in Fig. 3-1, the oscilloscope, gated amplifier, and receiver can be powered on but the high voltage should remain off. The frequency source is adjusted to the desired frequency setting. After a brief warmup period, including a self-test for the Nicolet oscilloscope, the "Receive Tuning" knob on the matching network is adjusted by viewing the noise on channel A and turning

the knob of the variable capacitor until the noise signal has maximum amplitude. This setting provides the maximum sensitivity to the input frequency. The usual settings for channel A during setup are $\pm$"100" mV full scale and "10 μs" dwell time.

The high voltage switch on the gated amplifier is then turned on and the high voltage pulse is viewed on channel B of the oscilloscope. A sequence interval of 10^3 is best for viewing the pulses. Gate #1 on the oscilloscope must be on; the pulse width should be set initially near "20 μs" for urea-type compounds. The pulse is being viewed through a 91:1 step down and the high voltage should be adjusted to "1.06" on the high voltage ten-turn potentiometer. This setting gives good repeatability with little chance of arcing under all conditions. The resulting pulse is $\sim$1400 V peak-to-peak. The usual settings for channel B during setup are "$\pm$40 V" full scale and "$<$5 ns" interpolated dwell time.

Data were collected for various sweep counts and pulse repetition rates. Due to the strong signal from the ν_+ line of urea, 1000 sweeps were averaged to form a data run with 0.6 x 10^4 ms between sweeps. The low intensity of the ν_- line of urea only allowed 200 sweeps with 0.8 x 10^5 ms between sweeps due to time and stability constraints. Temperature was maintained at 77 K in a dewar which kept the sample submerged in LN_2 for up to 12 hours.

Analytical Techniques

The analytical techniques to be used to analyze the raw data are the modulus-squared Fourier transform, state space singular value decomposition, and nonlinear least squares curve fitting. The techniques are presented in this order so that the amount of information available at each step in the analysis is increased and the next step's result will be a more accurate estimate of the physical parameters: the resonance amplitude, the resonance frequency, the relative phase, and the inverse linewidth parameter. Only a brief description of each technique is given here. For a more detailed explanation, see Iselin [1992]. After describing each technique, the data manipulation using these techniques will be described.

Fourier Transform

The best way to avoid phase errors is to calculate the modulus-squared Fourier transform, otherwise called the power spectrum or power spectral density (PSD). While the PSD is a mixture of the absorption and dispersion spectra, it does allow the experimenter to locate individual peaks in the frequency domain and to approximate the relative amplitudes of each frequency component. Known resonance sites can be identified as well as peaks due entirely to noise. The locations and line widths are only approximate when using the PSD, so their values should be considered only first approximations and not reported as actual experimentally determined values.

Singular Value Decomposition Methods

Analytical Techniques

The analytical techniques to be used to analyze the raw data are the modulus-squared Fourier transform, state space singular value decomposition, and nonlinear least squares curve fitting. The techniques are presented in this order so that the amount of information available at each step in the analysis is increased and the next step's result will be a more accurate estimate of the physical parameters: the resonance amplitude, the resonance frequency, the relative phase, and the inverse linewidth parameter. Only a brief description of each technique is given here. For a more detailed explanation, see Iselin [1992]. After describing each technique, the data manipulation using these techniques will be described.

Fourier Transform

The best way to avoid phase errors is to calculate the modulus-squared Fourier transform, otherwise called the power spectrum or power spectral density (PSD). While the PSD is a mixture of the absorption and dispersion spectra, it does allow the experimenter to locate individual peaks in the frequency domain and to approximate the relative amplitudes of each frequency component. Known resonance sites can be identified as well as peaks due entirely to noise. The locations and line widths are only approximate when using the PSD, so their values should be considered only first approximations and not reported as actual experimentally determined values.

Singular Value Decomposition Methods

The linear algebra method of singular value decomposition (SVD) is a powerful analytical tool which has only been applied to magnetic resonance data since 1985 [Barkhuijsen et al.]. The SVD theorem [Hill 1986] states that any matrix A with m rows and n columns (m x n) can be factored as

$$A = U \Lambda V^{\dagger} \qquad [3\text{-}1]$$

where U is m x n with orthonormal columns, Λ is n x n diagonal with positive, real values in the upper left and zeroes elsewhere, and $V^{\dagger}$ is the Hermitian conjugate of an n x n othogonal matrix. The positive non-zero values on the diagonal of Λ are called the singular values of A.

Hankel Singular Value Decomposition

A non-iterative SVD procedure for retrieving harmonics was developed by Kung and co-workers and published in 1983 using state space concepts. This method was implemented for magnetic resonance time domain spectra via linear algebra and published under the name Hankel Singular Value Decomposition (HSVD) by Barkhuijsen et al. in 1987. The name Hankel is used because the HSVD method takes advantage of the Hankel structure of the manipulated data matrix: all elements on a cross diagonal (running from lower left to upper right) have the same value. The model function is modified to

$$x_n = \sum_{k=1}^{K} c_k z_k^n \qquad [3\text{-}2]$$

where x_n is the nth data point up to the final Nth point, K is the number of signal poles present in the signal (two poles for each exponentially damped sinusoid), c_k is the kth complex coefficient which includes the associated phase information, and the z_ks are the signal poles defined as

$$z_k \equiv e^{[(-\frac{1}{T_2^*}+i\omega_k)\Delta t]} \quad . \qquad [3\text{-}3]$$

Once the signal poles are found, the frequencies and relaxation times can be determined and then the coefficients are found by a fit to the data. For further details, see Barkhuijsen et al. [1987], Iselin [1992], or de Beer and van Ormondt [1992].

Nonlinear Least Squares Curve Fitting

In nonlinear least squares, the goal is to find the values of the parameters which maximize the probability that the values of the fitted parameters are best. This is the Maximum Likelihood Method. Following de Beer and van Ormondt [1992], assume a model function $\hat{x}_n$, n=1,...,N (N data points) that exactly represents a noiseless real measurement x_n, n=1,...,N. Noise is added to the data x_n so that $x_n - \hat{x}_n = \epsilon_n$, where ϵ_n equals the noise contribution to the nth data point. The distribution of the noise is given as Gaussian with σ_r as the noise standard deviation.

The joint probability function P for the entire measurement is the product of the individual probabilities for each data point and is given as

$$P(\epsilon) = P(x-\hat{x}) = \prod_{n=1}^{N} p_n(x_n-\hat{x}_n)\,. \qquad [3\text{-}4]$$

When given a data set x and asked to determine $\hat{x}$, the values of the model parameters, $P(x-\hat{x})$ is called the likelihood function and the model parameters found are the Maximum Likelihood estimates. The log-likelihood function defined as

$$L(x-\hat{x}) \equiv \ln[P(x-\hat{x})] \qquad [3\text{-}5]$$

is often used in place of the likelihood function because of its particular form in the case of Gaussian noise:

$$L(x-\hat{x}) = -N\ln[2\pi\sigma^2] - \frac{1}{2\sigma_r^2}\sum_{n=1}^{N}(x_n-\hat{x}_n)^2\,. \qquad [3\text{-}6]$$

Maximizing the log-likelihood function also maximizes the likelihood function. This is the basis for minimizing the sum squared error when curve fitting. The log-likelihood function merit function is usually reported as χ^2 and shortened to

$$\chi^2 = \frac{1}{\sigma^2}\sum_{n=1}^{N}(x_n-\hat{x}_n)^2\,. \qquad [3\text{-}7]$$

Levenberg-Marquart Method

The Levenberg-Marquart method [Levenberg 1944, Marquart 1963, Davies and Whitting 1972, Press et al. 1989, Iselin 1992] is a hybrid of the method of steepest descent and Newton's method. Far (in relative terms) from the minimum, the method of steepest descent is used to target the minimum. As the minimum is approached, Newton's method is used. This is accomplished by introducing a varying factor into the Hessian matrix to weight the main diagonal. The parameter is raised to favor the method of steepest descent and then lower once the desired minimum is approached to use the faster convergence of Newton's method.

In practice, the Hessian matrix is usually approximated under Rao's (or Fisher's) "scoring" approximation [Rao 1973] which shortens the computation time while retaining good convergence characteristics [Maybeck 1979]. The Hessian matrix is replaced by the negative of the Fisher Information Matrix, also referred to by Rao and Maybeck as the conditional information matrix

$$\frac{\partial^2 L}{\partial \boldsymbol{\alpha}^2} \approx -\boldsymbol{F} = E\left\{\frac{\partial^2 L}{\partial \boldsymbol{\alpha}^2}\right\} \qquad [3\text{-}8]$$

where L is the log-likelihood function from Eq. [3-6] and $E\{\cdot\}$ means take the expectation value (also see Eq. [3-9] below). The approximation being made is that the Hessian matrix for a particular data set can be adequately represented by an average over all of the data points. The modified Hessian matrix represented by the Fisher Information Matrix has no second derivative terms, only the product of first

derivative terms. The form and function of the Fisher Information Matrix will be addressed further in the discussion on errors in the fitted parameters.

In general, there is never a guarantee of finding the values of the unknowns which give the global minimum for the merit function. There is no way to determine if the minimum values found are global or local. The search space may be very uneven near the global minimum and the search method may not quite reach that point.

Errors in Fitted Parameters

Estimating the standard deviation of a fitted parameter can be difficult. The two main sources of error are the experimental error and the analysis error. The experimental error can be approximated by replicating all experiments several times under identical conditions and determining the variation in the parameter values. The analysis errors can be approximated by giving the Cramér-Rao Lower Bounds [Fréchet 1943, Darmois 1945, Rao 1945, Cramér 1946]. While a program is available for estimating Cramér-Rao Lower Bounds for HSVD, the most useful error analysis is of the errors in the final curve fitting using the Levenberg-Marquart method, since the nonlinear least squares curve fit is a Maximum Likelihood method. The nonlinear least squares curve fitting program used in this work automatically calculates the Cramér-Rao Lower Bounds of each fitted parameter.

Following Norton [1986] (and [de Beer and van Ormondt 1992]), the lower limit for the covariance matrix for the α parameters, from 1 to J, used in $\mathcal{L}$ can be

shown to be the inverse of the Fisher Information Matrix F:

$$F \equiv E\left\{\frac{\partial L}{\partial \boldsymbol{\alpha}}\left(\frac{\partial L}{\partial \boldsymbol{\alpha}}\right)^T\right\} \tag{3-9}$$

where ^{T} means take the transpose. It can be shown that the Fisher Information Matrix can be simplified to

$$F = -E\left\{\frac{\partial^2}{\partial \boldsymbol{\alpha}^2}L\right\} = -E\left\{\frac{\partial^2 L}{\partial \alpha_k \partial \alpha_j}\right\}, \quad j,k=1,\ldots,J. \tag{3-10}$$

The partial derivatives of L with respect to the components α_j and α_k are as follows

$$\frac{\partial L}{\partial \alpha_j} = \frac{1}{\sigma_r^2}\sum_{i=1}^{N}(x_i-\hat{x}_i)\frac{\partial \hat{x}_i}{\partial \alpha_j} \tag{3-11}$$

and

$$\frac{\partial^2 L}{\partial \alpha_k \partial \alpha_j} = -\frac{1}{\sigma_r^2}\sum_{i=1}^{N}\left[\frac{\partial \hat{x}_i}{\partial \alpha_k}\frac{\partial \hat{x}_i}{\partial \alpha_j} - (x_i-\hat{x}_i)\frac{\partial^2 \hat{x}_i}{\partial \alpha_k \partial \alpha_j}\right]. \tag{3-12}$$

Note that the second derivative matrix given in Eq. [3-12] is the full Hessian matrix. The negative sign in Eq. [3-12] is negated by the negative sign in Eq. [3-10] and the Fisher Information Matrix becomes

$$F = E\left\{\frac{1}{\sigma_r^2}\sum_{i=1}^{N}\left[\frac{\partial \hat{x}_i}{\partial \alpha_k}\frac{\partial \hat{x}_i}{\partial \alpha_j} - (x_i-\hat{x}_i)\frac{\partial^2 \hat{x}_i}{\partial \alpha_k \partial \alpha_j}\right]\right\} \tag{3-13}$$

The expectation value of Eq. [3-13] removes all terms containing ϵ_i and thus Eq. [3-13] becomes

$$F = \frac{1}{\sigma_r^2}\sum_{i=1}^{N}\left[\frac{\partial \ell_i}{\partial \alpha_k}\frac{\partial \ell_i}{\partial \alpha_j}\right]. \qquad [3\text{-}14]$$

This is the result that makes Rao's "scoring" approximation attractive. Once the Maximum Likelihood parameters have been found, the lower bounds on the errors of those parameters can be found by inverting the Fisher Information Matrix, according to the Cramér-Rao Inequality [Norton 1986]:

$$Cov(\boldsymbol{\alpha}) \geq F^{-1}. \qquad [3\text{-}15]$$

Procedures

Data File Manipulation

The spectra were transferred from the Nicolet to a Zenith[16] PC/AT model 325 microcomputer via Henry. This transfer requires that there be a configuration file in the root directory of the computer named 4094.CNF. The configuration file is created by 4094CFG.EXE, a file supplied with HENRY, which questions the user about the hardware setup. The Henry transfer program used is named 4094LTU.EXE. The transfer can either be to the directory containing 4094LTU.EXE

---

[16] Zenith Data Systems Corporation, St. Joseph, MI 49085.

or another directory if the above executable file is in the path or is called by a batch file which is in the path. The file names were chosen in such a way to always be able to identify the location of the original spectrum on the Nicolet formatted data disks.

Before performing any data analysis, the PRN files are viewed in a graphing program such as Lotus® 1-2-3®[17] to determine how many initial points to remove to eliminate the detection response to the initial pulse. The data spectra always contain a square pulse which is the response to any input pulses. It was arbitrarily chosen to delete the initial points up to the first zero crossing of the FID signal. For a signal such as urea, this represents the loss of 4 to as many as 20 valid data points.
Before running any of the data analysis programs, the data files must be converted into the proper format. FFT requires that the data are in time and voltage columns as in the OUT file format produced by CONVERT. CONVERT changes the PRN condensed format of eight columns of voltage data with time described by start time and time increment into two columns of time versus voltage. HSVD requires a binary format in blocks of 64 points. The PXLTA and CXLTA programs convert the PRN and OUT files, respectively, to a formatted form with blocks of 64 points in ASCII text. ASBIN reads this block formatted data to produce the HSVD-required binary formatted data blocks. The nonlinear curve fitting programs read in the data from the OUT formatted files. Examples of all computer programs are in Appendix A; examples of all file types are in Appendix B.

---

[17] Lotus Development Corporation, Cambridge, MA 02142

Use of Fourier Transform

When searching for an unreported transition, the PSD FFT is useful to help locate the peak and to differentiate real resonances from noise (If the peak shifts exactly in response to a frequency shift it is most probably a resonance and not noise.). With a simple FID, like that of urea, the PSD FFT is not always run on each data set unless a question arises that can best (or most quickly) be answered by viewing the frequency domain. When needed, the data sets are converted to the OUT file format by CONVERT, retaining every data point. The FFT program is then run on each data set producing the PSD FFT.

HSVD Applied to Data

The HSVD program requires no starting guesses, so HSVD can be run after the data have been properly formatted by PXLTA and then converted to binary format by ASBIN. The HSVD inputs are the number of data points, the value of the Hankel parameter, L (here the number of data columns), and the number of singular values expected. The HSVD model associates two singular values with each resonance site. If the PSD FFT noise peak at low frequency is very large, there will be associated noise singular values which cannot be ignored. For urea, two singular values are usually enough unless dc noise (zero frequency) is present. If too many singular values are used, then HSVD will attempt to fit the peaks by overlapping Lorentzian peaks even if the data are not perfectly Lorentzian. An example of the actual output

file from HSVD, HSVSCR.PAR, is shown in Appendix A. Since linear algebra methods are not always Maximum Likelihood methods in the presence of noise, nonlinear curve fitting is necessary to find the Maximum Likelihood values of the NQR parameters.

Nonlinear Curve Fitting of Data

The values returned for the resonance peaks by HSVD are excellent starting values for nonlinear least squares curve fitting programs. Since the stability of nonlinear curve fitting programs depends on the starting values being as correct as possible, these values are exactly what is needed. The PSD FFT results were used to approximate the frequency and amplitude values, but the lack of phase information often makes the analysis difficult if not impossible if there are multiple peaks. The final results of the data analysis are based on the Levenberg-Marquart results. All data analysis errors in the parameters are assumed to be the minimums given by Eq. [3-15] as no systematic errors were identified.

CHAPTER 4
RESULTS

This chapter reports the results of the original extension to NQR analysis theory and all experiments and the analyses from fitting the data to the various models. The original data are FIDs of urea, urea-water, and urea-d_4. Only the urea and urea-water were subjected to ionizing radiation. Irradiations were done at room temperature and 77 K with all NQR data taken at 77 K with the sample submerged in LN_2. NQR experiments on urea-rock salt and urea-hydrogen peroxide which failed to detect a resonance site are also described. The sodium nitrite data used to test the method of linewidth analysis is from Petersen's doctoral work [1975, 1976].

Theoretical Results

NQR Linewidth Analysis

An expression used to describe the spin dynamics in experimental NMR can be applied to experimental NQR to yield information on the widths of electric field gradient (EFG) parameters. The width of the primary EFG component is usually assumed from the width of the resonance lines, although one previous NQR work used spin dynamics with the width of the EFG parameters assumed constant [Zussman 1973]. This assumption is not necessarily true.

In NMR, the inverse linewidth parameter T_2^* and the spin-spin relaxation time T_2 are related through the inhomogeneity in the magnetic field (H_0) used to split the energy levels. The equation used to describe this relationship for a resonance line having a Lorentzian shape [Farrar and Becker 1971] can be written as

$$\frac{1}{T_2^*} = \frac{1}{T_2} + \frac{\gamma(\Delta H_0)}{2} \qquad [4\text{-}1]$$

(with γ as the gyromagnetic ratio), but has appeared in the literature in an approximate form with no constants, i.e. $\gamma = 2$, for the general case [Fukushima and Roeder 1981]. The relationship for a resonance line having a Gaussian shape is

$$\frac{1}{T_2^*} = \frac{1}{T_2} + \frac{\gamma(\Delta H_0)}{4\sqrt{\ln 2}}. \qquad [4\text{-}2]$$

The Gaussian case will not be explicitly considered since it only differs from the Lorentzian case by a constant. In NQR, the energy level splitting is produced internally and no external magnetic fields are necessary; thus, the relationship between T_2^* and T_2 for NQR is different than Eq. [4-1]. Since the last term in Eq. [4-1] is simply a measure of the spread of the angular frequency of the transition that is not due to the spin system dynamics, the equivalent equation for NQR would be

$$\frac{1}{T_2^*} = \frac{1}{T_2} + \frac{\Delta\omega_Q}{2}. \qquad [4\text{-}3]$$

Referring to Eq. [2-33], the angular frequency for an NQR transition ω_Q is a function of the quadrupole moment eQ of the target nucleus, Planck's constant h, and the EFG

parameters eq and η. Since these EFG parameters are the only parts of ω_Q which are not constants, any width in ω_Q not due to the spin system interactions must be a direct result of widths in the EFG parameters. The asymmetric splitting of the energy levels in NQR (with $\eta \neq 0$), gives rise to multiple versions of Eq. [4-3], one for each observable transition.

For $I = 1$, three variations of Eq. [4-3] are available for inspection, corresponding to the ω_d difference line,

$$\frac{1}{T_2^*} = \frac{1}{T_2} + \frac{\pi e Q}{2h}\Delta[eq\eta], \qquad [4\text{-}4]$$

the ω_- line,

$$\frac{1}{T_2^*} = \frac{1}{T_2} + \frac{\pi e Q}{4h}\Delta[eq(3-\eta)], \qquad [4\text{-}5]$$

and the ω_+ line.

$$\frac{1}{T_2^*} = \frac{1}{T_2} + \frac{\pi e Q}{4h}\Delta[eq(3+\eta)]. \qquad [4\text{-}6]$$

Since the quadrupole energy tensor is symmetrical and traceless, there are only two degrees of freedom for the three versions of Eq. [4-3]. These two degrees of freedom are usually represented by eq and η or by χ and $\chi\eta$. The equations for ω_-, Eq. [4-5], and ω_+, Eq. [4-6], are expected to yield identical results since they differ only by a sign change inside the term with an associated width. The validity of this implied requirement

$$\left[\frac{1}{T_2^*}-\frac{1}{T_2}\right]_+ = \left[\frac{1}{T_2^*}-\frac{1}{T_2}\right]_- \qquad [4\text{-}7]$$

will be tested in the next chapter.

Rearranging Eq. [4-4] gives a directly measurable relationship for the width of the EFG function [V_{xx} - V_{yy}], the numerator of η, as

$$\Delta[eq\eta] = \frac{2h}{\pi eQ}\left(\frac{1}{T_2^*}-\frac{1}{T_2}\right)_d \qquad [4\text{-}8]$$

where the subscript denotes the line to which the time constants are associated, ω_d in the case of Eq. [4-8]. Often the ω_d line is at too low a frequency to be observed by traditional methods; however, advances in NQR detection methods and instrumentation have brought this relationship within the reach of experimenters through SQUID NQR [Conner 1990].

The other independent variable to be considered here is *eq*. Determining the width of this variable requires prior knowledge of the shape of the EFG distribution. An upper limit on the width can be obtained by assuming the widths to be completely correlated so as to add arithmetically [Taylor 1982]

$$\Delta[eq]_{max} \le \frac{h}{3\pi eQ}\left[2\left(\frac{1}{T_2^*}-\frac{1}{T_2}\right)_\pm - \left(\frac{1}{T_2^*}-\frac{1}{T_2}\right)_d\right]. \qquad [4\text{-}9]$$

If the spreads in the EFG components are independent and uncorrelated, then the widths add in quadrature [Taylor 1982] and the result is

$$\Delta[eq] = \frac{2h}{3\pi eQ}\sqrt{4\left(\frac{1}{T_2^*}-\frac{1}{T_2}\right)_{\pm}^2 - \left(\frac{1}{T_2^*}-\frac{1}{T_2}\right)_d^2}\,. \qquad [4\text{-}10]$$

For any case, ω_Q can be separated experimentally into its two components: spin dynamic width and EFG component width, for any given substance and transition starting with Eq. [4-1] for a Lorentzian lineshape, Eq. [4-2] for a Gaussian lineshape or an analogous equation for other lineshapes. By experimentally measuring the T_2 and T_2^* dynamic spin system time constants of NQR transitions, information on the widths of the EFG parameters can be determined. This method extends the traditional method of estimating the total width of *eq* (or χ) from the width of the resonance lines.

NQR Linewidth Analysis Test for ^{14}N

Since experimental values for T_2 and T_2^* are unavailable for the ν_d line for any ^{14}N containing compound, the NQR linewidth analysis method previously proposed cannot be *fully* tested. The best available test is to use available data from the literature to determine if it is true that ν_+ and ν_- give comparable results as described above. For this test, Petersen's data set on sodium nitrite was chosen. Values for T_2 and T_{2^*} for the ν_+ and ν_- lines were determined as a function of temperature from 77 K to over 400 K. The data were taken from Petersen's doctoral work in 1975 that was subsequently published in 1976. The data were originally presented on semi-log graphs of time constant vs. temperature. The data points presented here were

digitized from graphs sent by Petersen since the original data files were erased from computer storage in early 1992.[1] Figures 4-1 through 4-4 are the original digitized data points on linear graphs.[2] They are followed by smooth curves representing the data. The mean squared errors for the smooth curves given in Figs. 4-5 and 4-6 are 0.00827 for T_2 and 0.151 for T_2^* of the ν_+ line and in Figs. 4-7 and 4-8 are 0.294 for T_2 and 0.0199 for T_2^* of the ν_- line, respectively. Note the difference in *y*-axis scaling in each pair of figures; the first is linear and the second is logarithmic. The data could not be "fit" in a traditional fashion since there is no theoretical model to describe the data. The smooth curves simply reduce the scatter.

Experimental Results

Pulse Optimization

The initial experiment on the NQR spectrometry system is to set the pulse height and width for the substances to be probed. By trial and error it was determined that the maximum voltage that could be repeated almost indefinitely was around 1400 V to the coil or about 1.06 on the ten turn potentiometer on the amplifier. To provide a standard that would interact with as uniform a magnetic field as possible, samples of HMT and urea were made with paraffin filling the upper and lower one third of the sample vial. This eliminates any end effects but does not

---

[1] Personal Communication with Dr. Gary Petersen, RITEC, Inc., Warwick, RI 02886.

[2] The data were originally presented by Petersen only on logarithmic graphs.

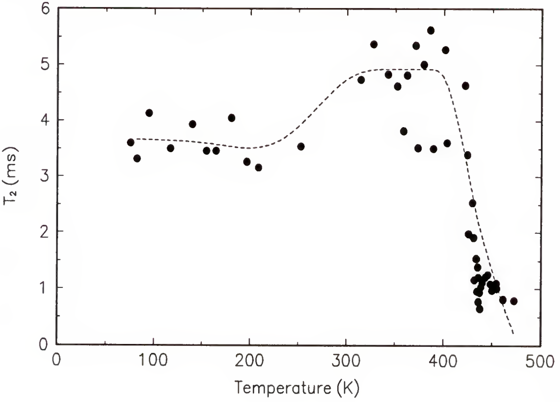

Figure 4-1 Petersen's data for the ν_+ line of sodium nitrite.

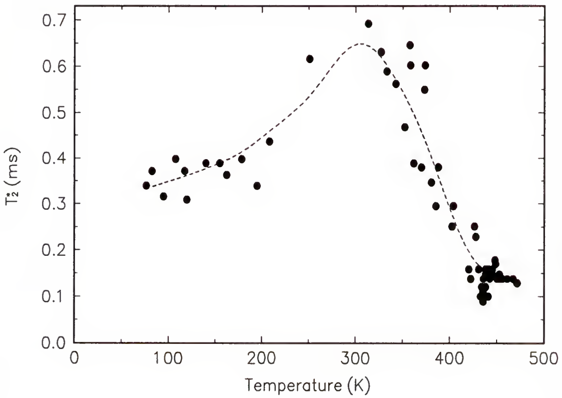

Figure 4-2 Petersen's data for the ν_+ line of sodium nitrite.

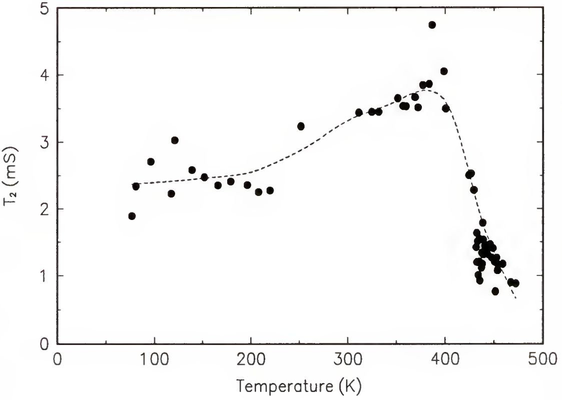

Figure 4-3 Petersen's data for the ν_- line of sodium nitrite.

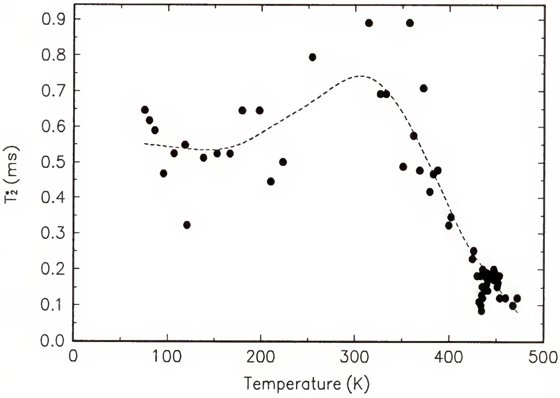

Figure 4-4 Petersen's data for the ν_- line of sodium nitrite.

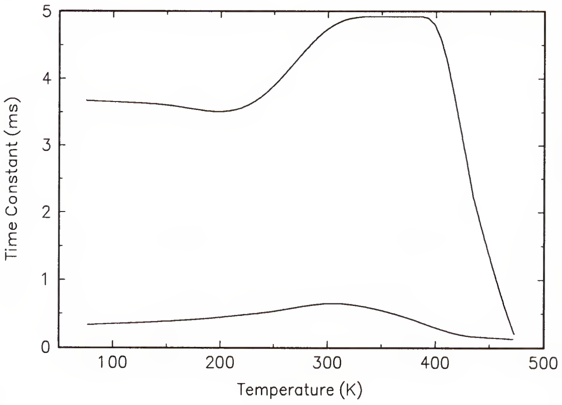

Figure 4-5 Smoothed values of Petersen's data for T_2 (upper line) and T_2^* (lower line) for the ν_+ line of sodium nitrite on a linear scale.

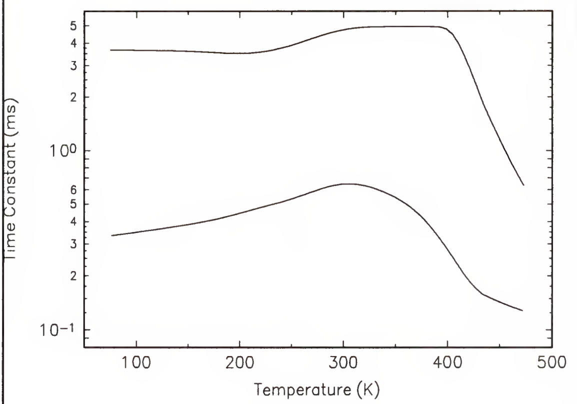

Figure 4-6 Smoothed values of Petersen's data for T_2 (upper line) and T_2^* (lower line) for the ν_+ line of sodium nitrite on a logarithmic scale.

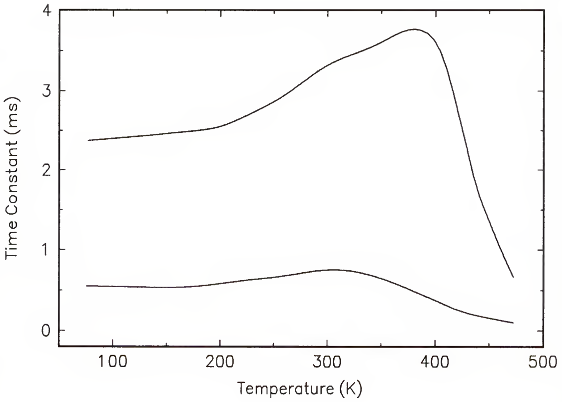

Figure 4-7 Smoothed values of Petersen's data for T_2 (upper line) and T_2^* (lower line) for the ν_- line of sodium nitrite on a linear scale.

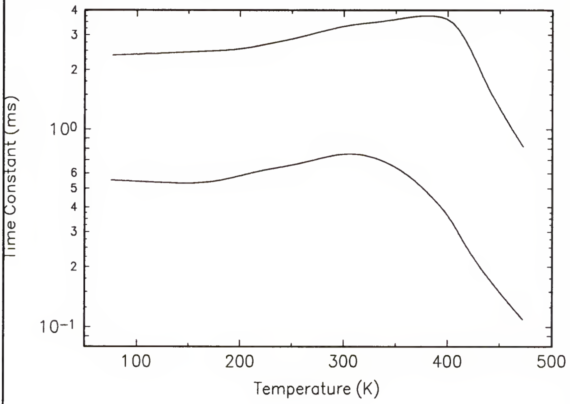

Figure 4-8 Smoothed values of Petersen's data for T_2 (upper line) and T_2^* (lower line) for the ν_- line of sodium nitrite on a logarithmic scale.

change possible radial effects on the magnetic field. These pulse calibration standards were used in addition to a full vial of crushed urea. Using HMT at room temperature as an initial standard, the pulse width was varied and the height of the FID was measured with the frequency set exactly 10 kHz above resonance. Attempts to observe changes in the FID while on resonance were unsuccessful. For this purpose, the height of the FID was the average difference on voltage from the top of the first peak to the bottom of the first valley to the top of the second peak for each FID. The results for HMT are given in Fig. 4-9. This graph demonstrates that the FID amplitude does indeed change in a measurable way with pulse width. Switching to the urea standards at 77 K gave the results shown in the next three figures. The frequency was again set 10 kHz above resonance. Figure 4-10 was taken at a pulse height voltage of 1200 V and Fig. 4-11 was taken at 1400 V, both using the urea standard consisting of a full vial. Figure 4-12 was taken at 1360 V using the urea calibration standard. The error in each measurement in Figs. 4-9 through 4-12 is 10-15%. Based on these graphs, the decision was made to use 20 μs pulse widths to obtain urea FIDs. All efforts to record consistent data with pulses longer than 1.5 times the FID maximum failed. This eliminated the possibility of performing experiments which require more than a single pulse such as spin echoes for measuring T_2.

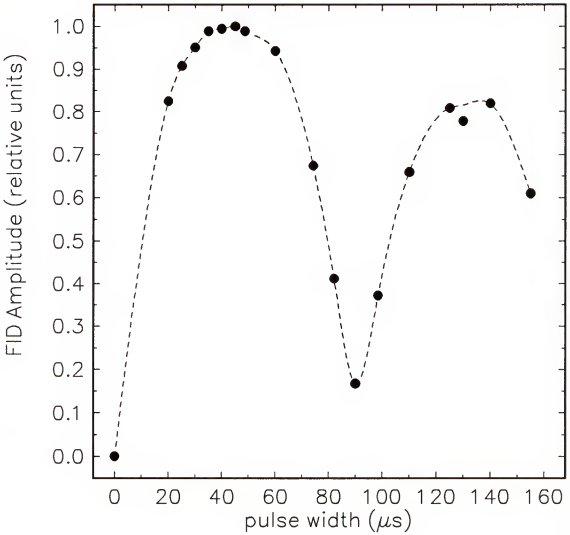

Figure 4-9 HMT FID Amplitude at 1400 V and Room Temperature.

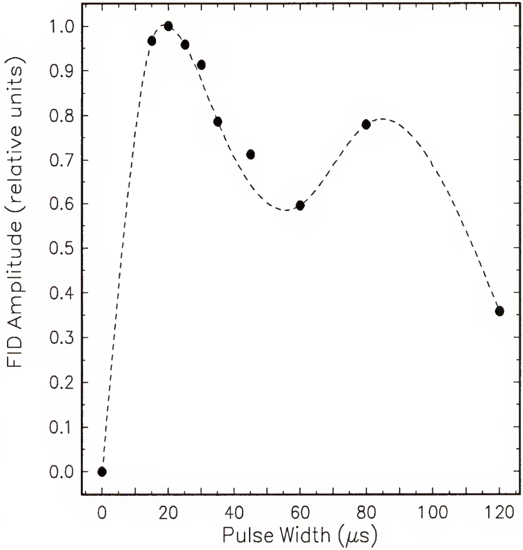

Figure 4-10 Urea FID Amplitude at 1200 V at 77 K.

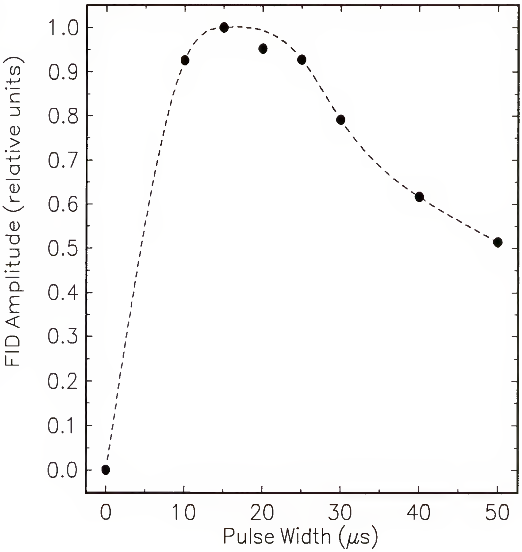

Figure 4-11 Urea FID Amplitude at 1400 V at 77 K.

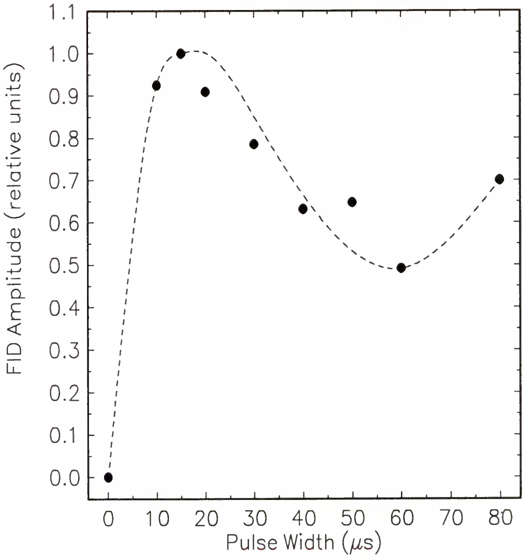

Figure 4-12 Urea FID Amplitude at 1360 V at 77 K.

Pure Urea and Urea-d_4

Of all available compounds containing nitrogen, urea is one of the most studied by ^{14}N NQR, with HMT probably being the most studied. Not only has pure polycrystalline urea been studied [Chiba et al. 1959, Minematsu 1959, Guibé 1960, Widman 1963, O'Konskia and Torizuka 1969, Zussman 1973, Oja 1973, Higgins 1990, Hintenlang et al. 1992], but also urea complexes [Negita et al. 1977, 1981, Murgich and Santana R. 1981], substituted ureas [Smith and Cotts 1964, Dinesh and Rogers 1972, Sauer and Bray 1973, Chen and Dodgen 1976], and structurally related guanidine compounds [Oja 1969a, 1969b, 1973]. The ν_+ resonance of urea routinely detected previously (not shown) was observed at 2913.32 $\pm$ 0.01 kHz and the ν_- resonance shown in Fig. 4-13 was observed at 2347.88 $\pm$ 0.08 kHz. These urea resonances were found at frequencies consistent with those previously reported. The T_2^* values for urea given in Table 4-1 agree reasonably well ($\pm$25%) with those given by Zussman [1973] at 77 K.

Urea-d_4 has significance in that the substitution of deuterium ($I = 1$) for light hydrogen ($I = ½$) in the amide groups raises the mass of the molecule leading to a difference in its NQR frequency temperature dependance. The center of the ν_+ resonance (2941.65 $\pm$ 0.01 kHz) of urea-d_4 was found at a frequency consistent with previous reports [Widman 1963]. The ν_- resonance of urea-d_4 was identified for the first time at 2381.46 $\pm$ 0.04 kHz. The inverse linewidth parameters (T_2^*) for the resonance lines are given in Table 4-1, along with the calculated χ and η, and compared to urea.

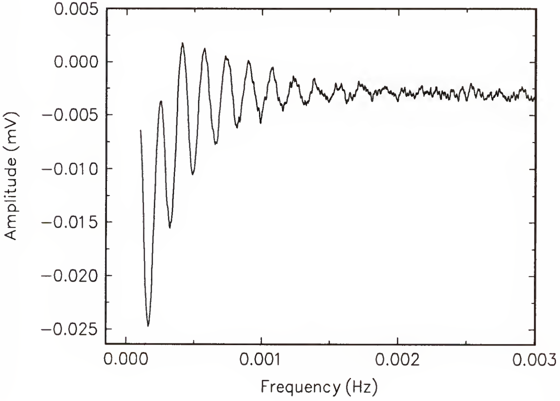

Figure 4-13 FID of urea. Resonance shown is v_-.

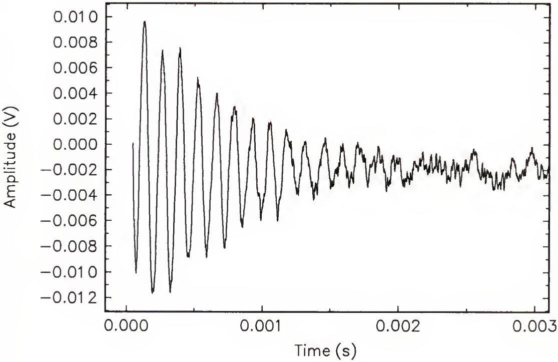

Figure 4-14 FID of urea-d_4. Resonance shown is ν_-.

Table 4-1 Nuclear quadrupole coupling constants, asymmetry parameters, and inverse linewidth parameters for urea and urea-d_4.

NQR Parameter	urea	urea-d_4
χ	3548.74 ± 0.03 kHz	3507.47 ± 0.06 kHz
η	0.32242 ± 0.00015	0.31571 ± 0.00007
$\nu_+ T_2^*$	780 ± 20 μS	928 ± 23 μS
$\nu_- T_2^*$	523 ± 24 μS	721 ± 12 μS

Errors given are the propagated fitting errors.
Different samples may yield T_2^* values that differ by as much as 10%.

Effect of Gamma Rays on Urea-Water

It has previously been reported by this laboratory that ^{60}Co γ-ray irradiations on urea-water leads to a decrease in the inverse linewidth parameter with increasing radiation dose [Higgins 1990, Hintenlang and Higgins 1992, Hintenlang et al. 1992]. Based on the original data and original analyses, the exact relationship was shown to correspond to a linear increase in linewidth by Iselin and Hintenlang[3]. This relationship is shown in Fig. 4-15. Repeated attempts to replicate this effect have been unsuccessful. Figure 4-16 illustrates the results of these attempts; the error in each datum is ±7.5% or 150 Hz.

[3] *The NQI Newsletter*. 1(3):39; 1994. Published under the auspices of the International Symposium on Nuclear Quadrupole Interactions by R. A. Marino, Hunter College of CUNY, 695 Park Ave., New York, NY 10021.

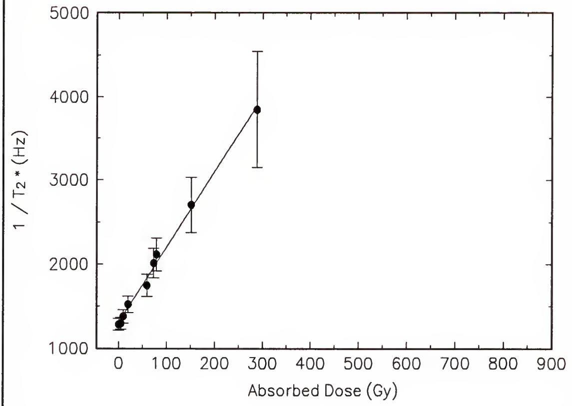

Figure 4-15 Reported increase in the urea ν_+ linewidth after exposure to increasing amounts of ^{60}Co γ rays.

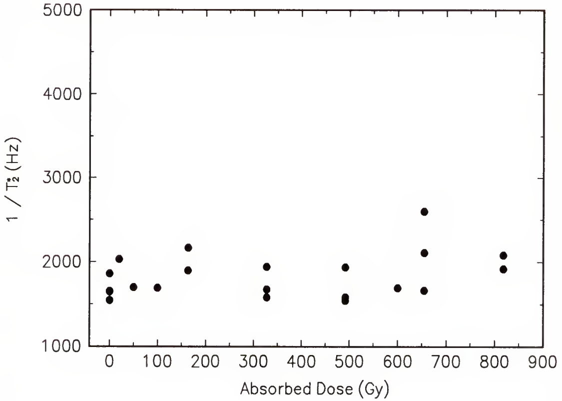

Figure 4-16 Data from an attempt to replicate the reported ^{60}Co radiation effect on the urea-water ν_+ inverse linewidth parameter.

Effect of Water on Urea

An experiment was carried out to determine if the changes reported by Higgins and later by Hintenlang could be attributed to the water added to the urea. Samples of urea were bottled as per Higgins with varying amounts of water to see if the amount of water caused a shift in T_2^*. Each sample's mass was determined and the molar amount calculated for determining the proper amount of water for the desired molar ratio for each sample. The urea and water were heated in a microwave just until the point of boiling. The sample vial was immediately removed from the oven and capped. The sample was then shaken to insure complete dissolution of the urea in the water. The samples were placed on their sides on an insulated surface to cool slowly. The cooling method differed from the method that Higgins was observed using. Higgins removed samples from the microwave and then placed a wooden dowel in the center of the solution so that the samples would have a hollow core. In both cases, the void space in the sample vials was needed to assure that the vials did not burst upon thawing from 77 K. The results are shown in Fig. 4-17. The value of T_2^* drops from the baseline value of 780 μs for pure urea to below 650 μs. The smallest amount of water that could be added to a sample was 9 molar percent. Using less than this amount caused the sample to become heterogeneous in nature with a part of the sample remaining unchanged. Since the urea samples must be heated quickly to avoid the urea + water reaction, there is no time for mixing the samples during heating to spread the water molecules throughout the urea sample.

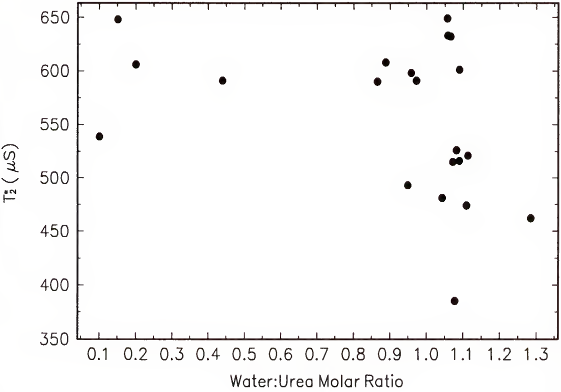

Figure 4-17 Effect of adding water to the $\nu+$ line of urea. (σ = ~45 μs)

Pulsed ^{14}N NQR of Urea-H_2O_2 and Urea-Rock Salt

Since the ^{14}N NQR spectrum of urea-H_2O_2 is known [Negita et al. 1977], and the structure is believed to be similar to urea-water due to the presence of hydrogen bonding in both "compounds", the decision was made to attempt to use urea-H_2O_2 for comparison. The literature on urea-hydrogen peroxide stated clearly that the material had to be stored below 35 °C or degradation would occur. At higher temperatures, the hydrogen peroxide is not contained in the urea matrix. Initial data runs were taken and analyzed. The ν_+ line was detected at 2922 kHz as published [Negita et al. 1977]. Careful and continued experimentation led to the discovery that the material was not as stable, even when kept refrigerated, as believed from reports in the literature. After finding that samples could not be stored for repeated analysis, further experiments with urea-H_2O_2 were dropped.

Early work in the literature on the use of NQR to study radiation effects involved ^{35}Cl containing compounds. The decision was made to attempt to use a ^{35}Cl- and ^{14}N containing compound to see if photon radiation effects could be observed. Being familiar with the ^{14}N NQR of urea compounds, urea-rock salt was chosen as a candidate material. The ^{14}N NQR frequencies have been reported by Negita et al. [1977] with resonance lines at 3592, 3599, 3596, and 3602 kHz. Although the method of preparation for urea-rock salt is given by Negita et al. [1977], two attempts to manufacture the complex were unsuccessful. The urea ν_+ resonance line was faintly observed at the extreme limits of detection, but no urea-rock salt transitions could be detected.

CHAPTER 5
DISCUSSION

This chapter gives a discussion of the results of the original extension to NQR analysis theory and the various experiments and analyses that were carried out. Several approximations to the NQR linewidth analysis method are given. From the testing of the method, the EFG widths for Petersen's sodium nitrite data are given. The pulse width calibration reveals the limitations of the NQR spectrometer, but the urea-d_4 ν_- line is still detected for the first time and characterized to show less electronic shifting upon deuteration than would be expected compared to other compounds. Townes and Dailey theory is used to analyze the results. Further EFG comparison is made to other urea compounds. The negative radiation effects study is analyzed by comparing the effect of adding water to urea and a further look at some of Higgins' original data.

Theoretical Results

NQR Linewidth Analysis

For ^{14}N NQR, measuring T_2 for ν_+ and ν_- or acquiring any information about the ν_d line may be difficult or practically impossible. Several approximations to the

linewidth analysis method given here are readily assumable and each simplifies the amount of information needed experimentally.

The first is to assume that $T_2 >> T_2^*$ for all transitions so that $1/T_2$ can be neglected. For most ^{14}N containing compounds, this is the case. In this case,

$$\Delta[eq\eta] \approx \frac{2h}{eQ}\left(\frac{1}{\pi T_2^*}\right)_d \qquad [5\text{-}1]$$

and

$$\Delta[eq]_{max} < \frac{h}{3eQ}\left[2\left(\frac{1}{\pi T_2^*}\right)_{\pm} - \left(\frac{1}{\pi T_2^*}\right)_d\right]. \qquad [5\text{-}2]$$

The primary result of this approximation is that twice the linewidth of the ν_d transition is proportional to the average width of V_{xx} and V_{yy}. Note that if the linewidths of all three transitions are similar in magnitude, then the width of *eq* is proportional to the linewidth and the width of χ is approximately one third of the linewidth. The only drawback to this approximation is that although the absolute value of the width is given, the error in the values can be substantially increased if the assumptions are poor.

The second approximation involves relative values of the EFG widths and is given by assuming that T_2 is relatively constant for all transitions under all experimental conditions. The main concerns in this case will be that temperature and pressure remain constant throughout. If, for example, a change in the EFG widths is

present before and after irradiation of the sample, then the differences δ_{2-1} could be written as

$$\delta_{eq\eta} = \Delta_2[eq\eta] - \Delta_1[eq\eta] = \frac{2h}{eQ}\left[\left(\frac{1}{\pi T_2^*}\right)_{d2} - \left(\frac{1}{\pi T_2^*}\right)_{d1}\right] \qquad [5\text{-}3]$$

and

$$\delta_{eq} = \frac{h}{3eQ}\left[2\left(\frac{1}{\pi {T_2^*}_2} - \frac{1}{\pi {T_2^*}_1}\right)_{\pm} - \left(\frac{1}{\pi {T_2^*}_2} + \frac{1}{\pi {T_2^*}_1}\right)_{d}\right]. \qquad [5\text{-}4]$$

The errors in this second case will depend solely on the measurement errors in determining the linewidths.

A third approximation, the one used in this work, is to assume that

$$\left[\frac{1}{T_2^*} - \frac{1}{T_2}\right]_{+} = \left[\frac{1}{T_2^*} - \frac{1}{T_2}\right]_{-} = \left[\frac{1}{T_2^*} - \frac{1}{T_2}\right]_{d}. \qquad [5\text{-}5]$$

Note that this applies to all three transitions and not just ν_+ and ν_- as given by Eq. [4-7]. This assumption is reasonable if the EFG is isotropic. In this case, Eq. [4-8] simplifies to

$$\Delta[eq\eta] = \frac{2h}{\pi eQ}\left(\frac{1}{T_2^*} - \frac{1}{T_2}\right) \qquad [5\text{-}6]$$

and leads to

$$\Delta[\chi\eta] = \frac{2}{\pi}\left(\frac{1}{T_2^*}-\frac{1}{T_2}\right), \qquad [5\text{-}7]$$

while Eq. [4-9] simplifies to

$$\Delta[eq]_{max} <\approx \frac{h}{3\pi eQ}\left(\frac{1}{T_2^*}-\frac{1}{T_2}\right) \qquad [5\text{-}8]$$

and leads to

$$\Delta[\chi]_{max} <\approx \frac{1}{3\pi}\left(\frac{1}{T_2^*}-\frac{1}{T_2}\right). \qquad [5\text{-}9]$$

This approximation allows T_2^* and T_2 data for a single transition to take the place of missing data from the other two transitions. In the case of a pure, homogeneous material, this may be an acceptable approximation. When inhomogeneities are introduced into the material, the error introduced may become unacceptable. Since there is no significant data on the ν_d line for any ^{14}N containing material, the errors introduced by this approximation cannot be tested at this time.

NQR Linewidth Analysis Test for ^{14}N

To get the Petersen data in the form necessary for testing the linewidth analysis method, the time constants must be inverted. The propagation of error in inversion, starting with an experimental value x with associated standard deviation σ_x is given by

$$y = \frac{1}{x}, \ \sigma_y = \frac{\sigma_x}{x^2} = \sigma_x y^2. \qquad [5\text{-}10]$$

The calculated values of the differences of the inverted time constants and the associated errors are given in tabular form in Appendix C. The data curves were expanded to 200 points, interpolated from the originals using cubic splines, and smoothed with a smoothing parameter of 0.25 using the Cleveland-Devlin [1988] algorithm for locally weighted regression. Figure 5-1 shows the final comparison of the ν_+ line and the ν_- line before constants are scaled into the values.

Within the known error bars, there is no difference between the ν_+ and ν_- lines for the differences of the inverted time constants, as tested. Thus, using the best available data, Eq. [4-5] and Eq. [4-6] give the same results as required by NQR linewidth analysis. This does not prove the validity of the method, only affirm that the data do not discredit it.

To provide a complete, thorough test of the NQR linewidth analysis method for ^{14}N NQR, the values of T_2 and T_2^* for all resonance lines, especially ν_d, of several groups of related compounds would be required. To acquire this data, high-T_c superconductors would be required to build SQUID NQR spectrometers that run at temperatures of 77 K or higher. At lower temperatures, the relaxation times increase exponentially.

EFG Widths for Sodium Nitrite

Using the experimental values for T_2 and T_2^* from Petersen and the assumption that the three transition lines will all have the same inhomogeneity characteristics, the

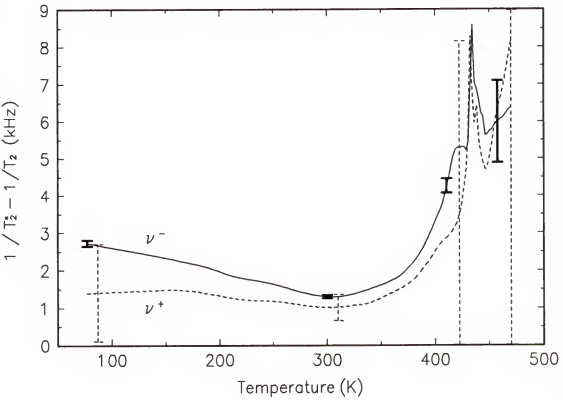

Figure 5-1 Difference of the inverted time constants for sodium nitrite. The broken lines represent the data for ν_+.

EFG width given as $\Delta[\chi]$ or $\Delta[eq]$ can be calculated. Since the experimental errors are smaller for the ν_- line, that data set will be used in the calculation of Eq. [2-81]. The result is shown in Fig. 5-2. The value[1] of the quadrupole moment for ^{14}N, used in the right-hand y axis in Fig. 5-2 is 1.6×10^{-26} cm^2. Values for $\Delta[\chi\eta]$ are not calculated as they would be proportional to $\Delta[\chi]$, a result of the assumption that all three resonance lines have equal inhomogeneity as defined as the difference of the inverted time constants.

Experimental Results

Pulse Optimization

Optimizing the pulse width for a given pulse height was more difficult than expected. Having previously run the NQR spectrometer at a "usable" setting without regard to maximizing the signal, the author was surprised to discover the large amount of drift and poor repeatability with the experimental setup, despite the known correlation of small changes in FID amplitude with changes in pulse width near the FID maximum response. Attempts to use two pulses with a variable separation to measure changes in the echo height were unsuccessful. The echo height appeared to decrease and then leveled off before disappearing completely. As the second pulse must be wider then the first, the NQR spectrometer continually drifted such that the errors voided any attempt to measure T_2.

---

[1] Bruker NMR NQR Periodic Table, Bruker Instruments, Inc., Manning Park, Billerica, MA 01812.

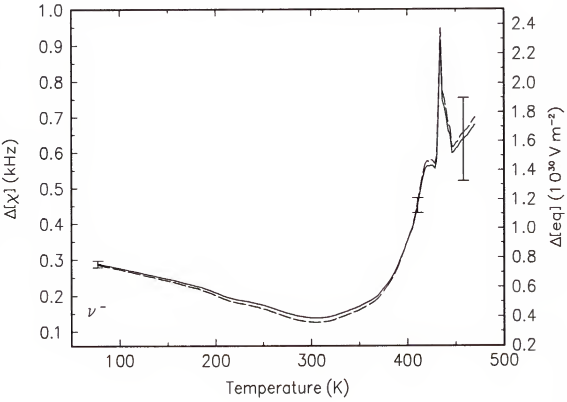

Figure 5-2 The widths of the NQCC (left y-axis, solid line) and the primary EFG component, V_{zz}, (right y-axis, broken line) for the ν_+ and ν_- lines of sodium nitrite.

NQR of Pure Urea Compounds

The bonding structure of urea is known to be a prime example of sp^2 hybridization. Under Townes and Dailey theory, the NQR parameters are related to the bonding parameters by Eqns. [2-55] and [2-56]. Following the work and notation of Negita et al. [1981] (probably after Oja [1973]), where only the differences between urea and urea-d_4 are important, we will assume that σ_{NC} is constant, since the N-C bond less likely to become polarized than the N-H bond due to the difference in electronegativity between C and H, and write [Negita et al., Eqn. 6]

$$\Delta\alpha = \Delta\pi - \frac{2}{3}\Delta\sigma_{NH} \qquad [5\text{-}11]$$

$$\Delta(\alpha\eta) = \Delta\sigma_{NH}\,. \qquad [5\text{-}12]$$

This analysis gives the following values when combined with the experimental results:

$$\chi_{2p}\Delta\pi = -34.27 \pm 0.13 \qquad [5\text{-}13]$$

$$\chi_{2p}\Delta\sigma_{NH} = 10.50 \pm 0.18\,. \qquad [5\text{-}14]$$

The exact value for χ_{2p} is not known but its range is known to be from 8 to 14 MHz [Marino 1968]. The exact value used is not very important considering the magnitude of the experimental errors, so we will use χ_{2p} = 10 MHz to yield the final results of

$$\Delta\pi = -0.004 \qquad \Delta\sigma_{NH} = 0.001\,. \qquad [5\text{-}15]$$

The experimental values for the nuclear quadrupole coupling constant and the asymmetry parameter of ^{14}N in urea-d_4 differ from urea by +1% and -2%, respectively. Townes and Dailey theory reveals that urea-d_4 has a 0.2% increase in the lone pair electronic density and an almost negligible decrease in the N-H σ bond density. These small differences between urea and urea-d_4 are believed to be due to the increase in mass upon deuteration. The differences between urea and urea-d_4 are similar to that between urea-NaCl-H_2O and urea-NaBr-H_2O and are greater than the differences between the two sites in thiourea or the change from ethylurea to methylurea.

To relate these results to other deuterated compounds, the work of Hunt and Mackay [1974] will be used as a reference. They found that derivatives of formamide, using *sp* hybrid orbitals, show on average a decrease of 0.004 electrons in the σ_{NH} orbitals for each 25 kHz increase in χ upon deuteration. Using *sp* or sp^2 bonding for urea gives similar results and suggests that for ^{14}N in symmetric molecules, less shifting of electrons is necessary for large changes in the nuclear quadrupole coupling constant. The shift of 41 kHz for urea-d_4 only resulted in a shift 0.001 electrons in the σ_{NH} orbitals as opposed to an expected 0.007 according to Hunt and Mackay. Even accounting for four N-H bonds instead of two, the electronic shift is smaller than predicted.

For comparison with other compounds with the same basic structure as urea, a plot of $\chi\eta$ versus χ is shown in Fig. 5-3. This choice of axes allows the graphical space to be uniform with the same units in both directions. Higher values of $\chi\eta$

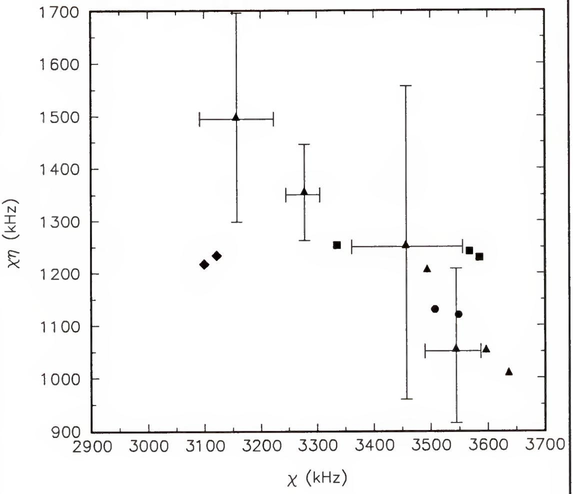

Moving from left to right, the diamonds (♦) are the two sites of thiourea [Smith and Cotts 1964, Jamil 1992], the triangles (▲) are urea nitrate, urea phosphate, urea oxalate [Murgich and Santana R. 1981], urea-hydrogen peroxide [Negita et al. 1977], urea-NH_4Cl [Murgich and Santana R. 1981], urea-rock salt, and urea-NaBr-H_2O [Negita et al. 1977], the squares (■) are hydroxyurea [Sauer and Bray 1973], ethylurea [Chen and Dodgen 1976] and methylurea [Dinesh and Rogers 1972], and the circles (●) represent urea and urea-d_4.

Figure 5-3 EFG-Space Diagram of urea and related compounds.

correspond to more polarization of the nitrogen bonds; higher values of χ correspond to more π bond character. The substitution of ^2H for ^1H in urea causes a change equivalent to the difference between urea-NaCl-H_2O and urea-NaBr-H_2O, but with less change in nitrogen bond polarization, and is greater than the differences between the two sites in thiourea or the change from ethylurea to methylurea.

The error bars for the positions of urea nitrate, urea phosphate, urea oxalate, and urea-NH_4Cl are given to remind the reader that the exact parings of the ν_+ and ν_- lines for these compounds is not known and that the position given on the graph is only the average position for these compounds. The possibilities are on opposing sides near the ends of the error bars for the first three compounds. There are six known lines for urea-NH_4Cl and thus three sets of pairs that would all fall within the limits of the error bars given.

Effect of Gamma Rays on Urea-Water

A decrease in T_2^* to a constant value [C.I. >95%] of 550 μs from 780 μs was measured. The spread in the data around the 550 μs central value is slightly larger than attributable to the measurement and analysis error attributed to each individual measurement. This suggests a source of change in the measured values other than the irradiation. Despite previous reports from this laboratory [Higgins 1990, Hintenlang and Higgins 1992, Hintenlang eta l. 1992], ^{60}Co irradiation of urea-water was not shown to cause a linear or exponential increase in the NQR linewidth even when the absorbed dose was extended from 300 to 900 Gy.

Review of Higgin's Original Data

Since verification of the previously reported work in this laboratory was not obtained, the laboratory records were searched for the original data sets taken on urea-water by Higgins [1990]. Five data runs from that work were identified. Details of this data are given in Appendix D. The comparison of the original analysis with the analysis obtained using the techniques cited in this work is shown in Fig. 5-4.

The use of nonlinear curve fitting gives drastically different results than just fitting the peaks of the FID to an exponential curve (or the logarithm of those values to a straight line) as was done by Higgins. The errors obtained after nonlinear curve fitting demonstrate that the errors originally reported for these points are underestimated. The reanalysis does not support the conclusion that ^{60}Co γ rays cause a measurable variable decrease in the T_2^* of urea-water. The original data that were published by Hintenlang and Higgins in 1992 were not available for review.[2] It is believed that the curve given by these authors was coincidental with the same underestimation of errors that plagued Higgins' original work.

[2] The data published by Hintenlang and Higgins in 1992 is believed to be different than the data given by Higgins in 1991 since Higgins reported a linear response and Hintenlang and Higgins reported an exponential response.

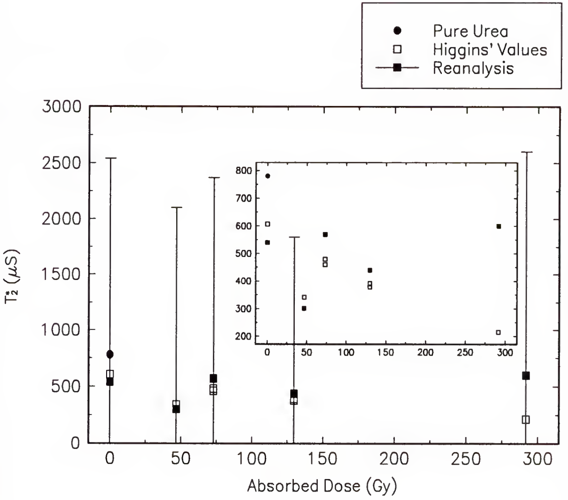

Figure 5-4 Reanalysis of Higgins' data on radiation effects on urea:water.

Effect of Water on Urea

Both Higgins [1990] and Hintenlang and Higgins [1992] reported that recrystallizing water into the urea crystalline structure did not cause a change in T_2^* when compared to dry, polycrystalline urea. In both previously reported cases, the datum for urea and the urea-water standard have T_2^* values around 800 μs. This result is not supported in this work. All standard samples (N=21) which were recrystallized with water added to pure urea had T_2^* values below 650 μs with one as low as 380 μs. As is shown in Fig. 4-17, the amount of water added as measured as a molar ratio, moles of water to moles of urea, always led to a decrease in T_2^*. The wide variations in the data in Fig. 4-17 are simply experimental scatter. Although there may appear to the eye to be a downward trend in the data given in Fig. 4-17, it is indistinguishable from a line with slope $m=0$ above a 95% confidence interval. The majority of data were taken around a molar ratio of 1.0 as this is the region which the previous researchers had used. The extreme value of 0.09 represents the lower limit of the amount of water that could be added. At and below this point, the water would boil away before the urea could dissolve in the water to be recrystallized. The upper limit of 1.3 represents the point where water would be left unincorporated after the urea recrystallized.

The process of adding water to polycrystalline urea results in the widening of the linewidth and therefore a shrinking of T_2^* down to the region of 550 μs. It is therefore the addition of water to the urea and the associated changes in the internal crystalline structure of the urea that is responsible for the "radiation effect" previously

measured. If chemical impurities, water in this case, are added to a crystal, the disruptions of the lattice lead to EFG changes that are propagated several crystalline units from the disruption site in spite of the r^{-3} dependance. These disruptions shift the distribution of EFGs, leading to line broadening and a lowering of the central amplitude of a peak.

Pulsed ^{14}N NQR of Urea-H_2O_2 and Urea-Rock Salt

Due to their similar crystalline structure, urea-H_2O_2 is a logical choice for comparison to urea-water. The structure of urea-H_2O_2 is known to have the hydrogen peroxide hydrogen bonded between the oxygen of one urea and the hydrogens of the next. The base urea structure of urea-H_2O_2 is almost exactly the same as pure urea [Lu et al. 1941, Fritchie and McMullan 1981]. Had the radiation effects on the NQR spectra of urea-water previously described been seen, the radiation effect on urea-H_2O_2 could have been key to understanding the effect on urea-water.

Pulsed NQR experiments require longer T_2 values than CW experiments with the worst case for pulsed NQR being a compound with short T_2 and long T_1. The original paper on urea-rock salt by Negita et al. (1977) utilized a CW apparatus. No time constants for urea-rock salt have ever been reported, but they are probably be too short to allow for detection by pulsed NQR methods.

CHAPTER 6
CONCLUSIONS

If radiation protection practice is to become biologically based instead of energy deposition based, then the radiation effects of radiations of different qualities must be measured directly on biological materials. One of the simplest organic compounds found in the human body with a strong ^{14}N NQR signal is urea. Urea is also known to form a variety of compounds and complexes, such as urea-hydrogen peroxide and urea-rock salt, giving a range of similar materials for study. To tie the results to radiation biology work, the presence of water, the universal solvent, is believed to be necessary. Ionizing photons are used as the radiation source for this radiation effects study.

The following specific objectives were considered.

1) Propose and test a method for quantifying changes in NQR signals. The proposed NQR linewidth analysis method uses the NQR relaxation times to calculate the natural widths of the EFG parameters exclusive of the effects of the spin dynamics. The use of this technique were successfully demonstrated using Petersen's ^{14}N NQR data of changes in the relaxation times of sodium nitrite as a function of temperature.

2) Demonstrate the validity of NQR measurements taken on the Ritec spectrometer system by detecting and quantifying one or more unreported resonances as well as resonances previously described in the literature.

The Ritec NQR spectrometer was calibrated for ^{14}N NQR using standard samples of HMT and urea. The previously unreported ν_- line of urea-d_4 was identified at 2381.46 kHz allowing the determination of χ and η for urea-d_4 for the first time.

3) Follow up the work of Higgins and Hintenlang by replicating their measurements of the ^{14}N NQR spin-spin relaxation times for urea-water and extending the range of ^{60}Co gamma ray absorbed doses above 300 Gy.

In the range of 0-900 Gy, there were no measurable changes observed in the relaxation times of urea-water that could be attributed to exposure to ionizing photons. The works of the previous researchers was not replicated and is not supported.

4) Compare and correlate changes in the NQR experimentally derived quantities of urea-water to gamma ray dose to quantify the broadening of the electric field gradient at the nitrogen sites.

It was determined that the inverse linewidth parameter of urea-water differs from dry, polycrystalline urea with values of 550 μs and 780 μs, respectively. These results were observed for urea-water with composition ranging from 0.1 to 1.3 molar ratio of water to urea.

5) Make recommendations for further study in this area.

Nuclear quadrupole resonance of ^{14}N nuclei is not currently useful as a radiation effects probe of organic solid solutions. No further experiments are recommended until such time as the theoretical basis for NQR has reached the point of providing adequate justification that the desired radiation effect will be observable.

In addition to the previous listing of objectives and conclusions, the following summarizes other important contributions of this work. An expression used to describe the spin dynamics in experimental NMR was applied to experimental NQR to yield quantitative information on the widths of the EFG parameters. For a Lorentzian lineshape the "NQR linewidth analysis" method yields the following relationships between the NQR EFG parameter widths and T_2 and T_2^*:[1]

$$\Delta[eq\eta] = \frac{2h}{\pi eQ}\left(\frac{1}{T_2^*} - \frac{1}{T_2}\right)_d \qquad [4\text{-}8]$$

and

$$\Delta[eq]_{max} \le \frac{h}{3\pi eQ}\left[2\left(\frac{1}{T_2^*} - \frac{1}{T_2}\right)_\pm - \left(\frac{1}{T_2^*} - \frac{1}{T_2}\right)_d\right]. \qquad [4\text{-}9]$$

As can be inferred from Eq. [4-9] there is an internal consistency requirement for

$$\left[\frac{1}{T_2^*} - \frac{1}{T_2}\right]_+ = \left[\frac{1}{T_2^*} - \frac{1}{T_2}\right]_- . \qquad [4\text{-}7]$$

By experimentally measuring the T_2 and T_2^* dynamic spin system time constants of NQR transitions, information on the widths of the EFG parameters can be determined. This method extends the traditional NQR method of estimating the total width of eq (or χ) from the width of the resonance lines.

---

[1] Note that all equations in this chapter are numbered as originally given to provide a reference back to the discussion where the equations were first used.

As a test of this new analysis method, a very complete data set, Petersen's data set on sodium nitrite, was chosen. Values for T_2 and T_2^* for the ν_+ and ν_- lines were determined by Petersen as a function of temperature from 77 K to over 400 K. Since experimental values for T_2 and T_2^* are unavailable for the ν_d line for any ^{14}N containing compound, several approximations the NQR linewidth analysis method were explored. The assumptions for each approximation were 1) that $T_2 >> T_2^*$ for all transitions so that $1/T_2$ can be neglected, 2) that T_2 is relatively constant for all transitions under all experimental conditions, and 3) that the following extension to Eq. [4-7] is true:

$$\left[\frac{1}{T_2^*}-\frac{1}{T_2}\right]_+ = \left[\frac{1}{T_2^*}-\frac{1}{T_2}\right]_- = \left[\frac{1}{T_2^*}-\frac{1}{T_2}\right]_d . \qquad [5\text{-}5]$$

Since the only assumption which eliminated the need for experimental values for ν_d is the last one, that simplification was adopted and applied to Petersen's sodium nitrite data. Under this assumption, Eq. [4-8] transforms into

$$\Delta[\chi\eta] = \frac{2}{\pi}\left(\frac{1}{T_2^*}-\frac{1}{T_2}\right) \qquad [5\text{-}7]$$

and Eq. [4-9] into

$$\Delta[\chi]_{max} \lessapprox \frac{1}{3\pi}\left(\frac{1}{T_2^*}-\frac{1}{T_2}\right). \qquad [5\text{-}9]$$

Note that this assumption leads to the result that the widths of the NQR EFG components are all proportional.

Petersen's sodium nitrite data provide support for Eq. [4-7] and the internal consistency requirement that ν_+ and ν_- yield the same results. The final results of applying the approximated NQR linewidth analysis method yields values for $\Delta[\chi]$ in the range of 100 Hz to 950 Hz. The lowest value for $\Delta[\chi]$ occurs just above 300 K and the highest occurs at an internal phase transition near 420 K.

Using standard samples of HMT and urea, the performance of the RITEC NQR spectrometer in the Department of Nuclear Engineering Sciences at the University of Florida was analyzed and the spectrometer was calibrated for ^{14}N NQR work. The proper pulse height and pulse width for urea and related compounds were experimentally determined for single pulse experiments to be $\sim$20 μs at $\sim$1400 V, but the equipment was determined to be too unstable when using wider pulses or pulse separation values or more than 1 ms to adequately determine T_2 values by use of multi-pulse sequences such as the 180°-τ-90° inversion-recovery method. As a test of the calibration for single pulse experiments, the previously unreported ν_- line for urea-d_4 was detected at 2381 $\pm$ 0.04 kHz and used to determine accurately the values for χ (=3548.74 $\pm$ 0.03 kHz) and η (=0.31571 $\pm$ 0.00007) for urea-d_4 along with the associated T_2^* values for ν_+ (=928 $\pm$ 23 μs) and ν_- (=721 $\pm$ 12 μs). In terms of Townes and Dailey theory, urea-d_4 has a 0.004 increase in the lone pair electronic density and a slight decrease in the N-H bond electronic density. The differences are smaller than were predicted by the correlations of Hunt and Mackay [1974]. To

further explore the differences between the various urea-based substances, an EFG graph [Fig. 5-3] was made and the locations of thirteen compounds were placed. It was determined that the substitution of ^2H for ^1H in urea causes a change equivalent to changing the Cl in urea-NaCl-H_2O to Br to form urea-NaBr-H_2O and is greater than the differences between the two sites in thiourea or the change from ethylurea to methylurea.

Urea recrystallized in the presence of water has a decrease in T_2^* that is found to be relatively constant regardless of exposure to ^{60}Co γ rays up to an absorbed dose of 900 Gy, twice the range in exposure reported previously. It is believed that the previously reported data were misinterpreted due to a low signal-to-noise ratio and a simplistic data analysis method prone to larger errors than were expected by the previous researchers. The conclusion of the radiation effects studies on urea-water by Higgins and Hintenlang and Higgins was not supported as their work could not be replicated.

Cobalt-60 irradiation of urea-water was not observed to lead to any change in the NQR linewidth for an absorbed dose in the range from 0 to 900 Gy. Since verification of the previously reported work in this laboratory was not obtained, the laboratory records were searched for the original data sets taken on urea-water by Higgins [1990]. The comparison of the original analysis with the analysis obtained using the techniques cited in this work shows that nonlinear curve fitting gives dramatically different results than just fitting the peaks of the FID to an exponential curve (or the logarithm of those values to a straight line) as was done by Higgins.

The errors obtained after nonlinear curve fitting demonstrate that the errors originally reported for these points were underestimated. Despite previous reports from this laboratory, ^{60}Co irradiation of urea-water was not shown to cause a linear or exponential increase in the NQR linewidth for an absorbed dose in the range from 0 to 900 Gy.

All standard samples of urea (N=21) which were recrystallized with water were measured with T_2^* values around 550 μs with all below 650 μs and one as low as 380 μs. As shown in Fig. 4-17, any amount of water added, measured as a molar ratio of moles of water to moles of urea, always led to a decrease in T_2^* as compared to dry, polycrystalline urea. Both Higgins [1990] and Hintenlang and Higgins [1992] reported that recrystallizing water into the urea crystalline structure did not cause a decrease in T_2^* when compared to dry, polycrystalline urea. In both previously reported cases, the datum for urea and the urea-water standard have T_2^* values around 800 μs. This result was not supported in this work.

The process of adding water to polycrystalline urea results in the widening of the linewidth and therefore a shrinking of T_2^* down to the region of 550 μs. It is therefore the addition of water to the urea and the associated changes in the internal crystalline structure of the urea that is responsible for the "radiation effect" previously measured.

The primary conclusion of this work is that ^{14}N NQR is still Not Quite Ready for high precision work in radiation effects as a probe of solid solutions. The experimental apparatus was state-of-the-art at the time it was purchased. It is not

capable of taking high enough accuracy data for radiation effects study attempted here. While multipulse experiments are becoming common in NMR, the NQR community is behind in both experimental and theoretical developments. This is probably due to the large amount of research funding available for medical imaging. Also, the high sensitivity of NQR experiments to the preparation and handling of the samples prevents highly accurate comparisons between samples. The continuing work into the fundamental theory of NQR pulses and radiofrequency interactions with matter by such researchers as Sanctuary and Krishnan may modify this conclusion in the future.

For NQR to be used as an effective radiation effects tools for exploring the effects of photons, the following items would need to be developed or found: more precise equipment for the measurement of NQR parameters with pulse width stability of $<3\%$ and pulse separation stability of $<3\%$ for separations of tens of thousands of pulse widths, multiple pulse sequences which isolate particular attributes of the system, a better understanding of the fundamental interactions of pulses and the spin system in organic systems, and an organic material which demonstrates changes in its bonding configuration after exposure to small amounts of photonic ionizing radiation. The best type of system would be a binary, well mixed mixture which reacted upon exposure. The two largest limitations on NQR for radiation effects studies are the long T_1 and T_2 time constants for most biologically active organics and NQR's sensitivity to small changes in pressure and temperature.

APPENDIX A
FORTRAN PROGRAMS

The following computer programs were written in FORTRAN to aid in manipulating and analyzing the NQR data. Each was compiled on a Zenith personal computer with Intel®[1] 386i™/387i™ processors with Microsoft®[2] FORTRAN version 5.1.

CONVERT

This program takes the PRN datafile that was imported from the Nicolet and converts it into an OUT file of time versus voltage. An example of the PRN and OUT files are in Appendix B. The required inputs are the input PRN filename, the output OUT filename, the size of the data spectrum, the number of initial points to be deleted, and the increment at which to discard the data points.

```
C*************************************************************************
C                                                                        *
C  PROGRAM TAKES THE OUTPUT .prn FILE FROM THE NICOLET AND CONVERTS      *
C  THE NICOLET FORMAT TO A USER-NAMED DATAFILE OF TIME VERSUS VOLTAGE    *
C                                                                        *
C  WRITTEN BY Louis H Iselin                                             *
C  VERSION 3.20  OF  13 JAN 91                                           *
C                                                                        *
C*************************************************************************
C
C  THE FOLLOWING IS THE DESCRIPTION OF THE VARIABLES USED:
C
```

[1] Intel Corporation, 2200 Mission College Blvd., Santa Clara, CA 95052-8119.

[2] Microsoft Corporation, Redmond, WA 98052-6399.

```
C  NIC         =  THE NICOLET INPUT FILE NAME
C  OUT         =  THE OUTPUT FILE NAME
C  ERRMSG  =  THE STANDARD ERROR MESSAGE
C  IC1         =  THE ERROR NUMBER FOR ERRORS READING INPUT FILE - NIC
C  IC2         =  THE ERROR NUMBER FOR ERRORS READING OUTPUT FILE - OUT
C  SIZE    =  THE INTEGER WHICH DETERMINES THE INPUT FILE
C            SIZE, (1)FULL-(2)HALF-(4)QUARTER
C  C     =  THE NUMBER OF COLUMNS OF DATA POINTS
C  D     =  THE NUMBER OF COLUMNS OF DATA POINTS IN USE
C  R     =  THE NUMBER OF ROWS OF DATA
C  S     =  THE NUMBER OF ROWS OF DATA IN USE
C  DELPTS  =  THE NUMBER OF INITIAL DATA POINTS TO DELETE FROM
C            THE OUTPUT FILE - OUT
C  X(D,S)  =  THE VOLTAGE DATA POINTS FROM THE INPUT FILE
C  SKIP    =  THE NUMBER OF DATA POINTS TO SKIP AFTER EACH RETAINED
C              POINT
C  DELTA   =  THE TIME BETWEEN EACH DATA POINT
C  START   =  THE TIME THE FIRST DATA POINT WAS TAKEN WITH RESPECT TO
C               THE TRIGGER OF THE NICOLET
C  MAX     =  THE MAXIMUM NUMBER OF DATA POINTS
C  IS      =  THE INITIAL COLUMN OF DATA
C  JS,JC   =  THE INITIAL ROW OF DATA
C              JS = STATIC, JC = CHANGES
C
C  VARIABLE DECLARATIONS AND INITIATIONS
C
      CHARACTER NIC*36, OUT*36, ERRMSG*41
      INTEGER   IC1, IC2, C, R, S, MAX, NUM
      INTEGER   DELPTS, SKIP, IS, JS, JC, SIZE
      REAL      DELTA, START
      DIMENSION X(8,2048)
      DATA ERRMSG /'** INVALID RESPONSE - PLEASE TRY AGAIN **'/
      DATA IC1 /0/, IC2 /0/, C /8/, R /1536/, S /2048/
      DATA MAX /15872/, NUM /0/
C     DATA X /16384*-99999./
C
C   MAIN PROGRAM STARTS
C
C   ASK FOR AND OPEN THE NICOLET INPUT "PRN" DATA FILE
C
      PRINT*,'**********************************'
      PRINT*,'*          C O N V E R T         *'
      PRINT*,'*   WRITTEN BY Louis H Iselin    *'
      PRINT*,'*  VERSION 3.10  OF  22 DEC 90   *'
      PRINT*,'**********************************'
      PRINT*,' '
      PRINT*,' Welcome to the CONVERT program to CONVERT'
      PRINT*,'    the Nicolet prn datafile to a datafile'
      PRINT*,'       of time vs. voltage'
      PRINT*,' '
 10   PRINT*,' What is the Nicolet INPUT file name?'
      PRINT*,'          (include path if necessary)'
      PRINT*,' '
      READ(*,'(A)') NIC
      OPEN (UNIT=1, FILE=NIC, STATUS='OLD', IOSTAT=IC1)
      IF (IC1.NE.0) THEN
       PRINT*, ERRMSG
       PRINT*,' Error ',IC1,' has occurred.'
       GOTO 10
      ENDIF
      PRINT*,' '
C
```

```
C   ASK THE SIZE OF THE NICOLET DATA FILE USED AS INPUT
C
      PRINT*,' Please give the size of the data spectrum.'
      PRINT*,'MAX POINTS - 15872       7936          3968'
      PRINT*,'               (1)Full     (2)Half     (4)Quarter'
      PRINT*,' '
      READ(*,*) SIZE
C
C   QUARTER SIZED INPUT FILE PARAMETERS
C
      IF (SIZE.GT.2) THEN
       C=2
       R=1920
       MAX=3968
C
C   HALF SIZED INPUT FILE  PARAMETERS
C
       ELSEIF (SIZE.EQ.2) THEN
            C=4
            R=1792
            MAX=7936
      ENDIF
C
C   ASK FOR AND OPEN THE OUTPUT FILE
C
      PRINT*,' '
 20   PRINT*,' What is the desired OUTPUT datafile name?'
      PRINT*,'             (include path if necessary)'
      PRINT*,' '
      READ(*,'(A)') OUT
      OPEN (UNIT=2, FILE=OUT, STATUS='NEW', IOSTAT=IC2)
      IF (IC2.NE.0) THEN
       PRINT*, ERRMSG
       PRINT*,' Error ',IC2,' has occurred.'
       GOTO 20
      ENDIF
      PRINT*,' '
C
C   ASK FOR THE NUBER OF INITIAL DATA POINTS TO STRIP FROM THE SPECTRUM
C
 30   PRINT*,' How many initial points do you wish to delete?'
      READ(*,*) DELPTS
      IF ((DELPTS.LT.0).OR.(DELPTS.GE.MAX)) THEN
       PRINT*, ERRMSG
       GOTO 30
      ENDIF
C
C   CALCULATE INITIAL COLUMN AND ROW PARAMETERS
C
      IF (DELPTS.GT.2047) THEN
       IS = (DELPTS / 2048) + 1
       JS = MOD (DELPTS , 2048) + 1
      ELSE
       IS = 1
       JS = DELPTS + 1
      ENDIF
      JC = JS
C
C   ASK FOR THE NUMBER OF DATA POINTS TO SKIP AFTER EACH RETAINED POINT
C
 40   PRINT*,' PLEASE GIVE THE DESIRED SAMPLING INTERVAL.'
      PRINT*,' How many data points should be skipped'
```

```
      PRINT*,'    after each retained data point?'
      PRINT*,' '
      READ(*,*) SKIP
      IF ((SKIP.LT.0).OR.(SKIP.GE.MAX)) THEN
       PRINT*, ERRMSG
       GOTO 40
      ENDIF
C
C   READ INPUT FILE
C
C   READ FIRST 2 LINES
C
      DO 50, J=1,2
       IF (C.EQ.8) READ (1,601) (X(I,J), I=1,C)
       IF (C.EQ.4) READ (1,602) (X(I,J), I=1,C)
       IF (C.EQ.2) READ (1,604) (X(I,J), I=1,C)
 50   CONTINUE
 601  FORMAT (14X, 8(1X,G8.6))
 602  FORMAT (14X, 4(1X,G8.6))
 604  FORMAT (14X, 2(1X,G8.6))
C
C   READ NEXT 2 LINES, INCLUDING START AND DELTA
C
      READ   (1,*) START, (X(I,3), I=1,C)
      READ   (1,*) DELTA, (X(I,4), I=1,C)
C
C   READ NEXT 3 DATA LINES
C
      DO 51, J=5,7
       IF (C.EQ.8) READ (1,601) (X(I,J), I=1,C)
       IF (C.EQ.4) READ (1,602) (X(I,J), I=1,C)
       IF (C.EQ.2) READ (1,604) (X(I,J), I=1,C)
 51   CONTINUE
C
C   READ THE REMAINING DATA LINES WITH FULL COLUMNS OF DATA
C
      DO 52, J=8,R
       IF (C.EQ.8) READ (1,611) (X(I,J), I=1,C)
       IF (C.EQ.4) READ (1,612) (X(I,J), I=1,C)
       IF (C.EQ.2) READ (1,614) (X(I,J), I=1,C)
 52   CONTINUE
 611   FORMAT (2X, 8(1X, G8.6))
 612   FORMAT (2X, 4(1X, G8.6))
 614   FORMAT (2X, 2(1X, G8.6))
C
C   READ THE REMAINING DATA LINES
C
      DO 53, J=R+1,2048
       IF(C.EQ.8) READ   (1,621) (X(I,J), I=1,C-1)
       IF(C.EQ.4) READ   (1,622) (X(I,J), I=1,C-1)
       IF(C.EQ.2) READ   (1,624) (X(I,J), I=1,C-1)
 621  FORMAT (2X, 7(1X, G8.6))
 622  FORMAT (2X, 3(1X, G8.6))
 624  FORMAT (2X, 1(1X, G8.6))
 53   CONTINUE
      CLOSE  (UNIT=1, STATUS='KEEP')
C
C   WRITE OUTPUT INFORMATION
C
C   WRITE INPUT NICOLET FILE NAME
C
      WRITE(2,*) NIC
```

```
C
C   COUNT THE NUMBER OF OUTPUT DATA POINTS
C
      DO 91, I = IS, C
       IF (I.EQ.C) S = R
       DO 90, J = JC, S, SKIP + 1
          NUM = NUM + 1
 90    CONTINUE
       JC = J - 2048
 91   CONTINUE
C
C   WRITE THE TIME INCREMENT AND NUMBER OF DATA POINTS
C   TO THE OUTPUT FILE
C
      WRITE(2,*) DELTA*(SKIP+1.)
      WRITE(2,*) NUM
C
C   WRITE THE TIME AND VOLTAGE
C
      S = 2048
      JC = JS
      DO 81, I = IS, C
      IF (I.EQ.C) S = R
       DO 80, J = JC, S, SKIP + 1
          WRITE (2,70) ((I-1-START)*2048+J)*DELTA, X(I,J)
 80    CONTINUE
       JC = J - 2048
 81   CONTINUE
 70   FORMAT (2X, F12.9, 2X, F10.6)
C
C   CLOSE THE OUTPUT FILE AND END PROGRAM
C
      CLOSE (UNIT=2, STATUS='KEEP')
      PRINT*,' PROGRAM FINISHED'
      PRINT*,' DATAFILE ',OUT,'IS READY FOR USE.'
      PRINT*,' '
      END
```

PSD FFT

This program reads in OUT files created by CONVERT and outputs the PSD FFT of the data after padding the data with zeroes out to a specified power of 2. The maximum number of data points allowed is 131072. Since this program compiles to an executable file larger than 640KB, it was compiled with Microsoft® FORTRAN 5.1 to run inside Microsoft® Windows™ 3.0 using the following command:

FL /MW0 /Gt FFT.FOR /link /SE:4096

It has also been ported to the Department of Nuclear Engineering Sciences DEC™ 3000 Model 400 AlphaStation™ running OpenVMS™.

The following subroutines from Price must be supplied or their functional equivalent: REALFT and FOUR1. The required inputs to the program are the input OUT filename, the output FFT filename, and the total number of points desired to be used in the FFT.

```
*****************************************************************
*  THIS PROGRAM IS FFT.FOR FROM FT77.FOR FROM PSD.FOR          *
*  DEVELOPED BY KHALID JAMIL AND MODIFIED BY LOUIS H ISELIN *
*  UPDATED DEC.29,1990 AND MODIFIED 9 APR 91                   *
*  THIS VERSION FOR MS WINDOWS 3.0 AND MS FORTRAN 5.1          *
*      17 NOV 91
*  SUBROUTINES TAKEN FROM NUMERICAL RECIPES                    *
*****************************************************************
C
C  THE FOLLOWING IS THE DESCRIPTION OF THE VARIABLES USED:
C
C  VARIABLE DECLARATIONS AND INITIATIONS
C
      CHARACTER INFILE*40, OUTFILE*40, TITLE*30
      REAL D1, DELTA
      REAL*8 PI
      INTEGER M, NUMPTS, ISIGN
      DIMENSION D1(131072)
      DATA PI /3.14159265358979D0/
C
C  MAIN PROGRAM STARTS
C
C  ASK FOR AND OPEN THE INPUT DATA FILE
C
      PRINT*,' *****************************************************'
      PRINT*,' *                  F F T. F O R                      *'
      PRINT*,' *              DEVELOPED BY KHALID JAMIL             *'
      PRINT*,' *              MODIFIED BY LOUIS H ISELIN            *'
      PRINT*,' *     UPDATED DEC.29,1990 / MODIFIED 9 APR 91        *'
      PRINT*,' *                  17 NOV 91                         *'
      PRINT*,' *****************************************************'
 10   PRINT*,' ENTER NAME OF YOUR INPUT FILE (UP TO 40 CHARACTERS)'
      READ(*,'(A)') INFILE
      OPEN(1, FILE=INFILE, STATUS='OLD', IOSTAT=IC1)
      IF (IC1.NE.0) THEN
         PRINT*,' Error ',IC1,' has occurred.'
         GOTO 10
      ENDIF
      PRINT*,' '
C
C  ASK FOR AND OPEN THE OUTPUT FILE
C
 11   PRINT*,' ENTER NAME FOR OUTPUT FILE (UP TO 40 CHARACTERS)'
      READ(*,'(A)') OUTFILE
      OPEN(2, FILE=OUTFILE, STATUS='NEW', IOSTAT=IC2)
```

```
      IF (IC2.NE.0) THEN
         PRINT*,' Error ',IC2,' has occurred.'
         GOTO 11
      ENDIF
      PRINT*,' '
C
C  GIVE NUMBER OF DATA POINTS
C
      PRINT*,' ENTER NUMBER OF DATA POINTS, MUST BE POWER OF 2'
      PRINT*,' SUGGESTED VALES ARE POWERS OF 2:'
      PRINT*,'  8192, 16384, 32768, 65536, 131072-MAX'
      PRINT*,' '
      READ(*,*)M
      PRINT*,' '
C
C  PROGRAM TAKES OVER
C
      PRINT*,' READING INPUT  DATA'
      READ(1,'(A)') TITLE
      READ(1,*) DELTA
      READ(1,*) NUMPTS
      K = 1
 12   READ(1,*,END=13) DUM, D1(K)
      K = K + 1
      GOTO 12
 13   PRINT*,' FAST FINITE FOURIER TRANSFORM STARTS'
      N=M/2
      ISIGN=1
      CALL REALFT(D1,N,ISIGN)
      PRINT*,' FFT COMPLETED'
      PRINT*,' WRITING POWER SPECTRUM DENSITY'
      B=0.0
      DO 20 J=1,M,2
         B=B+1.0
         A=D1(J)**2+D1(J+1)**2
      if(b-1..lt.2.e5*m*delta)WRITE(2,*)(B-1.0)/(M*DELTA),A
20    CONTINUE
      END
C
C
C
      SUBROUTINE REALFT(DATA,N,ISIGN)
      SUBROUTINE FOUR1(DATA,NN,ISIGN)
```

PXLTA & CXLTA

These two programs are related to CONVERT in that the base code for CONVERT was simply modified to produce modified output ASC files. These ASC files are ASCII code in the block format to be read by ASBIN to be converted to the binary input required for HSVD. PXLTA translates a PRN file to ASC and CXLTA takes an OUT file, from CONVERT or test data in the OUT format, and translates it

to ASC fromat. Although the code says it is for use on PC class personal computers, the same code was used on an IBM®[3] RISC System/6000™ computer running AIX® and a DECstation™[4] 5000 model 200 running ULTRIX™. The required inputs for PXLTA parallel those required for CONVERT; the only requirements for CXLTA are the input and output filenames.

```
C************************************************************************
C  PROGRAM TAKES THE OUTPUT .prn FILE FROM THE NICOLET, CONVERTS THE    *
C  NICOLET FORMAT TO A THE INPUT FORMAT REQUIRED FOR                    *
C  HSVD [(C) TU-DELFT] AS MODIFIED FOR USE ON PC'S UNDER                *
C  MICROSOFT FORTRAN 5.1 INSIDE THE MICROSOFT WINDOWS 3.0 PLATFORM      *
C                                                                       *
C  WRITTEN BY Louis H Iselin                                            *
C  VERSION 1.10 OF 12 OCT 91                                            *
C                                                                       *
C  BASED ON THE ESTABLISHED PROGRAM NAMED 'CONVERT' VERSION 3.20        *
C  DOCUMENTED BELOW                                                     *
C                                                                       *
C  PROGRAM TAKES THE OUTPUT .prn FILE FROM THE NICOLET AND CONVERTS     *
C  THE NICOLET FORMAT TO A USER-NAMED DATAFILE OF TIME VERSUS VOLTAGE   *
C                                                                       *
C  WRITTEN BY Louis H Iselin                                            *
C  VERSION 3.20  OF  13 JAN 91                                          *
C                                                                       *
C************************************************************************
C
C  THE FOLLOWING IS THE DESCRIPTION OF THE VARIABLES USED:
C
C  NIC     =  THE NICOLET INPUT FILE NAME
C  HSVDOUT =  THE OUTPUT FILE NAME FOR HSVD INPUT
C  ERRMSG  =  THE STANDARD ERROR MESSAGE
C  IC1     =  THE ERROR NUMBER FOR ERRORS READING INPUT FILE - NIC
C  IC3     =  THE ERROR NUMBER FOR ERRORS READING OUTPUT FILE - HSVDOUT
C  SIZE    =  THE INTEGER WHICH DETERMINES THE INPUT FILE
C                SIZE, (1)FULL-(2)HALF-(4)QUARTER
C  C       =  THE NUMBER OF COLUMNS OF DATA POINTS
C  D       =  THE NUMBER OF COLUMNS OF DATA POINTS IN USE
C  R       =  THE NUMBER OF ROWS OF DATA
C  S       =  THE NUMBER OF ROWS OF DATA IN USE
C  DELPTS  =  THE NUMBER OF INITIAL DATA POINTS TO DELETE FROM
C               THE OUTPUT FILE - OUT
C  X(D,S)  =  THE VOLTAGE DATA POINTS FROM THE INPUT FILE
C  SKIP    =  THE NUMBER OF DATA POINTS TO SKIP AFTER EACH RETAINED
POINT
C  DELTA   =  THE TIME BETWEEN EACH DATA POINT
C  START   =  THE TIME THE FIRST DATA POINT WAS TAKEN WITH RESPECT TO
C               THE TRIGGER OF THE NICOLET
```

[3] Internatinal Business Machines Corporation, White Plains, NY 10604.

[4] Digital Electronics Corporation, Maynard, MA 01754-1418.

```
C  MAX      =  THE MAXIMUM NUMBER OF DATA POINTS
C  IS       =  THE INITIAL COLUMN OF DATA
C  JS,JC    =  THE INITIAL ROW OF DATA
C                 JS = STATIC, JC = CHANGES
C  DELTAT   =  TIME BETWEEN DATA POINTS IN THE OUTPUT FILES
C  START    =  THE START TIME IN THE OUTPUT FILES
C  IVAR     =  THE ACTUAL NUMBER OF VARIABLES IN THE FILE HSVDOUT
C  JVAR     =  REMAINER OF IVAR/4
C
C  VARIABLE DECLARATIONS AND INITIATIONS
C
      PROGRAM PXLTA
C
      CHARACTER  NIC*36, HSVDOUT*36, ERRMSG*41
      INTEGER    IC1, IC3, C, R, S, MAX, NUM, IVAR, JVAR
      INTEGER    DELPTS, SKIP, IS, JS, JC, SIZE
      REAL       DELTA, START, X, V
      DIMENSION  X(8,2048), V(8192)
      DATA ERRMSG /'** INVALID RESPONSE - PLEASE TRY AGAIN **'/
      DATA IC1 /0/, IC2 /0/, C /8/, R /1536/, S /2048/
      DATA MAX /15872/, NUM /0/
C     DATA X /16384*-99999./
C
C   MAIN PROGRAM STARTS
C
C   ASK FOR AND OPEN THE NICOLET INPUT "PRN" DATA FILE
C
      PRINT*,'***********************************'
      PRINT*,'*      P   X   L   T   A          *'
      PRINT*,'*    WRITTEN BY Louis H Iselin    *'
      PRINT*,'*  VERSION 1.10  OF  12 OCT 91    *'
      PRINT*,'***********************************'
      PRINT*,' '
      PRINT*,' Welcome to the PXLTA program to XtransLaTe'
      PRINT*,'    the Nicolet prn datafile to datafiles'
      PRINT*,'       usable as input files for HSVD'
      PRINT*,' '
 10   PRINT*,' What is the Nicolet INPUT file name?'
      PRINT*,'             (include path if necessary)'
      PRINT*,' '
      READ(*,'(A)') NIC
      OPEN (UNIT=1, FILE=NIC, STATUS='OLD', IOSTAT=IC1)
      IF (IC1.NE.0) THEN
       PRINT*, ERRMSG
       PRINT*,' Error ',IC1,' has occurred.'
       GOTO 10
      ENDIF
      PRINT*,' '
C
C   ASK THE SIZE OF THE NICOLET DATA FILE USED AS INPUT
C
      PRINT*,' Please give the size of the data spectrum.'
      PRINT*,'MAX POINTS - 15872        7936          3968'
      PRINT*,'             (1)Full     (2)Half      (4)Quarter'
      PRINT*,' '
      READ(*,*) SIZE
C
C   QUARTER SIZED INPUT FILE PARAMETERS
C
      IF (SIZE.GT.2) THEN
       C=2
       R=1920
```

```
      MAX=3968
C
C   HALF SIZED INPUT FILE  PARAMETERS
C
      ELSEIF (SIZE.EQ.2) THEN
           C=4
           R=1792
           MAX=7936
      ENDIF
      PRINT*,' '
C
C   ASK FOR AND OPEN THE HSVD OUTPUT FILE NAME
C
      PRINT*,' '
 25   PRINT*,' What is the desired OUTPUT datafile name for HSVD?'
      PRINT*,'           (include path if necessary)'
      PRINT*,' '
      READ(*,'(A)') HSVDOUT
      OPEN (UNIT=3, FILE=HSVDOUT, STATUS='NEW', IOSTAT=IC3)
      IF (IC2.NE.0) THEN
         PRINT*, ERRMSG
         PRINT*,' Error ',IC3,' has occurred.'
         GOTO 25
      ENDIF
      PRINT*,' '
C
C   ASK FOR THE NUMBER OF INITIAL DATA POINTS TO STRIP FROM THE SPECTRUM
C
 30   PRINT*,' How many initial points do you wish to delete?'
      READ(*,*) DELPTS
      IF ((DELPTS.LT.0).OR.(DELPTS.GE.MAX)) THEN
       PRINT*, ERRMSG
       GOTO 30
      ENDIF
C
C   CALCULATE INITIAL COLUMN AND ROW PARAMETERS
C
      IF (DELPTS.GT.2047) THEN
       IS = (DELPTS / 2048) + 1
       JS = MOD (DELPTS , 2048) + 1
      ELSE
       IS = 1
       JS = DELPTS + 1
      ENDIF
      JC = JS
C
C   ASK FOR THE NUMBER OF DATA POINTS TO SKIP AFTER EACH RETAINED POINT
C
 40   PRINT*,' PLEASE GIVE THE DESIRED SAMPLING INTERVAL.'
      PRINT*,' How many data points should be skipped'
      PRINT*,'    after each retained data point?'
      PRINT*,' '
      READ(*,*) SKIP
      IF ((SKIP.LT.0).OR.(SKIP.GE.MAX)) THEN
       PRINT*, ERRMSG
       GOTO 40
      ENDIF
C
C   READ INPUT FILE
C
C   READ FIRST 2 LINES
C
```

```
      DO 50, J=1,2
       IF (C.EQ.8) READ (1,601) (X(I,J), I=1,C)
       IF (C.EQ.4) READ (1,602) (X(I,J), I=1,C)
       IF (C.EQ.2) READ (1,604) (X(I,J), I=1,C)
 50   CONTINUE
 601  FORMAT (14X, 8(1X,G8.6))
 602  FORMAT (14X, 4(1X,G8.6))
 604  FORMAT (14X, 2(1X,G8.6))
C
C   READ NEXT 2 LINES, INCLUDING START AND DELTA
C
      READ   (1,*) START, (X(I,3), I=1,C)
      READ   (1,*) DELTA, (X(I,4), I=1,C)
C
C   READ NEXT 3 DATA LINES
C
      DO 51, J=5,7
       IF (C.EQ.8) READ (1,601) (X(I,J), I=1,C)
       IF (C.EQ.4) READ (1,602) (X(I,J), I=1,C)
       IF (C.EQ.2) READ (1,604) (X(I,J), I=1,C)
 51   CONTINUE
C
C   READ THE REMAINING DATA LINES WITH FULL COLUMNS OF DATA
C
      DO 52, J=8,R
       IF (C.EQ.8) READ (1,611) (X(I,J), I=1,C)
       IF (C.EQ.4) READ (1,612) (X(I,J), I=1,C)
       IF (C.EQ.2) READ (1,614) (X(I,J), I=1,C)
 52   CONTINUE
 611   FORMAT (2X, 8(1X, G8.6))
 612   FORMAT (2X, 4(1X, G8.6))
 614   FORMAT (2X, 2(1X, G8.6))
C
C   READ THE REMAINING DATA LINES
C
      DO 53, J=R+1,2048
       IF(C.EQ.8) READ   (1,621) (X(I,J), I=1,C-1)
       IF(C.EQ.4) READ   (1,622) (X(I,J), I=1,C-1)
       IF(C.EQ.2) READ   (1,624) (X(I,J), I=1,C-1)
 621  FORMAT (2X, 7(1X, G8.6))
 622  FORMAT (2X, 3(1X, G8.6))
 624  FORMAT (2X, 1(1X, G8.6))
 53   CONTINUE
      CLOSE  (UNIT=1, STATUS='KEEP')
C
C   COUNT THE NUMBER OF OUTPUT DATA POINTS
C
      DO 91, I = IS, C
       IF (I.EQ.C) S = R
       DO 90, J = JC, S, SKIP + 1
          NUM = NUM + 1
 90    CONTINUE
       JC = J - 2048
 91   CONTINUE
C
C   WRITE THE TIME AND VOLTAGE
C
      IV = 1
      S = 2048
      JC = JS
      DO 81, I = IS, C
      IF (I.EQ.C) S = R
```

```
      DO 80, J = JC, S, SKIP + 1
         IF (IV . LE . 8192 ) THEN
            V(IV) = X(I,J)
            IV = IV + 1
         ENDIF
 80   CONTINUE
      JC = J - 2048
 81   CONTINUE
C
C   CREATE THE HSVDOUT OUTPUT FILE
C
      IVAR = MIN ( NUM , 8192 )
      WRITE(3,100) REAL(IVAR), DELTA*(SKIP+1.)*1000.,
     +        REAL((IS-1-START)*2048+JS)*1000.*DELTA, 0.0
 100  FORMAT(4E15.5)
      DO 110, I = 1, 15
 110     WRITE(3,100) 0.0, 0.0, 0.0, 0.0
      DO 130, I = 4, IVAR, 4
 130  WRITE(3,135) V(I-3), V(I-2), V(I-1), V(I)
 135  FORMAT(4E18.10)
      JVAR = MOD(IVAR,4)
      IF (JVAR.NE.0) THEN
         WRITE(3,135) (V(J), J = IVAR-JVAR+1, IVAR)
      ENDIF
C
C
C
      PRINT*,' '
      PRINT*,' PXLTA -- FINISHED -- PXLTA'
      PRINT*,' '
      PRINT*,' THE DESIRED DATAFILE IS READY FOR USE.'
      PRINT*,'    ',HSVDOUT
      PRINT*,' '
      END

C**********************************************************************
C  PROGRAM TAKES AN OUTPUT FILE OF TIME VERSUS VOLTAGE IN THE 'CONVERT'*
C  FROMAT AND TRANSLATES IT TO THE FILE FORMAT AS INPUT               *
C  FOR HSVD [(C) TU-DELFT] AS MODIFIED FOR USE AT UFlorida            *
C                                                                     *
C  WRITTEN BY Louis H Iselin                                          *
C  VERSION 1.10 OF 13 OCT 91                                          *
C                                                                     *
C**********************************************************************
C
C  THE FOLLOWING IS THE DESCRIPTION OF THE VARIABLES USED:
C
C  FFTIN   =  THE INPUT FILE NAME
C  HSVDOUT =  THE OUTPUT FILE NAME FOR HSVD INPUT
C  ERRMSG  =  THE STANDARD ERROR MESSAGE
C  DUMMY   =  DUMMY CHARACTER*36 VARIABLE
C  IC1     =  THE ERROR NUMBER FOR ERRORS READING INPUT FILE  - FFTIN
C  IC3     =  THE ERROR NUMBER FOR ERRORS READING OUTPUT FILE - HSVDOUT
C  MAX     =  THE MAXIMUM NUMBER OF DATA POINTS
C  DELTAT  =  TIME BETWEEN DATA POINTS IN THE OUTPUT FILES
C  START   =  THE START TIME IN THE OUTPUT FILES
C  DUM     =  DUMMY REAL*4 VARIABLE
C
C  VARIABLE DECLARATIONS AND INITIATIONS
C
      PROGRAM CXLTA
```

```
C
      CHARACTER  FFTIN*36, HSVDOUT*36, ERRMSG*41, DUMMY*36
      INTEGER    IC1, IC3, MAX, NUM
      REAL       DELTAT, START, V, DUM
      DIMENSION  V(8192)
      DATA ERRMSG /'** INVALID RESPONSE - PLEASE TRY AGAIN **'/
      DATA IC1 /0/, IC3 /0/
      DATA MAX /8192/, V /8192*0./
C
C   MAIN PROGRAM STARTS
C
C   ASK FOR AND OPEN THE INPUT "OUT" DATA FILE
C
      PRINT*,'***********************************'
      PRINT*,'*        C   X   L   T   A        *'
      PRINT*,'*    WRITTEN BY Louis H Iselin    *'
      PRINT*,'*   VERSION 1.10  OF  13 OCT 91   *'
      PRINT*,'***********************************'
      PRINT*,' '
      PRINT*,' Welcome to the CXLTA program to TRANSLATE'
      PRINT*,'    a time vs voltage datafile to a datafile'
      PRINT*,'       usable as an input file for HSVD'
      PRINT*,' '
 10   PRINT*,' What is the Nicolet INPUT file name?'
      PRINT*,'            (include path if necessary)'
      PRINT*,' '
      READ(*,'(A)') FFTIN
      OPEN (UNIT=1, FILE=FFTIN, STATUS='OLD', IOSTAT=IC1)
      IF (IC1.NE.0) THEN
          PRINT*, ERRMSG
          PRINT*,' Error ',IC1,' has occurred.'
          GOTO 10
      ENDIF
      PRINT*,' '
C
C   ASK FOR AND OPEN THE HSVD OUTPUT FILE
C
      PRINT*,' '
 20   PRINT*,' What is the desired ASC datafile name for HSVD?'
      PRINT*,'            (include path if necessary)'
      PRINT*,' '
      READ(*,'(A)') HSVDOUT
      OPEN (UNIT=2, FILE=HSVDOUT, STATUS='NEW', IOSTAT=IC3)
      IF (IC3.NE.0) THEN
          PRINT*, ERRMSG
          PRINT*,' Error ',IC3,' has occurred.'
          GOTO 20
      ENDIF
      PRINT*,' '
C
C
C   READ INPUT FILE
C
      READ(1,'(A)') DUMMY
      READ(1,*) DELTAT
      READ(1,*) NUM
      READ(1,*) START, V(1)
      IF (NUM.GT.MAX) NUM = MAX
      DO 30, I = 2, NUM
         READ(1,*) DUM, V(I)
 30   CONTINUE
      CLOSE  (UNIT=1, STATUS='KEEP')
```

```
C
C   WRITE OUTPUT INFORMATION TO HSVDOUT
C
      WRITE(2,100) REAL(NUM), DELTAT*1000., START*1000., 0.0
 100  FORMAT(4E15.5)
      DO 110, I = 1, 15
         WRITE(2,100) 0.0, 0.0, 0.0, 0.0
 110  CONTINUE
      DO 130, I = 4, NUM, 4
 130  WRITE(2,135) V(I-3), V(I-2), V(I-1), V(I)
 135  FORMAT(4E18.10)
      JVAR = MOD(NUM,4)
      IF (JVAR.NE.0) THEN
         WRITE(2,135) (V(J), J = NUM-JVAR+1, NUM)
      ENDIF
      END
```

HSVD

The code for HSVD and the associated programs, such as ASBIN, are copyrighted by the Delft University of Technology and the use of the programs is controlled by Dr. Ron de Beer. The source code is available from Dr. de Beer only upon his receipt of a letter stating that the programs will only be used in a non-industrial setting. The version used in this work is HSVD 91.1. More information is available from

Dr. Ron de Beer
Applied Physics Laboratory
Delft University of Technology
P.O. Box 5046
2600 GA Delft
THE NETHERLANDS

phone: 31 15786394 e-mail: beer@dutnsi2.tudelft.nl

HSVD has two output files: HSVSCR.PAR and SINVAL.DAT. HSVSCR.PAR is the data regression output file. An example of this file is in Appendix B. HSVD also wants to write a file of the amplitudes versus the singular values, named SINVAL.DAT, to help determine which singular values are due to the

resonance signal and which are due to the noise. This file was not used since similar information can also be obtained from the FFT. The basic inputs to HSVD are the input ASC filename, the number of data points, and the value of the Hankel parameter (number of columns in the data matrix). The HSVD package also contains an ERROR program to compute the two sigma errors from the HSVSCR.PAR file.

FIT

This program uses the Levenberg-Marquart weighted diagonal method of nonlinear least squares curve fitting. All calculations are done in double precision and 10000 data points are fit. The input data must be in a file named "fit.d", the initial parameter guesses must be in a file named "fit.i" and the output file will be named "fit.o". FIT requires the subroutines MRQMIN, MRQCOF, COVSRT, and GAUSSJ from Price, or their functional equivalents. The frequencies must be entered in hertz, the phase in radians, and the relaxation times in seconds.

```
      PROGRAM FIT
      REAL*8 S,T,DEV,COEF,COVAR,ALPHA,ALAMDA,CHISQ,SUM,noise
      integer nc,nca,mfit,lista
      character*40 title, blank
      DIMENSION S(10000),T(10000),DEV(10000),COEF(12),COVAR(12,12)
      DIMENSION ALPHA(12,12),LISTA(12)
      EXTERNAL FCOSE
      DATA NC /12/, ALAMDA /-5./, CHISQ /0.D0/, noise /0.d0/
      DATA COVAR /144*0./, ALPHA /144*0./, NCA /12/,MFIT /12/
      OPEN(UNIT=1, FILE='fit.d')
      sum=0.d0
      read(1,'(a)') title
      read(1,'(a)') blank
      read(1,'(a)') blank
      DO 10, I=1,10000
         READ(1,*) S(I), T(I)
         sum=sum+t(i)
         if (i.gt.9500) noise=noise+dabs(t(i))
 10   continue
      close(1)
```

```
      DO 11, I=1,MFIT
 11      LISTA(I)=I
      DO 12, I=1,10000
 12      DEV(I)=noise/500.d0
      open(unit=2, file='fit.i')
      DO 13, I=1,MFIT
 13      read(2,*) coef(i)
      close(2)
      coef(2)=coef(2)*6.283185308d0
      coef(6)=coef(6)*6.283185308d0
      coef(10)=coef(10)*6.283185308d0
      do 14, i=1,10000
 14      t(i)=t(i)-sum/10000.d0
 20   CALL MRQMIN(S,T,DEV,10000,COEF,NC,LISTA,MFIT,COVAR,
     1        ALPHA,NCA,CHISQ,FCOSE,ALAMDA)
      IF (CHISQ.LE.1.d-10) GOTO 25
      if (alamda.lt.1.d-250) goto 25
      if (alamda.gt.1.d+250) goto 25
      GOTO 20
 25   ALAMDA=0.D0
      CALL MRQMIN(S,T,DEV,10000,COEF,NC,LISTA,MFIT,COVAR,
     1    ALPHA,NCA,CHISQ,FCOSE,ALAMDA)
      coef(2)=coef(2)/6.283185308d0
      coef(6)=coef(6)/6.283185308d0
      coef(10)=coef(10)/6.283185308d0
      OPEN(UNIT=3, FILE='fit.o')
      write(3,*)title
      DO 31 I=1,MFIT
         WRITE(3,*) COEF(I),1.d0/dsqrt(alpha(i,i)*(10000.d0-13.d0))
 31   continue
      write(3,*) ' '
      write(3,*) ' noise level =',noise/500.d0
      END
C
      SUBROUTINE FCOSE(X,A,YFIT,DYDA,MA)
      REAL*8 X,A,YFIT,DYDA,YFIT1,YFIT2,YFIT3
      integer ma
      DIMENSION A(MA), DYDA(MA)
      YFIT1=A(1)*DCOS(A(2)*X+A(3))*DEXP(-X/A(4))
      YFIT2=A(5)*DCOS(A(6)*X+A(7))*DEXP(-X/A(8))
      YFIT3=A(9)*DCOS(A(10)*X+A(11))*DEXP(-X/A(12))
      YFIT=YFIT1+YFIT2+YFIT3
      DYDA(1)=YFIT1/A(1)
      DYDA(3)=-A(1)*DSIN(A(2)*X+A(3))*DEXP(-X/A(4))
      DYDA(2)=DYDA(3)*X
      DYDA(4)=YFIT1*X/A(4)/A(4)
      DYDA(5)=YFIT1/A(5)
      DYDA(7)=-A(5)*DSIN(A(6)*X+A(7))*DEXP(-X/A(8))
      DYDA(6)=DYDA(7)*X
      DYDA(8)=YFIT1*X/A(8)/A(8)
      DYDA(9)=YFIT1/A(9)
      DYDA(11)=-A(9)*DSIN(A(10)*X+A(11))*DEXP(-X/A(12))
      DYDA(10)=DYDA(11)*X
      DYDA(12)=YFIT1*X/A(12)/A(12)
      RETURN
      END
C
      SUBROUTINE MRQMIN(X,Y,SIG,NDATA,A,MA,LISTA,MFIT,
     *      COVAR,ALPHA,NCA,CHISQ,FUNCS,ALAMDA)
      SUBROUTINE MRQCOF(X,Y,SIG,NDATA,A,MA,LISTA,MFIT,ALPHA,BETA,NALP,
     *      CHISQ,FUNCS)
      SUBROUTINE COVSRT(COVAR,NCVM,MA,LISTA,MFIT)
      SUBROUTINE GAUSSJ(A,N,NP,B,M,MP)
```

APPENDIX B
EXAMPLE FILES

Only the first page is given for each file except where necessary to include important data. The format is shifted to multiple columns in some cases to allow for more of the file to be printed on a page. The ν_{-} line of urea-d_4 is used as for illustrative purposes. Data was collected with a reference frequency of 2389.00 $\pm$ 0.05 kHz.

PRN

```
"wave # 1"     0.000950 0.004044 -.000319 -.001322 -.003428 -.002956 -.002819 -.002594
"PI 1/A"       0.001419 0.003906 -.000463 -.001375 -.003522 -.002947 -.002812 -.002656
 0             0.001344 0.003941 -.000413 -.001347 -.003456 -.002891 -.002787 -.002556
 .0000002      0.000975 0.003841 -.000419 -.001459 -.003447 -.002844 -.002750 -.002472
"From B"       0.002072 0.003866 -.000541 -.001409 -.003450 -.002837 -.002769 -.002484
"  To I"       0.002353 0.003800 -.000547 -.001419 -.003334 -.002800 -.002744 -.002419
"....."        0.003594 0.003753 -.000597 -.001425 -.003319 -.002747 -.002728 -.002450
"" 0.004959 0.003678 -.000641 -.001441 -.003322 -.002716 -.002706 -.002434
"" 0.006384 0.003641 -.000734 -.001484 -.003306 -.002694 -.002684 -.002459
"" 0.009587 0.003597 -.000741 -.001438 -.003256 -.002669 -.002700 -.002509
"" 0.011231 0.003544 -.000853 -.001419 -.003269 -.002609 -.002719 -.002466
"" 0.015950 0.003478 -.000897 -.001531 -.003262 -.002684 -.002700 -.002447
"" 0.018209 0.003416 -.000963 -.001534 -.003291 -.002694 -.002812 -.002516
"" 0.023569 0.003341 -.000984 -.001547 -.003234 -.002703 -.002763 -.002500
"" 0.026278 0.003347 -.001034 -.001575 -.003269 -.002691 -.002797 -.002516
"" 0.031806 0.003250 -.001137 -.001650 -.003216 -.002816 -.002791 -.002597
"" 0.034094 0.003284 -.001159 -.001769 -.003231 -.002763 -.002819 -.002594
"" 0.040262 0.003187 -.001231 -.001887 -.003234 -.002875 -.002781 -.002666
"" 0.041897 0.003206 -.001247 -.001947 -.003197 -.002884 -.002806 -.002681
"" 0.048809 0.003172 -.001312 -.002119 -.003112 -.002863 -.002725 -.002691
"" 0.050316 0.003138 -.001344 -.002219 -.003163 -.002888 -.002706 -.002647
"" 0.056822 0.003172 -.001425 -.002219 -.003019 -.002837 -.002647 -.002675
"" 0.058872 0.003131 -.001434 -.002331 -.003000 -.002797 -.002584 -.002678
"" 0.064753 0.003128 -.001528 -.002391 -.002969 -.002828 -.002469 -.002706
"" 0.067512 0.002991 -.001550 -.002431 -.002975 -.002806 -.002400 -.002669
"" 0.072875 0.002922 -.001653 -.002450 -.002984 -.002797 -.002384 -.002753
"" 0.076037 0.002866 -.001691 -.002491 -.002959 -.002756 -.002291 -.002763
"" 0.081056 0.002834 -.001775 -.002484 -.003013 -.002734 -.002275 -.002812
"" 0.084387 0.002700 -.001850 -.002528 -.002934 -.002759 -.002197 -.002784
"" 0.088231 0.002691 -.001875 -.002537 -.002950 -.002644 -.002141 -.002784
"" 0.091500 0.002672 -.001991 -.002534 -.002906 -.002653 -.002103 -.002778
"" 0.093916 0.002572 -.002041 -.002497 -.002962 -.002728 -.002069 -.002766
```

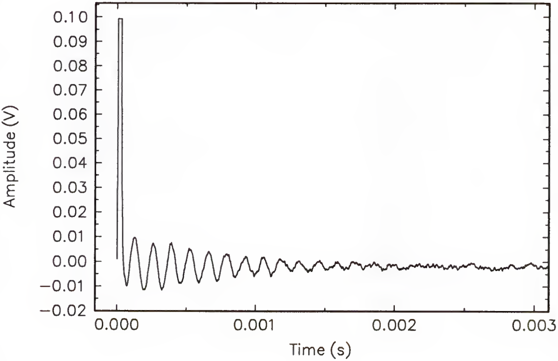

Figure B-1 PRN file for data set UD106.

OUT

The following OUT file is the same as the above PRN file, except that the first 456 points have been deleted and than every 5 points after the first has been skipped. The file has been divided into three columns to conserve space.

```
ud106.prn
   2.000000E-07
     2607
   .000046200      .000100
   .000047400     -.000991
   .000048600     -.001947
   .000049800     -.003041
   .000051000     -.003947
   .000052200     -.004803
   .000053400     -.005375
   .000054600     -.005906
   .000055800     -.005934
   .000057000     -.005962
   .000058200     -.006381
   .000059400     -.006897
   .000060600     -.007391
   .000061800     -.008019
   .000063000     -.008341
   .000064200     -.008672
   .000065400     -.008762
   .000066600     -.009084
   .000067800     -.009634
   .000069000     -.009828
   .000070200     -.009856
   .000071400     -.010091
   .000072600     -.009913
   .000073800     -.009662
   .000075000     -.009363
   .000076200     -.009184
   .000077400     -.008913
   .000078600     -.008556
   .000079800     -.008016
   .000081000     -.007391
   .000082200     -.006831
   .000083400     -.006191
   .000084600     -.005691
   .000085800     -.005341
   .000087000     -.004775
   .000088200     -.004028
   .000089400     -.003231
   .000090600     -.002463
   .000091800     -.001684
   .000093000     -.000819
   .000094200     -.000037
   .000095400      .000616
   .000096600      .001125
   .000097800      .001500
   .000099000      .002150
   .000100200      .002488
   .000101400      .003000
   .000102600      .003716
   .000103800      .004181
   .000105000      .004409
   .000106200      .004769
   .000107400      .005359
   .000108600      .005881
   .000109800      .006172
   .000111000      .006562
   .000112200      .006984
   .000113400      .007322
   .000114600      .007659
   .000115800      .007997
   .000117000      .008347
   .000118200      .008850
   .000119400      .009094
   .000120600      .009153
   .000121800      .009216
   .000123000      .009494
   .000124200      .009553
   .000125400      .009556
   .000126600      .009625
   .000127800      .009625
   .000129000      .009553
   .000130200      .009638
   .000131400      .009641
   .000132600      .009550
   .000133800      .009231
   .000135000      .009291
   .000136200      .009203
   .000137400      .009066
   .000138600      .008759
   .000139800      .008331
   .000141000      .007531
   .000142200      .006819
   .000143400      .006431
   .000144600      .005975
   .000145800      .005575
   .000147000      .005034
   .000148200      .004453
   .000149400      .003950
   .000150600      .003375
   .000151800      .002900
   .000153000      .002531
   .000154200      .001819
   .000155400      .001053
   .000156600      .000444
   .000157800      .000100
   .000159000     -.000303
   .000160200     -.000800
   .000161400     -.001425
   .000162600     -.002141
   .000163800     -.002800
   .000165000     -.003112
   .000166200     -.003563
   .000167400     -.004362
   .000168600     -.005219
   .000169800     -.005803
   .000171000     -.006356
   .000172200     -.006862
   .000173400     -.007078
   .000174600     -.007350
   .000175800     -.007769
   .000177000     -.008384
   .000178200     -.008984
   .000179400     -.009325
   .000180600     -.009722
   .000181800     -.010084
   .000183000     -.010334
   .000184200     -.010569
   .000185400     -.010969
   .000186600     -.011175
   .000187800     -.011375
   .000189000     -.011597
   .000190200     -.011625
   .000191400     -.011672
   .000192600     -.011481
   .000193800     -.011391
   .000195000     -.011291
   .000196200     -.011278
   .000197400     -.011378
   .000198600     -.011431
   .000199800     -.011487
   .000201000     -.011512
   .000202200     -.011419
   .000203400     -.011256
   .000204600     -.011053
   .000205800     -.010716
   .000207000     -.010362
   .000208200     -.010306
   .000209400     -.010181
   .000210600     -.010147
   .000211800     -.009787
   .000213000     -.009325
   .000214200     -.008828
   .000215400     -.008391
   .000216600     -.007847
   .000217800     -.007141
   .000219000     -.006550
   .000220200     -.005937
   .000221400     -.005219
   .000222600     -.004684
   .000223800     -.004294
   .000225000     -.003662
   .000226200     -.003178
   .000227400     -.002841
   .000228600     -.002362
   .000229800     -.001797
   .000231000     -.001378
   .000232200     -.000950
   .000233400     -.000506
   .000234600      .000100
   .000235800      .000862
   .000237000      .001603
   .000238200      .002169
   .000239400      .002306
```

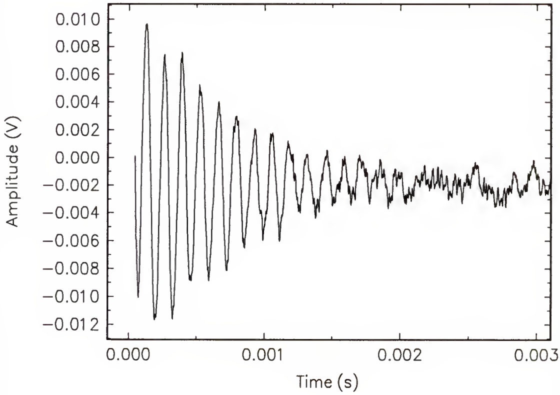

Figure B-2 OUT file for data set UD106.

FFT

This is the PSD FFT of the above OUT file padded with zeroes to 32768 points. A second page is filled to show the peak values.

0.0000000E+00	760.9504	2212.524	1.143985
38.14697	729.1951	2250.671	0.7383693
76.29395	640.0808	2288.818	1.803383
114.4409	510.5210	2326.965	4.478462
152.5879	363.9980	2365.112	8.078354
190.7349	224.9005	2403.259	11.31133
228.8818	112.9581	2441.406	12.83292
267.0288	39.26183	2479.553	11.88906
305.1758	4.839679	2517.700	8.741746
343.3228	1.980404	2555.847	4.655894
381.4697	17.68378	2593.994	1.422951
419.6167	38.04451	2632.141	0.6133943
457.7637	52.19839	2670.288	2.884444
495.9106	54.72288	2708.435	7.655189
534.0576	45.97632	2746.582	13.30301
572.2046	30.57127	2784.729	17.80412
610.3516	14.75859	2822.876	19.54365
648.4985	3.765519	2861.023	17.94721
686.6455	1.1685744E-02	2899.170	13.66924
724.7925	2.696752	2937.317	8.273064
762.9395	8.692378	2975.464	3.560611
801.0864	14.19740	3013.611	0.8544950
839.2334	16.39766	3051.758	0.5388385
877.3804	14.46995	3089.905	2.032551
915.5273	9.614935	3128.052	4.166529
953.6743	4.236131	3166.199	5.760629
991.8213	0.7190000	3204.346	6.126069
1029.968	0.3768323	3242.493	5.279334
1068.115	2.993566	3280.640	3.807483
1106.262	7.089060	3318.787	2.492533
1144.409	10.70587	3356.934	1.904005
1182.556	12.31145	3395.081	2.160213
1220.703	11.40428	3433.228	2.953340
1258.850	8.590425	3471.375	3.790556
1296.997	5.161522	3509.521	4.297481
1335.144	2.428280	3547.668	4.412319
1373.291	1.146707	3585.815	4.372459
1411.438	1.291605	3623.962	4.516652
1449.585	2.237180	3662.109	5.028404
1487.732	3.200548	3700.256	5.776313
1525.879	3.689956	3738.403	6.350087
1564.026	3.724335	3776.550	6.279818
1602.173	3.731587	3814.697	5.320628
1640.320	4.210831	3852.844	3.642908
1678.467	5.365650	3890.991	1.812829
1716.614	6.921056	3929.138	0.5563740
1754.761	8.228678	3967.285	0.4166425
1792.908	8.603058	4005.432	1.476738
1831.055	7.703892	4043.579	3.295191
1869.202	5.751913	4081.726	5.098189
1907.349	3.453485	4119.873	6.143721
1945.496	1.664772	4158.020	6.082418
1983.643	0.9675586	4196.167	5.135392
2021.790	1.381133	4234.314	3.994831
2059.937	2.368170	4272.461	3.487818
2098.083	3.140391	4310.608	4.161575
2136.230	3.109677	4348.755	5.990752
2174.377	2.246246	4386.902	8.352397

4425.049	10.28769	7057.190	89.41947
4463.196	10.93240	7095.337	89.06531
4501.343	9.916217	7133.484	94.25574
4539.490	7.544309	7171.631	110.4981
4577.637	4.676003	7209.778	141.3306
4615.784	2.356279	7247.925	186.6604
4653.931	1.369394	7286.072	242.2114
4692.078	1.916727	7324.219	300.3946
4730.225	3.559567	7362.366	352.3742
4768.372	5.443081	7400.513	390.6268
4806.519	6.689876	7438.660	411.0755
4844.666	6.780005	7476.807	414.0274
4882.813	5.749754	7514.954	403.5919
4920.959	4.132702	7553.101	385.8449
4959.106	2.687369	7591.248	366.4799
4997.253	2.048668	7629.395	348.8558
5035.400	2.464096	7667.542	333.1668
5073.547	3.724101	7705.688	316.9741
5111.694	5.298605	7743.835	296.7903
5149.841	6.597362	7781.982	269.9909
5187.988	7.224140	7820.129	236.2471
5226.135	7.111959	7858.276	197.9065
5264.282	6.494284	7896.423	159.2261
5302.429	5.748394	7934.570	124.8379
5340.576	5.202096	7972.717	98.12273
5378.723	4.999944	8010.864	80.16123
5416.870	5.083504	8049.011	69.64269
5455.017	5.277388	8087.158	63.68530
5493.164	5.421806	8125.305	59.14591
5531.311	5.476997	8163.452	53.83155
5569.458	5.548172	8201.599	47.12376
5607.605	5.825448	8239.746	39.82930
5645.752	6.475920	8277.893	33.42569
5683.899	7.544211	8316.040	29.11920
5722.046	8.907525	8354.187	27.17266
5760.193	10.30124	8392.334	26.78976
5798.340	11.39964	8430.480	26.55659
5836.487	11.91803	8468.628	25.17804
5874.634	11.70295	8506.774	22.12668
5912.781	10.78876	8544.922	17.88940
5950.928	9.412022	8583.068	13.70854
5989.075	7.981226	8621.216	10.96120
6027.222	7.000308	8659.362	10.48554
6065.369	6.948027	8697.510	12.17386
6103.516	8.129026	8735.656	15.01320
6141.663	10.53481	8773.804	17.53797
6179.810	13.77208	8811.950	18.47137
6217.957	17.11401	8850.098	17.25757
6256.104	19.69605	8888.244	14.25271
6294.250	20.81633	8926.392	10.51087
6332.397	20.23823	8964.538	7.287132
6370.544	18.36128	9002.686	5.496964
6408.691	16.15549	9040.832	5.372013
6446.838	14.84264	9078.979	6.444166
6484.985	15.42540	9117.126	7.831418
6523.132	18.25643	9155.273	8.667295
6561.279	22.85389	9193.420	8.467973
6599.426	28.08397	9231.567	7.282268
6637.573	32.67095	9269.714	5.586030
6675.720	35.82940	9307.861	4.003677
6713.867	37.72206	9346.008	3.008503
6752.014	39.49038	9384.155	2.743257
6790.161	42.77959	9422.302	3.026457
6828.308	48.92173	9460.449	3.511908
6866.455	58.13803	9498.596	3.898499
6904.602	69.17286	9536.743	4.076335
6942.749	79.62966	9574.890	4.142400
6980.896	86.98392	9613.037	4.294917
7019.043	89.91930	9651.184	4.678635

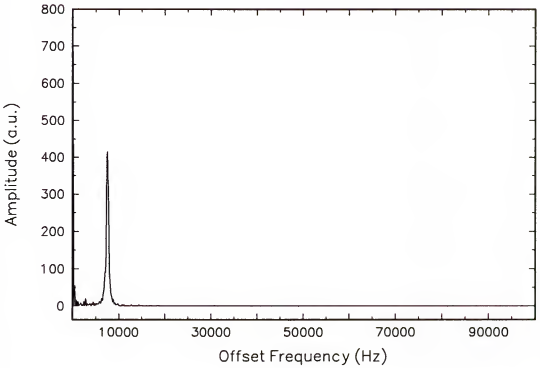

Figure B-3 Full PSD FFT for data set UD106.

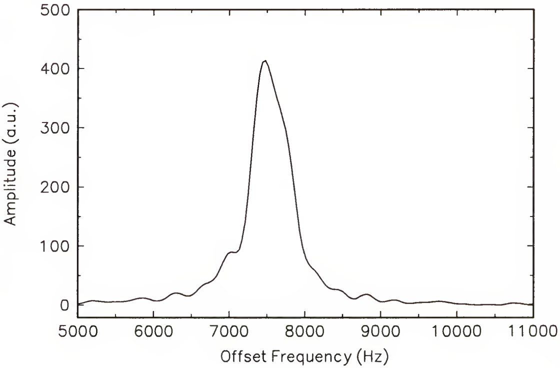

Figure B-4 Detail of PSD FFT of data set UD106.

ASC

0.81920E+04	0.20000E-03	0.46200E-01	0.00000E+00
0.00000E+00	0.00000E+00	0.00000E+00	0.00000E+00
0.00000E+00	0.00000E+00	0.00000E+00	0.00000E+00
0.00000E+00	0.00000E+00	0.00000E+00	0.00000E+00
0.00000E+00	0.00000E+00	0.00000E+00	0.00000E+00
0.00000E+00	0.00000E+00	0.00000E+00	0.00000E+00
0.00000E+00	0.00000E+00	0.00000E+00	0.00000E+00
0.00000E+00	0.00000E+00	0.00000E+00	0.00000E+00
0.00000E+00	0.00000E+00	0.00000E+00	0.00000E+00
0.00000E+00	0.00000E+00	0.00000E+00	0.00000E+00
0.00000E+00	0.00000E+00	0.00000E+00	0.00000E+00
0.00000E+00	0.00000E+00	0.00000E+00	0.00000E+00
0.00000E+00	0.00000E+00	0.00000E+00	0.00000E+00
0.00000E+00	0.00000E+00	0.00000E+00	0.00000E+00
0.00000E+00	0.00000E+00	0.00000E+00	0.00000E+00
0.00000E+00	0.00000E+00	0.00000E+00	0.00000E+00
0.9999999747E-04	-0.1630000042E-03	-0.3689999867E-03	-0.5690000253E-03
-0.6590000121E-03	-0.8500000113E-03	-0.9909999790E-03	-0.1119000022E-02
-0.1306000049E-02	-0.1430999953E-02	-0.1550000045E-02	-0.1827999949E-02
-0.1947000041E-02	-0.2150000073E-02	-0.2338000108E-02	-0.2536999993E-02
-0.2666000044E-02	-0.2906000009E-02	-0.3041000105E-02	-0.3247000044E-02
-0.3375000088E-02	-0.3540999955E-02	-0.3690999933E-02	-0.3834000090E-02
-0.3947000019E-02	-0.4172000103E-02	-0.4302999936E-02	-0.4433999769E-02
-0.4519000184E-02	-0.4641000181E-02	-0.4803000018E-02	-0.4834000021E-02
-0.4999999888E-02	-0.5063000135E-02	-0.5191000178E-02	-0.5297000054E-02
-0.5375000183E-02	-0.5481000058E-02	-0.5634000059E-02	-0.5638000090E-02
-0.5783999804E-02	-0.5830999929E-02	-0.5905999802E-02	-0.5977999885E-02
-0.5983999930E-02	-0.5996999796E-02	-0.6025000010E-02	-0.5925000180E-02
-0.5934000015E-02	-0.5905999802E-02	-0.5849999841E-02	-0.5863000173E-02
-0.5872000009E-02	-0.5931000225E-02	-0.5962000228E-02	-0.6006000098E-02
-0.6033999845E-02	-0.6190999877E-02	-0.6211999804E-02	-0.6359000225E-02
-0.6380999926E-02	-0.6519000046E-02	-0.6606000010E-02	-0.6661999971E-02
-0.6721999962E-02	-0.6819000002E-02	-0.6897000130E-02	-0.6984000094E-02
-0.7025000174E-02	-0.7141000126E-02	-0.7228000090E-02	-0.7321999874E-02
-0.7391000167E-02	-0.7509000134E-02	-0.7577999961E-02	-0.7747000083E-02
-0.7790999953E-02	-0.7927999832E-02	-0.8019000292E-02	-0.7950000465E-02
-0.8105999790E-02	-0.8147000335E-02	-0.8209000342E-02	-0.8247000165E-02
-0.8341000415E-02	-0.8352999575E-02	-0.8415999822E-02	-0.8456000127E-02
-0.8553000167E-02	-0.8596999571E-02	-0.8671999909E-02	-0.8693999611E-02
-0.8728000335E-02	-0.8744000457E-02	-0.8768999949E-02	-0.8750000037E-02
-0.8762000129E-02	-0.8809000254E-02	-0.8828000166E-02	-0.8909000084E-02
-0.8946999907E-02	-0.9022000246E-02	-0.9084000252E-02	-0.9169000201E-02
-0.9286999702E-02	-0.9347000159E-02	-0.9449999779E-02	-0.9655999951E-02
-0.9634000249E-02	-0.9677999653E-02	-0.9734000079E-02	-0.9747000411E-02
-0.9793999605E-02	-0.9812000208E-02	-0.9828000329E-02	-0.9836999699E-02
-0.9862000123E-02	-0.9906000458E-02	-0.9831000119E-02	-0.9847000241E-02
-0.9855999611E-02	-0.9875000454E-02	-0.9897000156E-02	-0.1001300011E-01
-0.9965999983E-02	-0.1003700029E-01	-0.1009100024E-01	-0.1002799999E-01
-0.1002200041E-01	-0.9975000285E-02	-0.1001300011E-01	-0.9975000285E-02
-0.9913000278E-02	-0.9840999730E-02	-0.9812000208E-02	-0.9769000113E-02
-0.9712000377E-02	-0.9655999951E-02	-0.9662000462E-02	-0.9662000462E-02
-0.9575000033E-02	-0.9506000206E-02	-0.9496999905E-02	-0.9406000376E-02
-0.9363000281E-02	-0.9328000247E-02	-0.9269000031E-02	-0.9262000211E-02
-0.9212000296E-02	-0.9212000296E-02	-0.9184000082E-02	-0.9119000286E-02
-0.9084000252E-02	-0.9084000252E-02	-0.8968999609E-02	-0.9008999914E-02
-0.8913000114E-02	-0.8868999779E-02	-0.8828000166E-02	-0.8740999736E-02
-0.8650000207E-02	-0.8612000383E-02	-0.8555999957E-02	-0.8506000042E-02
-0.8396999910E-02	-0.8318999782E-02	-0.8249999955E-02	-0.8128000423E-02
-0.8015999570E-02	-0.7922000252E-02	-0.7833999582E-02	-0.7712000050E-02
-0.7577999961E-02	-0.7422000170E-02	-0.7391000167E-02	-0.7263000123E-02
-0.7184000220E-02	-0.7046999875E-02	-0.7019000128E-02	-0.6928000133E-02
-0.6831000093E-02	-0.6719000172E-02	-0.6653000135E-02	-0.6469000131E-02
-0.6393999793E-02	-0.6275000051E-02	-0.6190999877E-02	-0.6134000141E-02
-0.6025000010E-02	-0.5965999793E-02	-0.5888000131E-02	-0.5783999804E-02
-0.5690999795E-02	-0.5669000093E-02	-0.5559000187E-02	-0.5541000050E-02

HSVSCR.PAR

This is the output file from HSVD. It has been modified to remove the printing of the singular values and the signal roots. These parameters have only been commented out in the printing of the output file and could easily be returned to the file if they were desired. The damping factor reported here is T_2^*, the inverse linewidth parameter, and the amplitudes are in arbitrary (relative) units.

```
name of signal file:                ud106.dat

number of data-points of signal:          8192
step-size of signal (milli-seconds):   0.000200
begin time of signal (milli-seconds):    0.0462
number of data-points in hsvd:            6144
size parameter of hankel matrix:          3072
number of frequencies:                       1
signal noise level:                 0.16447E-03
root mean square of hsvd fit:       0.20322E-02
test parameter:                              1

     fre(khz)        dam(ms)        amp(a.u.)   phase(degr.)
  0.755161E+01  -0.933070E+00   0.110758E-01   0.135269E+03
```

The ERROR program with HSVD calculates the two-sigma errors.

```
name of signal file:                ud106.dat
number of data-points of signal:          8192
step-size of signal (milli-seconds):     0.000
begin time of signal (milli-seconds):    0.046
number of data-points in hsvd:            6144
size parameter of hankel matrix:          3072
number of frequencies:                       1
signal noise level:                  0.1645E+00
root mean square of hsvd fit:        0.2032E+00
test parameter:                              1

result of hsvd:

freq    f2sd      decay    d2sd      ampor     a2sd     phasor  p2sd
(khz)             (khz)              (a. u.)            (degrees)

7.55161 0.47403  -1.07173 2.97845  0.01164 0.01581  10.214   81.797
```

FIT.O

This is the output file of FIT, the nonlinear least squares curve fitting program using the Levenberg-Marquart method. The values are in the order of amplitude, frequency (Hz), phase (rad), and relaxation time (s), for the fitted peak. The values for *alpha* and *covar* are the upper triangular matrix values. The *alpha* column is directly from the fitting program. The *covar* column is the covariance matrix values. Since variances must be positive, note that *covar* entries 1, 5, 8 and 10 are indeed positive (emphasis added).

```
ud106.prn
1.397072791946770E-002
 7548.42692677702
0.192156800836138
7.213702176382539E-004

CHISQ =    1.965733364180134E-003
dev   =    1.926644355989993E-003

  alpha                     covar
 92802447.8515003          2.993034257636894E-008
 3.47182899708311          1.588257543932525E-004
 37684.8360559455         -1.243098079541661E-007
 1117605271.79131         -1.586853535868848E-009
5.721593453057895E-003     477.141996238359
 8.13691770249254         -0.212679857744911
0.725177718655479         -7.499220742641315E-006
 18279.8292216466          1.496014832744504E-004
 93209.6644723470          5.938532471083577E-009
 21072415440.6407          1.315904099702059E-010
```

While HSVD returns a useful estimate of the frequency, the damping factor is too high and with a large standard deviation due to the errors associated with the poor noise response of the HSVD algorithm. Final NQR parameters for the UD106 data run are resonance frequency 2381.45 $\pm$ 0.05 kHz with a T_2^* value of 721 $\pm$ 12 μs.

APPENDIX C
PETERSEN'S SODIUM NITRITE DATA

The sodium nitrite data used as a test of the NQR linewidth analysis method are from Petersen's doctoral thesis [Petersen 1975, 1976]. The graphs used were digitized, smoothed and parameterized and then manipulated.

Raw Data

The first column is temperature (K) and the second is the value of the time constant. Note that the second value in each pair is the logarithmic value from the graph as digitized linearly.

Upper Line - Spin-Spin Relaxation Time

The raw T_2 data for the ν_+ line are given here.

75.104230	5.560800E-01	385.750600	7.498900E-01
81.933030	5.205900E-01	401.086700	7.223400E-01
94.094400	6.160200E-01	421.574700	6.667700E-01
116.383900	5.443500E-01	358.187100	5.823600E-01
139.551400	5.943800E-01	373.278500	5.462100E-01
154.090100	5.394000E-01	389.103300	5.446200E-01
163.811600	5.392200E-01	402.955100	5.575500E-01
179.970000	6.073600E-01	424.056200	5.308000E-01
196.157100	5.137900E-01	429.452900	4.038100E-01
208.150100	4.998200E-01	425.704700	2.961400E-01
252.048800	5.491500E-01	430.761800	2.825600E-01
313.884100	6.756700E-01	433.685700	1.866400E-01
327.199200	7.299100E-01	435.123400	1.429100E-01
342.663700	6.842100E-01	445.435300	9.830000E-02
351.992400	6.647800E-01	442.837000	8.061000E-02
361.897600	6.831400E-01	435.844100	8.163000E-02
370.565400	7.280500E-01	431.767700	6.456000E-02
379.132700	6.998100E-01	439.663500	4.433000E-02

448.028600	3.685000E-02	449.874900	-1.012000E-02
454.319200	4.130000E-02	461.398300	-8.911000E-02
438.594700	1.712000E-02	472.712300	-9.983000E-02
434.619400	-1.880000E-02	435.908100	-1.119900E-01
437.212700	-2.725000E-02	437.496100	-1.857900E-01
454.634600	4.540000E-03		

Upper Line - Inverse Linewidth Parameter

The T_2^* data for the ν_+ line are:

76.570000	-4.700000E-01	426.600000	-6.000000E-01
82.720000	-4.300000E-01	428.040000	-6.400000E-01
94.880000	-5.000000E-01	448.210000	-7.500000E-01
120.050000	-5.100000E-01	448.670000	-7.700000E-01
107.920000	-4.000000E-01	420.400000	-8.000000E-01
117.420000	-4.300000E-01	430.830000	-8.000000E-01
140.030000	-4.100000E-01	438.080000	-8.000000E-01
154.830000	-4.100000E-01	441.420000	-8.000000E-01
162.270000	-4.400000E-01	445.500000	-8.000000E-01
194.890000	-4.700000E-01	438.260000	-8.300000E-01
178.160000	-4.000000E-01	443.860000	-8.300000E-01
208.210000	-3.600000E-01	445.370000	-8.300000E-01
250.800000	-2.100000E-01	452.780000	-8.300000E-01
313.350000	-1.600000E-01	422.720000	-8.600000E-01
326.970000	-2.000000E-01	436.020000	-8.600000E-01
333.080000	-2.300000E-01	442.520000	-8.600000E-01
342.790000	-2.500000E-01	450.090000	-8.600000E-01
357.970000	-1.900000E-01	453.560000	-8.600000E-01
358.660000	-2.200000E-01	456.140000	-8.600000E-01
373.990000	-2.200000E-01	461.120000	-8.600000E-01
373.480000	-2.600000E-01	467.330000	-8.600000E-01
352.410000	-3.300000E-01	471.590000	-8.900000E-01
362.050000	-4.100000E-01	434.020000	-9.200000E-01
370.310000	-4.200000E-01	438.250000	-9.200000E-01
387.890000	-4.200000E-01	435.610000	-9.600000E-01
380.840000	-4.600000E-01	432.840000	-1.000000
385.830000	-5.300000E-01	435.260000	-1.000000
403.990000	-5.300000E-01	440.840000	-1.000000
402.530000	-6.000000E-01	435.690000	-1.050000

Lower Line - Spin-Spin Relaxation Time

The raw T_2 data for the ν_- line are given here.

76.765730	2.764500E-01	121.172300	4.815600E-01
80.623050	3.691900E-01	138.832900	4.124400E-01
96.277300	4.326400E-01	151.633900	3.935900E-01
117.352700	3.482200E-01	165.835400	3.720600E-01

179.018600	3.823500E-01
196.053600	3.730900E-01
208.108700	3.534400E-01
219.451900	3.581400E-01
251.658200	5.105100E-01
311.300900	5.364100E-01
324.804000	5.376200E-01
331.609600	5.378200E-01
351.413500	5.627700E-01
356.796900	5.488200E-01
360.037200	5.479900E-01
369.134700	5.639400E-01
372.136700	5.457300E-01
377.157700	5.847300E-01
383.535600	5.865400E-01
386.674000	6.760600E-01
398.907200	6.072600E-01
400.450600	5.436000E-01
426.450600	4.031300E-01
424.065800	3.986100E-01
429.427600	3.581300E-01
438.396100	2.522400E-01
432.399400	2.126500E-01
434.753900	1.893100E-01
439.078600	1.852400E-01
433.334800	1.786000E-01
445.984600	1.658600E-01
440.348400	1.592300E-01
431.681100	1.520900E-01
448.995900	1.478700E-01
440.758400	1.385800E-01
442.814500	1.380200E-01
441.944100	1.340100E-01
437.713300	1.260100E-01
438.572400	1.198400E-01
439.762000	1.187500E-01
443.767200	1.184400E-01
447.539200	1.028400E-01
452.735200	1.019800E-01
451.415000	8.269000E-02
450.547600	8.162000E-02
432.680100	7.861000E-02
435.280100	8.019000E-02
437.975200	6.997000E-02
453.674300	6.925000E-02
459.088300	6.892000E-02
437.193000	4.826000E-02
453.635200	3.304000E-02
434.003700	4.570000E-03
435.586200	-3.247000E-02
467.308000	-4.493000E-02
472.283200	-5.277000E-02
451.308200	-1.153200E-01

Lower Line - Inverse Linewidth Parameter

The T_2^* data for the ν_- line are:

75.950000	-1.900000E-01
80.620000	-2.100000E-01
86.090000	-2.300000E-01
96.080000	-3.300000E-01
105.410000	-2.800000E-01
118.510000	-2.600000E-01
138.080000	-2.900000E-01
151.520000	-2.800000E-01
166.040000	-2.800000E-01
208.830000	-3.600000E-01
219.300000	-3.000000E-01
178.830000	-1.900000E-01
196.440000	-1.900000E-01
251.170000	-1.000000E-01
311.250000	-5.000000E-02
355.480000	-5.000000E-02
325.660000	-1.500000E-01
331.750000	-1.500000E-01
370.930000	-1.500000E-01
360.790000	-2.400000E-01
350.520000	-3.100000E-01
368.060000	-3.200000E-01
387.120000	-3.200000E-01
382.970000	-3.300000E-01
378.470000	-3.800000E-01
400.800000	-4.600000E-01
398.750000	-4.900000E-01
425.790000	-6.000000E-01
423.350000	-6.400000E-01
435.180000	-7.000000E-01
446.020000	-7.000000E-01
440.350000	-7.200000E-01
447.490000	-7.200000E-01
430.170000	-7.500000E-01
432.820000	-7.400000E-01
439.170000	-7.400000E-01
445.110000	-7.500000E-01
450.270000	-7.400000E-01
452.510000	-7.400000E-01
441.410000	-7.700000E-01
446.830000	-7.700000E-01
449.210000	-7.700000E-01
440.070000	-8.000000E-01
450.380000	-8.000000E-01

433.980000	-8.200000E-01	453.920000	-9.200000E-01
437.410000	-8.200000E-01	460.260000	-9.200000E-01
450.880000	-8.300000E-01	471.230000	-9.200000E-01
438.710000	-8.500000E-01	431.650000	-9.600000E-01
440.280000	-8.600000E-01	433.690000	-1.000000
435.220000	-8.900000E-01	467.100000	-1.000000
435.550000	-9.200000E-01	434.740000	-1.070000

Linearized Raw Data

Upper Line - Spin-Spin Relaxation Time

The linearized raw T_2 data for the ν_+ line are given here.

75.10423	3.59816	421.57471	4.64269
81.93303	3.31581	424.05620	3.39469
94.0944	4.13067	425.70472	1.97761
116.3839	3.50227	429.45293	2.53402
139.5514	3.92989	430.76184	1.91673
154.09013	3.46258	431.76774	1.16027
163.81158	3.46115	433.68571	1.53688
179.96998	4.04911	434.61937	0.95763
196.15707	3.2643	435.12342	1.38966
208.1501	3.16097	435.84407	1.20679
252.04879	3.5412	435.90804	0.7727
313.88412	4.73882	437.21272	0.93918
327.19921	5.36921	437.49605	0.65194
342.66367	4.83292	438.59469	1.04021
351.99238	4.62147	439.66354	1.10746
358.18707	3.82261	442.83698	1.20395
361.89758	4.82103	445.43533	1.25401
370.56536	5.34626	448.02862	1.08855
373.27849	3.5173	449.87488	0.97697
379.13266	5.00968	454.31914	1.09977
385.7506	5.62199	454.63463	1.01051
389.10332	3.50445	461.39825	0.8145
401.08668	5.27643	472.71231	0.79464
402.95511	3.61036		

Upper Line - Inverse Linewidth Parameter

The linearized T_2^* data for the ν_+ line are:

76.57	0.33884	154.83	0.38905
82.72	0.37154	162.27	0.36308
94.88	0.31623	178.16	0.39811
107.92	0.39811	194.89	0.33884
117.42	0.37154	208.21	0.43652
120.05	0.30903	250.80	0.61660
140.03	0.38905	313.35	0.69183

326.97	0.63096	435.26	0.10000
333.08	0.58884	435.61	0.10965
342.79	0.56234	435.69	0.08913
352.41	0.46774	436.02	0.13804
357.97	0.64565	438.08	0.15849
358.66	0.60256	438.25	0.12023
362.05	0.38905	438.26	0.14791
370.31	0.38019	440.84	0.10000
373.48	0.54954	441.42	0.15849
373.99	0.60256	442.52	0.13804
380.84	0.34674	443.86	0.14791
385.83	0.29512	445.37	0.14791
387.89	0.38019	445.50	0.15849
402.53	0.25119	448.21	0.17783
403.99	0.29512	448.67	0.16982
420.40	0.15849	450.09	0.13804
422.72	0.13804	452.78	0.14791
426.60	0.25119	453.56	0.13804
428.04	0.22909	456.14	0.13804
430.83	0.15849	461.12	0.13804
432.84	0.10000	467.33	0.13804
434.02	0.12023	471.59	0.12882

Lower Line - Spin-Spin Relaxation Time

The linearized T_2 data for the ν_- line are given here.

76.76573	1.88995	432.6801	1.19842
80.62305	2.33986	433.3348	1.50869
96.27730	2.70795	434.0037	1.01058
117.3527	2.22956	434.7539	1.54636
121.1723	3.03082	435.2801	1.20279
138.8329	2.58488	435.5861	0.92796
151.6339	2.47508	437.1930	1.11753
165.8354	2.35537	437.7133	1.33663
179.0186	2.41185	437.9752	1.17482
196.0536	2.36097	438.3961	1.78748
208.1087	2.25652	438.5724	1.31777
219.4519	2.28108	439.0786	1.53193
251.6583	3.23974	439.7620	1.31447
311.3009	3.43882	440.3484	1.44288
324.8040	3.44842	440.7584	1.37588
331.6096	3.45001	441.9441	1.36148
351.4135	3.65401	442.8145	1.37411
356.7969	3.53851	443.7672	1.31353
360.0372	3.53175	445.9846	1.46508
369.1347	3.66387	447.5392	1.26718
372.1367	3.51342	448.9959	1.40563
377.1577	3.84353	450.5476	1.20676
383.5356	3.85958	451.3082	0.7668
386.6740	4.74308	451.4150	1.20973
398.9072	4.04818	452.7352	1.26468
400.4506	3.49623	453.6352	1.07905
424.0658	2.50386	453.6743	1.17287
426.4506	2.53006	459.0883	1.17198
429.4276	2.28102	467.3080	0.90172
431.6811	1.41935	472.2832	0.88558
432.3994	1.63174		

Lower Line - Inverse Linewidth Parameter

The linearized T_2^* data for the ν_- line are:

75.27	0.64565	429.78	0.18197
79.79	0.61660	431.70	0.10965
86.11	0.58884	433.40	0.18197
95.54	0.46774	433.89	0.10000
106.52	0.52481	434.28	0.08511
118.05	0.54954	434.55	0.12882
120.52	0.32359	435.25	0.15136
137.92	0.51286	435.48	0.12023
152.53	0.52481	435.73	0.19953
166.43	0.52481	437.06	0.15136
179.02	0.64565	438.83	0.17783
197.61	0.64565	439.24	0.14125
210.15	0.44668	439.90	0.19055
222.77	0.50119	439.94	0.15849
253.91	0.79433	440.87	0.14125
313.70	0.89125	441.19	0.16982
326.76	0.69183	445.70	0.18197
332.73	0.69183	447.13	0.19953
350.89	0.48978	447.34	0.16982
357.63	0.89125	448.41	0.19055
361.88	0.57544	450.24	0.16982
368.43	0.47863	450.77	0.18197
372.51	0.70795	450.81	0.15136
379.31	0.41687	451.52	0.16218
382.90	0.46774	451.70	0.16218
387.78	0.47863	453.30	0.18197
399.44	0.32359	453.75	0.12023
401.96	0.34674	459.91	0.12023
424.66	0.22909	467.55	0.10000
425.91	0.25119	472.21	0.12023

Manipulated Data

The ν_+ line data after smoothing and parameterization are given here.

Temp	T_2	T_2^*	$1/T_2^*$	$1/T_2$	$y=1/T_2^*-1/T_2$	$1/y$
75.47	3.69	0.35	0.002857	0.000271	0.002586	0.386677
75.94	3.69	0.35	0.002857	0.000271	0.002586	0.386677
75.95	3.68	0.35	0.002857	0.000272	0.002585	0.386787
77.14	3.68	0.35	0.002857	0.000272	0.002585	0.386787
77.16	3.69	0.35	0.002857	0.000271	0.002586	0.386677
80.00	3.69	0.35	0.002857	0.000271	0.002586	0.386677
80.30	3.70	0.35	0.002857	0.000270	0.002587	0.386567
82.72	3.70	0.35	0.002857	0.000270	0.002587	0.386567
82.87	3.71	0.35	0.002857	0.000270	0.002588	0.386458
85.77	3.71	0.35	0.002857	0.000270	0.002588	0.386458
85.89	3.72	0.35	0.002857	0.000269	0.002588	0.386350

Temp	T_2	T_2^*	$1/T_2^*$	$1/T_2$	$y=1/T_2^*-1/T_2$	$1/y$
89.96	3.72	0.35	0.002857	0.000269	0.002588	0.386350
90.21	3.73	0.35	0.002857	0.000268	0.002589	0.386243
109.78	3.73	0.35	0.002857	0.000268	0.002589	0.386243
110.01	3.74	0.35	0.002857	0.000267	0.002590	0.386136
119.76	3.74	0.35	0.002857	0.000267	0.002590	0.386136
119.81	3.75	0.35	0.002857	0.000267	0.002590	0.386029
121.24	3.75	0.35	0.002857	0.000267	0.002590	0.386029
121.47	3.74	0.35	0.002857	0.000267	0.002590	0.386136
136.23	3.74	0.35	0.002857	0.000267	0.002590	0.386136
136.37	3.74	0.36	0.002778	0.000267	0.002510	0.398343
141.49	3.74	0.36	0.002778	0.000267	0.002510	0.398343
141.64	3.73	0.36	0.002778	0.000268	0.002510	0.398457
146.76	3.73	0.36	0.002778	0.000268	0.002510	0.398457
146.91	3.72	0.36	0.002778	0.000269	0.002509	0.398571
147.87	3.72	0.36	0.002778	0.000269	0.002509	0.398571
148.00	3.73	0.36	0.002778	0.000268	0.002510	0.398457
148.95	3.73	0.36	0.002778	0.000268	0.002510	0.398457
149.22	3.72	0.36	0.002778	0.000269	0.002509	0.398571
155.84	3.72	0.36	0.002778	0.000269	0.002509	0.398571
156.07	3.72	0.37	0.002703	0.000269	0.002434	0.410866
160.11	3.72	0.37	0.002703	0.000269	0.002434	0.410866
160.17	3.71	0.37	0.002703	0.000270	0.002433	0.410988
166.11	3.71	0.37	0.002703	0.000270	0.002433	0.410988
166.26	3.71	0.38	0.002632	0.000270	0.002362	0.423363
167.76	3.71	0.38	0.002632	0.000270	0.002362	0.423363
167.87	3.70	0.38	0.002632	0.000270	0.002361	0.423494
172.71	3.70	0.38	0.002632	0.000270	0.002361	0.423494
172.88	3.69	0.38	0.002632	0.000271	0.002361	0.423625
176.31	3.69	0.38	0.002632	0.000271	0.002361	0.423625
176.54	3.68	0.38	0.002632	0.000272	0.002360	0.423758
178.85	3.68	0.39	0.002564	0.000272	0.002292	0.436231
179.12	3.67	0.39	0.002564	0.000272	0.002292	0.436372
180.74	3.67	0.39	0.002564	0.000272	0.002292	0.436372
180.95	3.66	0.39	0.002564	0.000273	0.002291	0.436514
183.05	3.66	0.39	0.002564	0.000273	0.002291	0.436514
183.32	3.65	0.39	0.002564	0.000274	0.002290	0.436656
185.36	3.65	0.39	0.002564	0.000274	0.002290	0.436656
185.49	3.64	0.40	0.002500	0.000275	0.002225	0.449383
192.25	3.64	0.40	0.002500	0.000275	0.002225	0.449383
192.46	3.64	0.41	0.002439	0.000275	0.002164	0.462043
192.52	3.64	0.41	0.002439	0.000275	0.002164	0.462043
192.76	3.63	0.41	0.002439	0.000275	0.002164	0.462205
199.03	3.63	0.41	0.002439	0.000275	0.002164	0.462205
199.18	3.63	0.42	0.002381	0.000275	0.002105	0.474953
205.09	3.63	0.42	0.002381	0.000275	0.002105	0.474953
205.30	3.63	0.43	0.002326	0.000275	0.002050	0.487781
212.25	3.63	0.43	0.002326	0.000275	0.002050	0.487781
212.33	3.63	0.44	0.002273	0.000275	0.001997	0.500690
216.35	3.63	0.44	0.002273	0.000275	0.001997	0.500690
216.43	3.64	0.44	0.002273	0.000275	0.001998	0.500500
217.24	3.64	0.44	0.002273	0.000275	0.001998	0.500500
217.51	3.64	0.45	0.002222	0.000275	0.001947	0.513480
218.59	3.64	0.45	0.002222	0.000275	0.001947	0.513480
218.85	3.65	0.45	0.002222	0.000274	0.001948	0.513281
221.01	3.65	0.45	0.002222	0.000274	0.001948	0.513281
221.25	3.66	0.45	0.002222	0.000273	0.001949	0.513084
221.27	3.66	0.45	0.002222	0.000273	0.001949	0.513084
221.54	3.66	0.46	0.002174	0.000273	0.001901	0.526125
222.62	3.66	0.46	0.002174	0.000273	0.001901	0.526125
222.73	3.67	0.46	0.002174	0.000272	0.001901	0.525919
224.51	3.67	0.46	0.002174	0.000272	0.001901	0.525919
224.66	3.68	0.46	0.002174	0.000272	0.001902	0.525714
225.98	3.68	0.47	0.002128	0.000272	0.001856	0.538816

Temp	T_2	T_2^*	$1/T_2^*$	$1/T_2$	$y=1/T_2^*-1/T_2$	$1/y$
226.15	3.69	0.47	0.002128	0.000271	0.001857	0.538602
228.38	3.69	0.47	0.002128	0.000271	0.001857	0.538602
228.53	3.70	0.47	0.002128	0.000270	0.001857	0.538390
229.61	3.70	0.47	0.002128	0.000270	0.001857	0.538390
229.71	3.71	0.48	0.002083	0.000270	0.001814	0.551331
231.79	3.71	0.48	0.002083	0.000270	0.001814	0.551331
231.89	3.72	0.48	0.002083	0.000269	0.001815	0.551111
232.97	3.72	0.48	0.002083	0.000269	0.001815	0.551111
233.10	3.73	0.48	0.002083	0.000268	0.001815	0.550892
233.37	3.73	0.48	0.002083	0.000268	0.001815	0.550892
233.57	3.73	0.49	0.002041	0.000268	0.001773	0.564105
234.18	3.73	0.49	0.002041	0.000268	0.001773	0.564105
234.31	3.74	0.49	0.002041	0.000267	0.001773	0.563877
235.94	3.74	0.49	0.002041	0.000267	0.001773	0.563877
236.19	3.75	0.49	0.002041	0.000267	0.001774	0.563650
236.99	3.75	0.49	0.002041	0.000267	0.001774	0.563650
237.13	3.76	0.49	0.002041	0.000266	0.001775	0.563425
237.28	3.76	0.49	0.002041	0.000266	0.001775	0.563425
237.43	3.76	0.50	0.002000	0.000266	0.001734	0.576687
238.06	3.76	0.50	0.002000	0.000266	0.001734	0.576687
238.32	3.77	0.50	0.002000	0.000265	0.001735	0.576453
239.81	3.77	0.50	0.002000	0.000265	0.001735	0.576453
239.96	3.78	0.50	0.002000	0.000265	0.001735	0.576220
240.75	3.78	0.50	0.002000	0.000265	0.001735	0.576220
241.00	3.79	0.50	0.002000	0.000264	0.001736	0.575988
242.05	3.79	0.50	0.002000	0.000264	0.001736	0.575988
242.19	3.79	0.51	0.001961	0.000264	0.001697	0.589299
242.34	3.79	0.51	0.001961	0.000264	0.001697	0.589299
242.49	3.80	0.51	0.001961	0.000263	0.001698	0.589058
243.68	3.80	0.51	0.001961	0.000263	0.001698	0.589058
243.69	3.81	0.51	0.001961	0.000262	0.001698	0.588818
245.32	3.81	0.51	0.001961	0.000262	0.001698	0.588818
245.72	3.82	0.51	0.001961	0.000262	0.001699	0.588580
246.26	3.82	0.51	0.001961	0.000262	0.001699	0.588580
246.51	3.83	0.51	0.001961	0.000261	0.001700	0.588343
246.79	3.83	0.52	0.001923	0.000261	0.001662	0.601692
247.19	3.83	0.52	0.001923	0.000261	0.001662	0.601692
247.41	3.84	0.52	0.001923	0.000260	0.001663	0.601446
248.46	3.84	0.52	0.001923	0.000260	0.001663	0.601446
248.53	3.85	0.52	0.001923	0.000260	0.001663	0.601201
248.93	3.85	0.52	0.001923	0.000260	0.001663	0.601201
249.20	3.86	0.52	0.001923	0.000259	0.001664	0.600958
250.00	3.86	0.52	0.001923	0.000259	0.001664	0.600958
250.10	3.87	0.52	0.001923	0.000258	0.001665	0.600716
250.99	3.87	0.52	0.001923	0.000258	0.001665	0.600716
251.21	3.88	0.52	0.001923	0.000258	0.001665	0.600476
251.59	3.88	0.52	0.001923	0.000258	0.001665	0.600476
251.74	3.89	0.54	0.001852	0.000257	0.001595	0.627045
252.28	3.89	0.54	0.001852	0.000257	0.001595	0.627045
252.48	3.90	0.54	0.001852	0.000256	0.001595	0.626786
253.21	3.90	0.54	0.001852	0.000256	0.001595	0.626786
253.38	3.91	0.54	0.001852	0.000256	0.001596	0.626528
254.15	3.91	0.54	0.001852	0.000256	0.001596	0.626528
254.42	3.92	0.54	0.001852	0.000255	0.001597	0.626272
255.23	3.92	0.54	0.001852	0.000255	0.001597	0.626272
255.32	3.93	0.54	0.001852	0.000254	0.001597	0.626018
256.03	3.93	0.54	0.001852	0.000254	0.001597	0.626018
256.16	3.94	0.54	0.001852	0.000254	0.001598	0.625765
256.56	3.94	0.54	0.001852	0.000254	0.001598	0.625765
256.69	3.94	0.55	0.001818	0.000254	0.001564	0.639233
256.70	3.94	0.55	0.001818	0.000254	0.001564	0.639233
256.81	3.95	0.55	0.001818	0.000253	0.001565	0.638971
257.41	3.95	0.55	0.001818	0.000253	0.001565	0.638971

Temp	T_2	T_2^*	$1/T_2^*$	$1/T_2$	$y=1/T_2^*-1/T_2$	$1/y$
257.63	3.96	0.55	0.001818	0.000253	0.001566	0.638710
258.17	3.96	0.55	0.001818	0.000253	0.001566	0.638710
258.31	3.97	0.55	0.001818	0.000252	0.001566	0.638450
259.35	3.97	0.55	0.001818	0.000252	0.001566	0.638450
259.50	3.98	0.55	0.001818	0.000251	0.001567	0.638192
260.10	3.98	0.55	0.001818	0.000251	0.001567	0.638192
260.26	3.99	0.55	0.001818	0.000251	0.001568	0.637936
260.85	3.99	0.55	0.001818	0.000251	0.001568	0.637936
260.98	4.00	0.55	0.001818	0.000250	0.001568	0.637681
261.92	4.00	0.55	0.001818	0.000250	0.001568	0.637681
262.19	4.01	0.55	0.001818	0.000249	0.001569	0.637428
262.72	4.01	0.55	0.001818	0.000249	0.001569	0.637428
262.85	4.02	0.55	0.001818	0.000249	0.001569	0.637176
263.53	4.02	0.55	0.001818	0.000249	0.001569	0.637176
263.70	4.03	0.55	0.001818	0.000248	0.001570	0.636925
263.79	4.03	0.56	0.001786	0.000248	0.001538	0.650375
264.45	4.03	0.56	0.001786	0.000248	0.001538	0.650375
264.60	4.04	0.56	0.001786	0.000248	0.001538	0.650115
265.40	4.04	0.56	0.001786	0.000248	0.001538	0.650115
265.53	4.05	0.56	0.001786	0.000247	0.001539	0.649857
266.40	4.05	0.56	0.001786	0.000247	0.001539	0.649857
266.47	4.06	0.56	0.001786	0.000246	0.001539	0.649600
267.01	4.06	0.56	0.001786	0.000246	0.001539	0.649600
267.14	4.07	0.56	0.001786	0.000246	0.001540	0.649345
267.75	4.07	0.56	0.001786	0.000246	0.001540	0.649345
267.81	4.08	0.56	0.001786	0.000245	0.001541	0.649091
268.35	4.08	0.56	0.001786	0.000245	0.001541	0.649091
268.47	4.09	0.56	0.001786	0.000244	0.001541	0.648839
268.65	4.10	0.56	0.001786	0.000244	0.001542	0.648588
269.14	4.10	0.56	0.001786	0.000244	0.001542	0.648588
269.25	4.11	0.56	0.001786	0.000243	0.001542	0.648338
270.00	4.11	0.56	0.001786	0.000243	0.001542	0.648338
270.15	4.12	0.56	0.001786	0.000243	0.001543	0.648090
270.21	4.12	0.56	0.001786	0.000243	0.001543	0.648090
270.34	4.13	0.56	0.001786	0.000242	0.001544	0.647843
271.14	4.13	0.56	0.001786	0.000242	0.001544	0.647843
271.27	4.14	0.56	0.001786	0.000242	0.001544	0.647598
271.35	4.14	0.56	0.001786	0.000242	0.001544	0.647598
271.50	4.14	0.58	0.001724	0.000242	0.001483	0.674494
271.68	4.14	0.58	0.001724	0.000242	0.001483	0.674494
271.80	4.15	0.58	0.001724	0.000241	0.001483	0.674230
271.81	4.15	0.58	0.001724	0.000241	0.001483	0.674230
271.95	4.15	0.58	0.001724	0.000241	0.001483	0.674230
272.08	4.15	0.58	0.001724	0.000241	0.001483	0.674230
272.10	4.15	0.58	0.001724	0.000241	0.001483	0.674230
272.35	4.16	0.58	0.001724	0.000240	0.001484	0.673966
272.75	4.16	0.58	0.001724	0.000240	0.001484	0.673966
272.88	4.17	0.58	0.001724	0.000240	0.001484	0.673705
273.28	4.17	0.58	0.001724	0.000240	0.001484	0.673705
273.45	4.18	0.58	0.001724	0.000239	0.001485	0.673444
274.08	4.18	0.58	0.001724	0.000239	0.001485	0.673444
274.20	4.19	0.58	0.001724	0.000239	0.001485	0.673186
274.65	4.19	0.58	0.001724	0.000239	0.001485	0.673186
274.75	4.20	0.58	0.001724	0.000238	0.001486	0.672928
275.55	4.20	0.58	0.001724	0.000238	0.001486	0.672928
275.69	4.21	0.58	0.001724	0.000238	0.001487	0.672672
276.36	4.21	0.58	0.001724	0.000238	0.001487	0.672672
276.45	4.22	0.58	0.001724	0.000237	0.001487	0.672418
276.89	4.22	0.58	0.001724	0.000237	0.001487	0.672418
277.16	4.23	0.58	0.001724	0.000236	0.001488	0.672164
277.43	4.23	0.58	0.001724	0.000236	0.001488	0.672164
277.56	4.23	0.59	0.001695	0.000236	0.001459	0.685632
277.64	4.23	0.59	0.001695	0.000236	0.001459	0.685632

Temp	T_2	T_2^*	$1/T_2^*$	$1/T_2$	$y=1/T_2^*-1/T_2$	$1/y$
277.83	4.24	0.59	0.001695	0.000236	0.001459	0.685370
278.10	4.24	0.59	0.001695	0.000236	0.001459	0.685370
278.23	4.25	0.59	0.001695	0.000235	0.001460	0.685109
278.90	4.25	0.59	0.001695	0.000235	0.001460	0.685109
279.00	4.26	0.59	0.001695	0.000235	0.001460	0.684850
279.59	4.26	0.59	0.001695	0.000235	0.001460	0.684850
279.70	4.27	0.59	0.001695	0.000234	0.001461	0.684592
280.35	4.27	0.59	0.001695	0.000234	0.001461	0.684592
280.50	4.28	0.59	0.001695	0.000234	0.001461	0.684336
281.10	4.28	0.59	0.001695	0.000234	0.001461	0.684336
281.17	4.29	0.59	0.001695	0.000233	0.001462	0.684081
281.44	4.29	0.59	0.001695	0.000233	0.001462	0.684081
281.54	4.30	0.59	0.001695	0.000233	0.001462	0.683827
282.14	4.30	0.59	0.001695	0.000233	0.001462	0.683827
282.30	4.31	0.59	0.001695	0.000232	0.001463	0.683575
282.91	4.31	0.59	0.001695	0.000232	0.001463	0.683575
283.05	4.32	0.59	0.001695	0.000231	0.001463	0.683324
283.72	4.32	0.59	0.001695	0.000231	0.001463	0.683324
283.80	4.33	0.59	0.001695	0.000231	0.001464	0.683075
283.85	4.33	0.59	0.001695	0.000231	0.001464	0.683075
283.98	4.34	0.59	0.001695	0.000230	0.001465	0.682827
284.55	4.34	0.59	0.001695	0.000230	0.001465	0.682827
284.65	4.35	0.59	0.001695	0.000230	0.001465	0.682580
285.30	4.35	0.59	0.001695	0.000230	0.001465	0.682580
285.45	4.36	0.59	0.001695	0.000229	0.001466	0.682334
285.85	4.36	0.59	0.001695	0.000229	0.001466	0.682334
286.05	4.37	0.60	0.001667	0.000229	0.001438	0.695491
286.25	4.37	0.60	0.001667	0.000229	0.001438	0.695491
286.35	4.38	0.60	0.001667	0.000228	0.001438	0.695238
287.11	4.38	0.60	0.001667	0.000228	0.001438	0.695238
287.19	4.39	0.60	0.001667	0.000228	0.001439	0.694987
287.59	4.39	0.60	0.001667	0.000228	0.001439	0.694987
287.71	4.40	0.60	0.001667	0.000227	0.001439	0.694737
288.26	4.40	0.60	0.001667	0.000227	0.001439	0.694737
288.39	4.41	0.60	0.001667	0.000227	0.001440	0.694488
288.60	4.41	0.60	0.001667	0.000227	0.001440	0.694488
288.79	4.42	0.60	0.001667	0.000226	0.001440	0.694241
289.46	4.42	0.60	0.001667	0.000226	0.001440	0.694241
289.66	4.43	0.60	0.001667	0.000226	0.001441	0.693995
290.41	4.43	0.60	0.001667	0.000226	0.001441	0.693995
290.66	4.44	0.60	0.001667	0.000225	0.001441	0.693750
290.86	4.44	0.60	0.001667	0.000225	0.001441	0.693750
291.07	4.45	0.60	0.001667	0.000225	0.001442	0.693506
291.47	4.45	0.60	0.001667	0.000225	0.001442	0.693506
291.60	4.46	0.60	0.001667	0.000224	0.001442	0.693264
292.07	4.46	0.60	0.001667	0.000224	0.001442	0.693264
292.14	4.47	0.60	0.001667	0.000224	0.001443	0.693023
292.68	4.47	0.60	0.001667	0.000224	0.001443	0.693023
292.81	4.48	0.60	0.001667	0.000223	0.001443	0.692784
293.27	4.48	0.60	0.001667	0.000223	0.001443	0.692784
293.57	4.49	0.60	0.001667	0.000223	0.001444	0.692545
294.42	4.49	0.60	0.001667	0.000223	0.001444	0.692545
294.63	4.50	0.60	0.001667	0.000222	0.001444	0.692308
294.78	4.50	0.60	0.001667	0.000222	0.001444	0.692308
294.82	4.50	0.61	0.001639	0.000222	0.001417	0.705656
294.92	4.50	0.62	0.001613	0.000222	0.001391	0.719072
295.23	4.50	0.62	0.001613	0.000222	0.001391	0.719072
295.49	4.51	0.62	0.001613	0.000222	0.001391	0.718817
295.76	4.51	0.62	0.001613	0.000222	0.001391	0.718817
295.83	4.52	0.62	0.001613	0.000221	0.001392	0.718564
296.43	4.52	0.62	0.001613	0.000221	0.001392	0.718564
296.70	4.53	0.62	0.001613	0.000221	0.001392	0.718312
296.97	4.53	0.62	0.001613	0.000221	0.001392	0.718312

Temp	T_2	T_2^*	$1/T_2^*$	$1/T_2$	$y=1/T_2^*-1/T_2$	$1/y$
297.18	4.54	0.62	0.001613	0.000220	0.001393	0.718061
297.79	4.54	0.62	0.001613	0.000220	0.001393	0.718061
297.90	4.55	0.62	0.001613	0.000220	0.001393	0.717812
298.30	4.55	0.62	0.001613	0.000220	0.001393	0.717812
298.54	4.56	0.62	0.001613	0.000219	0.001394	0.717563
298.57	4.56	0.62	0.001613	0.000219	0.001394	0.717563
298.69	4.56	0.62	0.001613	0.000219	0.001394	0.717563
298.84	4.56	0.62	0.001613	0.000219	0.001394	0.717563
298.84	4.56	0.62	0.001613	0.000219	0.001394	0.717563
298.97	4.57	0.62	0.001613	0.000219	0.001394	0.717316
299.14	4.57	0.62	0.001613	0.000219	0.001394	0.717316
299.37	4.58	0.62	0.001613	0.000218	0.001395	0.717071
299.78	4.58	0.62	0.001613	0.000218	0.001395	0.717071
299.90	4.59	0.62	0.001613	0.000218	0.001395	0.716826
300.44	4.59	0.62	0.001613	0.000218	0.001395	0.716826
300.71	4.60	0.62	0.001613	0.000217	0.001396	0.716583
300.84	4.61	0.62	0.001613	0.000217	0.001396	0.716341
301.51	4.61	0.62	0.001613	0.000217	0.001396	0.716341
301.64	4.62	0.62	0.001613	0.000216	0.001396	0.716100
301.91	4.62	0.62	0.001613	0.000216	0.001396	0.716100
302.05	4.63	0.62	0.001613	0.000216	0.001397	0.715860
302.31	4.63	0.62	0.001613	0.000216	0.001397	0.715860
302.44	4.64	0.62	0.001613	0.000216	0.001397	0.715622
302.71	4.64	0.62	0.001613	0.000216	0.001397	0.715622
302.98	4.65	0.62	0.001613	0.000215	0.001398	0.715385
303.38	4.65	0.62	0.001613	0.000215	0.001398	0.715385
303.51	4.66	0.62	0.001613	0.000215	0.001398	0.715149
303.78	4.67	0.62	0.001613	0.000214	0.001399	0.714914
304.32	4.67	0.62	0.001613	0.000214	0.001399	0.714914
304.45	4.68	0.62	0.001613	0.000214	0.001399	0.714680
304.58	4.68	0.62	0.001613	0.000214	0.001399	0.714680
304.85	4.69	0.62	0.001613	0.000213	0.001399	0.714563
305.12	4.69	0.62	0.001613	0.000213	0.001400	0.714447
305.25	4.70	0.62	0.001613	0.000213	0.001400	0.714216
305.65	4.70	0.62	0.001613	0.000213	0.001400	0.714216
305.92	4.71	0.62	0.001613	0.000212	0.001401	0.713985
306.05	4.71	0.62	0.001613	0.000212	0.001401	0.713985
306.32	4.72	0.62	0.001613	0.000212	0.001401	0.713756
306.59	4.72	0.62	0.001613	0.000212	0.001401	0.713756
306.85	4.73	0.62	0.001613	0.000211	0.001401	0.713528
307.39	4.73	0.62	0.001613	0.000211	0.001401	0.713528
307.66	4.74	0.62	0.001613	0.000211	0.001402	0.713301
307.92	4.75	0.63	0.001587	0.000211	0.001377	0.726335
308.46	4.75	0.63	0.001587	0.000211	0.001377	0.726335
308.59	4.76	0.63	0.001587	0.000210	0.001377	0.726102
309.00	4.76	0.63	0.001587	0.000210	0.001377	0.726102
309.13	4.77	0.63	0.001587	0.000210	0.001378	0.725870
309.40	4.77	0.63	0.001587	0.000210	0.001378	0.725870
309.53	4.78	0.63	0.001587	0.000209	0.001378	0.725639
309.80	4.78	0.63	0.001587	0.000209	0.001378	0.725639
309.93	4.79	0.63	0.001587	0.000209	0.001378	0.725523
310.60	4.79	0.63	0.001587	0.000209	0.001379	0.725409
310.73	4.80	0.63	0.001587	0.000208	0.001379	0.725180
311.28	4.80	0.63	0.001587	0.000208	0.001379	0.725180
311.67	4.81	0.63	0.001587	0.000208	0.001379	0.724952
312.21	4.81	0.63	0.001587	0.000208	0.001379	0.724952
312.34	4.82	0.63	0.001587	0.000207	0.001380	0.724726
312.61	4.83	0.63	0.001587	0.000207	0.001380	0.724500
313.42	4.83	0.63	0.001587	0.000207	0.001380	0.724500
313.69	4.84	0.63	0.001587	0.000207	0.001381	0.724276
313.96	4.84	0.63	0.001587	0.000207	0.001381	0.724276
314.22	4.85	0.63	0.001587	0.000206	0.001381	0.724052
314.77	4.85	0.63	0.001587	0.000206	0.001381	0.724052

Temp	T_2	T_2^*	$1/T_2^*$	$1/T_2$	$y=1/T_2^*-1/T_2$	$1/y$
315.03	4.86	0.63	0.001587	0.000206	0.001382	0.723830
315.97	4.86	0.63	0.001587	0.000206	0.001382	0.723830
316.24	4.87	0.63	0.001587	0.000205	0.001382	0.723608
316.51	4.87	0.63	0.001587	0.000205	0.001382	0.723608
316.64	4.88	0.63	0.001587	0.000205	0.001382	0.723388
317.18	4.88	0.63	0.001587	0.000205	0.001382	0.723388
317.45	4.89	0.63	0.001587	0.000204	0.001383	0.723169
318.12	4.89	0.63	0.001587	0.000204	0.001383	0.723169
318.39	4.90	0.63	0.001587	0.000204	0.001383	0.722951
319.06	4.90	0.63	0.001587	0.000204	0.001383	0.722951
319.19	4.91	0.63	0.001587	0.000204	0.001384	0.722734
319.74	4.91	0.63	0.001587	0.000204	0.001384	0.722734
319.87	4.92	0.63	0.001587	0.000203	0.001384	0.722517
320.14	4.92	0.63	0.001587	0.000203	0.001384	0.722517
320.27	4.93	0.63	0.001587	0.000203	0.001384	0.722302
321.62	4.93	0.63	0.001587	0.000203	0.001384	0.722302
321.75	4.94	0.63	0.001587	0.000202	0.001385	0.722088
322.29	4.94	0.63	0.001587	0.000202	0.001385	0.722088
322.42	4.95	0.63	0.001587	0.000202	0.001385	0.721875
322.69	4.95	0.63	0.001587	0.000202	0.001385	0.721875
322.83	4.95	0.63	0.001587	0.000202	0.001385	0.721875
322.96	4.95	0.63	0.001587	0.000202	0.001385	0.721875
323.23	4.95	0.63	0.001587	0.000202	0.001385	0.721875
323.37	4.95	0.63	0.001587	0.000202	0.001385	0.721875
323.64	4.95	0.63	0.001587	0.000202	0.001385	0.721875
323.91	4.95	0.63	0.001587	0.000202	0.001385	0.721875
324.04	4.96	0.63	0.001587	0.000202	0.001386	0.721663
325.66	4.96	0.63	0.001587	0.000202	0.001386	0.721663
325.93	4.97	0.63	0.001587	0.000201	0.001386	0.721452
326.61	4.97	0.63	0.001587	0.000201	0.001386	0.721452
326.87	4.98	0.63	0.001587	0.000201	0.001386	0.721241
327.68	4.98	0.63	0.001587	0.000201	0.001386	0.721241
328.22	4.99	0.63	0.001587	0.000200	0.001387	0.721032
329.30	4.99	0.63	0.001587	0.000200	0.001387	0.721032
329.57	5.00	0.63	0.001587	0.000200	0.001387	0.720824
329.98	5.00	0.63	0.001587	0.000200	0.001387	0.720824
330.38	5.01	0.63	0.001587	0.000200	0.001388	0.720616
331.19	5.01	0.63	0.001587	0.000200	0.001388	0.720616
331.59	5.02	0.62	0.001613	0.000199	0.001414	0.707364
332.67	5.02	0.62	0.001613	0.000199	0.001414	0.707364
332.94	5.03	0.62	0.001613	0.000199	0.001414	0.707166
334.43	5.03	0.62	0.001613	0.000199	0.001414	0.707166
334.56	5.04	0.62	0.001613	0.000198	0.001414	0.706968
335.37	5.04	0.62	0.001613	0.000198	0.001414	0.706968
335.64	5.05	0.62	0.001613	0.000198	0.001415	0.706772
336.31	5.05	0.62	0.001613	0.000198	0.001415	0.706772
336.58	5.06	0.62	0.001613	0.000198	0.001415	0.706577
337.53	5.06	0.62	0.001613	0.000198	0.001415	0.706577
337.66	5.07	0.62	0.001613	0.000197	0.001416	0.706382
339.82	5.07	0.62	0.001613	0.000197	0.001416	0.706382
340.09	5.07	0.61	0.001639	0.000197	0.001442	0.693430
340.50	5.07	0.60	0.001667	0.000197	0.001469	0.680537
340.77	5.08	0.60	0.001667	0.000197	0.001470	0.680357
344.56	5.08	0.60	0.001667	0.000197	0.001470	0.680357
344.82	5.09	0.60	0.001667	0.000196	0.001470	0.680178
345.23	5.09	0.60	0.001667	0.000196	0.001470	0.680178
345.50	5.09	0.59	0.001695	0.000196	0.001498	0.667356
347.94	5.09	0.59	0.001695	0.000196	0.001498	0.667356
348.35	5.08	0.59	0.001695	0.000197	0.001498	0.667528
348.48	5.08	0.59	0.001695	0.000197	0.001498	0.667528
348.89	5.08	0.58	0.001724	0.000197	0.001527	0.654756
349.97	5.08	0.58	0.001724	0.000197	0.001527	0.654756
350.38	5.09	0.58	0.001724	0.000196	0.001528	0.654590

Temp	T_2	T_2^*	$1/T_2^*$	$1/T_2$	$y=1/T_2^*-1/T_2$	$1/y$
350.65	5.09	0.58	0.001724	0.000196	0.001528	0.654590
351.06	5.08	0.58	0.001724	0.000197	0.001527	0.654756
351.73	5.08	0.58	0.001724	0.000197	0.001527	0.654756
352.01	5.08	0.57	0.001754	0.000197	0.001558	0.642040
352.14	5.08	0.56	0.001786	0.000197	0.001589	0.629381
354.04	5.08	0.56	0.001786	0.000197	0.001589	0.629381
354.31	5.07	0.56	0.001786	0.000197	0.001588	0.629534
356.62	5.07	0.56	0.001786	0.000197	0.001588	0.629534
356.89	5.06	0.56	0.001786	0.000198	0.001588	0.629689
357.30	5.07	0.56	0.001786	0.000197	0.001588	0.629534
357.43	5.07	0.56	0.001786	0.000197	0.001588	0.629534
357.84	5.07	0.55	0.001818	0.000197	0.001621	0.616925
357.97	5.07	0.55	0.001818	0.000197	0.001621	0.616925
358.25	5.06	0.55	0.001818	0.000198	0.001621	0.617073
360.28	5.06	0.55	0.001818	0.000198	0.001621	0.617073
360.69	5.06	0.54	0.001852	0.000198	0.001654	0.604513
362.18	5.06	0.54	0.001852	0.000198	0.001654	0.604513
362.32	5.05	0.54	0.001852	0.000198	0.001654	0.604656
362.72	5.05	0.52	0.001923	0.000198	0.001725	0.579691
363.67	5.05	0.52	0.001923	0.000198	0.001725	0.579691
363.81	5.04	0.52	0.001923	0.000198	0.001725	0.579823
364.35	5.04	0.52	0.001923	0.000198	0.001725	0.579823
364.49	5.04	0.51	0.001961	0.000198	0.001762	0.567417
364.76	5.04	0.51	0.001961	0.000198	0.001762	0.567417
365.03	5.03	0.51	0.001961	0.000199	0.001762	0.567544
366.12	5.03	0.51	0.001961	0.000199	0.001762	0.567544
366.39	5.02	0.51	0.001961	0.000199	0.001762	0.567672
366.80	5.02	0.50	0.002000	0.000199	0.001801	0.555310
366.94	5.01	0.50	0.002000	0.000200	0.001800	0.555432
367.76	5.01	0.50	0.002000	0.000200	0.001800	0.555432
367.89	5.00	0.50	0.002000	0.000200	0.001800	0.555556
368.44	5.00	0.50	0.002000	0.000200	0.001800	0.555556
368.71	5.00	0.49	0.002041	0.000200	0.001841	0.543237
368.85	5.00	0.49	0.002041	0.000200	0.001841	0.543237
369.12	4.99	0.49	0.002041	0.000200	0.001840	0.543356
369.66	4.99	0.49	0.002041	0.000200	0.001840	0.543356
369.94	4.98	0.49	0.002041	0.000201	0.001840	0.543474
370.35	4.98	0.49	0.002041	0.000201	0.001840	0.543474
370.48	4.97	0.49	0.002041	0.000201	0.001840	0.543594
370.75	4.97	0.48	0.002083	0.000201	0.001882	0.531314
370.89	4.97	0.48	0.002083	0.000201	0.001882	0.531314
371.16	4.96	0.48	0.002083	0.000202	0.001882	0.531429
372.25	4.96	0.48	0.002083	0.000202	0.001882	0.531429
372.39	4.96	0.47	0.002128	0.000202	0.001926	0.519198
372.80	4.95	0.47	0.002128	0.000202	0.001926	0.519308
373.21	4.95	0.47	0.002128	0.000202	0.001926	0.519308
373.34	4.94	0.47	0.002128	0.000202	0.001925	0.519418
373.75	4.94	0.47	0.002128	0.000202	0.001925	0.519418
374.16	4.93	0.47	0.002128	0.000203	0.001925	0.519529
374.43	4.93	0.47	0.002128	0.000203	0.001925	0.519529
374.70	4.93	0.46	0.002174	0.000203	0.001971	0.507338
375.11	4.92	0.46	0.002174	0.000203	0.001971	0.507444
375.66	4.92	0.46	0.002174	0.000203	0.001971	0.507444
375.80	4.91	0.46	0.002174	0.000204	0.001970	0.507551
376.21	4.90	0.46	0.002174	0.000204	0.001970	0.507658
376.62	4.90	0.46	0.002174	0.000204	0.001970	0.507658
376.89	4.89	0.45	0.002222	0.000204	0.002018	0.495608
377.30	4.89	0.45	0.002222	0.000204	0.002018	0.495608
377.71	4.88	0.45	0.002222	0.000205	0.002017	0.495711
378.12	4.87	0.44	0.002273	0.000205	0.002067	0.483702
378.67	4.86	0.44	0.002273	0.000206	0.002067	0.483801
379.08	4.85	0.43	0.002326	0.000206	0.002119	0.471833
379.49	4.84	0.43	0.002326	0.000207	0.002119	0.471927

Temp	T_2	T_2^*	$1/T_2^*$	$1/T_2$	$y=1/T_2^*-1/T_2$	$1/y$
379.90	4.84	0.43	0.002326	0.000207	0.002119	0.471927
380.31	4.83	0.43	0.002326	0.000207	0.002119	0.472023
380.45	4.82	0.43	0.002326	0.000207	0.002118	0.472118
380.86	4.82	0.43	0.002326	0.000207	0.002118	0.472118
381.13	4.81	0.42	0.002381	0.000208	0.002173	0.460182
381.27	4.81	0.42	0.002381	0.000208	0.002173	0.460182
381.41	4.80	0.42	0.002381	0.000208	0.002173	0.460274
381.68	4.80	0.42	0.002381	0.000208	0.002173	0.460274
381.82	4.79	0.42	0.002381	0.000209	0.002172	0.460366
382.23	4.79	0.42	0.002381	0.000209	0.002172	0.460366
382.50	4.79	0.41	0.002439	0.000209	0.002230	0.448379
382.64	4.78	0.41	0.002439	0.000209	0.002230	0.448467
382.91	4.78	0.41	0.002439	0.000209	0.002230	0.448467
383.19	4.77	0.41	0.002439	0.000210	0.002229	0.448555
383.32	4.77	0.41	0.002439	0.000210	0.002229	0.448555
383.60	4.76	0.41	0.002439	0.000210	0.002229	0.448644
383.73	4.76	0.41	0.002439	0.000210	0.002229	0.448644
383.87	4.75	0.41	0.002439	0.000211	0.002228	0.448733
383.88	4.75	0.41	0.002439	0.000211	0.002228	0.448733
384.15	4.74	0.40	0.002500	0.000211	0.002289	0.436866
384.42	4.73	0.40	0.002500	0.000211	0.002289	0.436952
384.70	4.72	0.40	0.002500	0.000212	0.002288	0.437037
384.84	4.72	0.40	0.002500	0.000212	0.002288	0.437037
385.11	4.71	0.40	0.002500	0.000212	0.002288	0.437123
385.39	4.70	0.40	0.002500	0.000213	0.002287	0.437209
385.67	4.69	0.39	0.002564	0.000213	0.002351	0.425372
386.08	4.68	0.39	0.002564	0.000214	0.002350	0.425455
386.49	4.67	0.39	0.002564	0.000214	0.002350	0.425537
386.77	4.66	0.39	0.002564	0.000215	0.002350	0.425621
387.05	4.64	0.38	0.002632	0.000216	0.002416	0.413897
387.46	4.63	0.38	0.002632	0.000216	0.002416	0.413976
387.73	4.62	0.38	0.002632	0.000216	0.002415	0.414057
388.01	4.62	0.38	0.002632	0.000216	0.002415	0.414057
388.28	4.61	0.37	0.002703	0.000217	0.002486	0.402288
388.42	4.60	0.37	0.002703	0.000217	0.002485	0.402364
388.56	4.60	0.37	0.002703	0.000217	0.002485	0.402364
388.70	4.59	0.37	0.002703	0.000218	0.002485	0.402441
388.84	4.59	0.37	0.002703	0.000218	0.002485	0.402479
388.97	4.58	0.37	0.002703	0.000218	0.002484	0.402518
389.11	4.58	0.37	0.002703	0.000218	0.002484	0.402518
389.25	4.57	0.37	0.002703	0.000219	0.002484	0.402595
389.39	4.57	0.37	0.002703	0.000219	0.002484	0.402621
389.53	4.55	0.37	0.002703	0.000220	0.002483	0.402751
389.80	4.55	0.36	0.002778	0.000220	0.002558	0.390931
389.94	4.54	0.36	0.002778	0.000220	0.002558	0.391005
390.08	4.54	0.36	0.002778	0.000220	0.002558	0.391005
390.36	4.53	0.36	0.002778	0.000221	0.002557	0.391079
390.63	4.52	0.36	0.002778	0.000221	0.002557	0.391154
390.91	4.51	0.36	0.002778	0.000222	0.002556	0.391229
391.32	4.50	0.35	0.002857	0.000222	0.002635	0.379518
391.46	4.49	0.35	0.002857	0.000223	0.002634	0.379589
391.87	4.49	0.35	0.002857	0.000223	0.002634	0.379625
392.01	4.48	0.35	0.002857	0.000223	0.002634	0.379661
392.15	4.47	0.35	0.002857	0.000224	0.002633	0.379733
392.29	4.46	0.35	0.002857	0.000224	0.002633	0.379805
392.42	4.47	0.35	0.002857	0.000224	0.002633	0.379733
392.56	4.45	0.35	0.002857	0.000225	0.002632	0.379878
392.70	4.45	0.35	0.002857	0.000225	0.002632	0.379878
392.84	4.44	0.35	0.002857	0.000225	0.002632	0.379951
392.98	4.44	0.35	0.002857	0.000225	0.002632	0.379988
393.12	4.43	0.35	0.002857	0.000226	0.002631	0.380025
393.26	4.43	0.35	0.002857	0.000226	0.002631	0.380025
393.39	4.42	0.35	0.002857	0.000226	0.002631	0.380098

Temp	T_2	T_2^*	$1/T_2^*$	$1/T_2$	$y=1/T_2^*-1/T_2$	$1/y$
393.40	4.42	0.35	0.002857	0.000227	0.002631	0.380135
393.54	4.41	0.35	0.002857	0.000227	0.002630	0.380172
393.68	4.40	0.35	0.002857	0.000228	0.002630	0.380284
393.82	4.39	0.35	0.002857	0.000228	0.002629	0.380322
393.96	4.38	0.35	0.002857	0.000228	0.002629	0.380397
394.10	4.38	0.35	0.002857	0.000229	0.002629	0.380435
394.24	4.37	0.35	0.002857	0.000229	0.002628	0.380511
394.38	4.36	0.35	0.002857	0.000230	0.002628	0.380587
394.52	4.35	0.34	0.002941	0.000230	0.002711	0.368828
394.66	4.34	0.34	0.002941	0.000230	0.002711	0.368900
394.67	4.33	0.34	0.002941	0.000231	0.002710	0.368972
394.80	4.32	0.34	0.002941	0.000231	0.002710	0.369045
394.81	4.32	0.34	0.002941	0.000231	0.002710	0.369045
394.95	4.31	0.34	0.002941	0.000232	0.002709	0.369118
395.09	4.30	0.34	0.002941	0.000233	0.002708	0.369217
395.23	4.29	0.34	0.002941	0.000233	0.002708	0.369303
395.37	4.28	0.34	0.002941	0.000234	0.002707	0.369377
395.51	4.27	0.34	0.002941	0.000234	0.002707	0.369415
395.65	4.26	0.34	0.002941	0.000235	0.002706	0.369490
395.66	4.25	0.34	0.002941	0.000235	0.002706	0.369565
395.80	4.25	0.34	0.002941	0.000235	0.002706	0.369565
395.93	4.24	0.34	0.002941	0.000236	0.002705	0.369641
396.21	4.23	0.34	0.002941	0.000237	0.002704	0.369755
396.36	4.21	0.33	0.003030	0.000238	0.002793	0.358067
396.63	4.21	0.33	0.003030	0.000238	0.002793	0.358067
396.91	4.20	0.33	0.003030	0.000238	0.002792	0.358140
397.05	4.19	0.33	0.003030	0.000239	0.002792	0.358212
397.18	4.19	0.33	0.003030	0.000239	0.002792	0.358212
397.32	4.18	0.33	0.003030	0.000239	0.002791	0.358286
397.60	4.17	0.33	0.003030	0.000240	0.002790	0.358359
397.74	4.16	0.33	0.003030	0.000240	0.002790	0.358433
397.88	4.16	0.33	0.003030	0.000240	0.002790	0.358433
398.15	4.15	0.32	0.003125	0.000241	0.002884	0.346736
398.30	4.14	0.32	0.003125	0.000242	0.002883	0.346806
398.44	4.13	0.32	0.003125	0.000242	0.002883	0.346877
398.57	4.12	0.32	0.003125	0.000243	0.002882	0.346947
398.98	4.12	0.32	0.003125	0.000243	0.002882	0.346947
399.12	4.11	0.32	0.003125	0.000243	0.002882	0.347018
399.27	4.09	0.32	0.003125	0.000244	0.002881	0.347162
399.68	4.09	0.32	0.003125	0.000244	0.002881	0.347162
399.82	4.08	0.32	0.003125	0.000245	0.002880	0.347234
400.09	4.07	0.32	0.003125	0.000246	0.002879	0.347307
400.23	4.06	0.32	0.003125	0.000246	0.002879	0.347380
400.37	4.05	0.32	0.003125	0.000247	0.002878	0.347453
400.65	4.05	0.32	0.003125	0.000247	0.002878	0.347453
400.79	4.04	0.31	0.003226	0.000248	0.002978	0.335764
400.93	4.03	0.31	0.003226	0.000248	0.002978	0.335833
401.07	4.02	0.31	0.003226	0.000249	0.002977	0.335903
401.21	4.01	0.31	0.003226	0.000249	0.002976	0.335973
401.35	4.01	0.31	0.003226	0.000249	0.002976	0.335973
401.49	4.00	0.31	0.003226	0.000250	0.002976	0.336043
401.63	3.99	0.31	0.003226	0.000251	0.002975	0.336114
401.77	3.99	0.31	0.003226	0.000251	0.002975	0.336150
401.91	3.98	0.30	0.003333	0.000251	0.003082	0.324457
402.05	3.97	0.30	0.003333	0.000252	0.003081	0.324523
402.33	3.96	0.30	0.003333	0.000253	0.003081	0.324590
402.47	3.95	0.30	0.003333	0.000253	0.003080	0.324658
402.61	3.94	0.30	0.003333	0.000254	0.003080	0.324725
402.75	3.93	0.30	0.003333	0.000254	0.003079	0.324793
402.89	3.92	0.30	0.003333	0.000255	0.003078	0.324862
403.03	3.92	0.30	0.003333	0.000255	0.003078	0.324862
403.17	3.91	0.30	0.003333	0.000256	0.003077	0.324965
403.31	3.90	0.30	0.003333	0.000257	0.003077	0.325035

Temp	T_2	T_2^*	$1/T_2^*$	$1/T_2$	$y=1/T_2^*-1/T_2$	$1/y$
403.45	3.89	0.30	0.003333	0.000257	0.003076	0.325070
403.46	3.88	0.30	0.003333	0.000258	0.003076	0.325140
403.59	3.88	0.30	0.003333	0.000258	0.003076	0.325140
403.73	3.87	0.30	0.003333	0.000258	0.003075	0.325210
403.74	3.86	0.30	0.003333	0.000259	0.003074	0.325281
403.88	3.86	0.30	0.003333	0.000259	0.003074	0.325281
404.02	3.85	0.30	0.003333	0.000260	0.003074	0.325352
404.16	3.84	0.29	0.003448	0.000260	0.003188	0.313690
404.30	3.83	0.29	0.003448	0.000261	0.003187	0.313791
404.58	3.82	0.29	0.003448	0.000262	0.003186	0.313824
404.72	3.80	0.29	0.003448	0.000263	0.003185	0.313960
404.86	3.80	0.29	0.003448	0.000263	0.003185	0.313960
405.00	3.79	0.28	0.003571	0.000264	0.003308	0.302336
405.14	3.78	0.28	0.003571	0.000265	0.003307	0.302400
405.15	3.77	0.28	0.003571	0.000265	0.003306	0.302464
405.29	3.77	0.28	0.003571	0.000265	0.003306	0.302464
405.43	3.76	0.28	0.003571	0.000266	0.003305	0.302529
405.57	3.75	0.28	0.003571	0.000267	0.003305	0.302594
405.70	3.75	0.28	0.003571	0.000267	0.003305	0.302594
405.71	3.74	0.28	0.003571	0.000267	0.003304	0.302659
405.99	3.73	0.28	0.003571	0.000268	0.003303	0.302725
406.12	3.73	0.28	0.003571	0.000268	0.003303	0.302725
406.26	3.72	0.28	0.003571	0.000269	0.003303	0.302791
406.27	3.72	0.28	0.003571	0.000269	0.003303	0.302791
406.40	3.71	0.28	0.003571	0.000270	0.003302	0.302857
406.54	3.71	0.28	0.003571	0.000270	0.003302	0.302857
406.55	3.70	0.28	0.003571	0.000270	0.003301	0.302924
406.68	3.70	0.28	0.003571	0.000270	0.003301	0.302924
406.82	3.69	0.27	0.003704	0.000271	0.003433	0.291316
406.83	3.68	0.27	0.003704	0.000272	0.003432	0.291378
406.97	3.68	0.27	0.003704	0.000272	0.003432	0.291378
407.11	3.67	0.27	0.003704	0.000272	0.003431	0.291441
407.25	3.66	0.27	0.003704	0.000273	0.003430	0.291504
407.39	3.66	0.27	0.003704	0.000274	0.003430	0.291536
407.53	3.65	0.26	0.003846	0.000274	0.003572	0.279941
407.67	3.64	0.26	0.003846	0.000275	0.003571	0.280000
407.81	3.63	0.26	0.003846	0.000276	0.003570	0.280089
408.09	3.62	0.26	0.003846	0.000276	0.003570	0.280119
408.23	3.61	0.26	0.003846	0.000277	0.003569	0.280199
408.38	3.59	0.26	0.003846	0.000279	0.003568	0.280300
408.51	3.59	0.26	0.003846	0.000279	0.003568	0.280300
408.52	3.58	0.26	0.003846	0.000279	0.003567	0.280361
408.66	3.57	0.26	0.003846	0.000280	0.003566	0.280423
408.80	3.56	0.26	0.003846	0.000281	0.003565	0.280485
408.94	3.55	0.26	0.003846	0.000282	0.003564	0.280547
409.08	3.55	0.26	0.003846	0.000282	0.003564	0.280547
409.09	3.54	0.26	0.003846	0.000282	0.003564	0.280610
409.23	3.53	0.26	0.003846	0.000283	0.003563	0.280673
409.37	3.53	0.26	0.003846	0.000283	0.003563	0.280673
409.51	3.52	0.26	0.003846	0.000284	0.003562	0.280768
409.65	3.51	0.25	0.004000	0.000285	0.003715	0.269172
409.79	3.50	0.25	0.004000	0.000286	0.003714	0.269231
409.93	3.49	0.25	0.004000	0.000287	0.003713	0.269290
410.07	3.48	0.25	0.004000	0.000287	0.003713	0.269350
410.21	3.47	0.25	0.004000	0.000288	0.003712	0.269410
410.22	3.47	0.25	0.004000	0.000288	0.003712	0.269410
410.49	3.46	0.25	0.004000	0.000289	0.003711	0.269470
410.50	3.45	0.25	0.004000	0.000290	0.003710	0.269531
410.64	3.45	0.25	0.004000	0.000290	0.003710	0.269562
410.78	3.43	0.25	0.004000	0.000292	0.003708	0.269654
410.79	3.43	0.25	0.004000	0.000292	0.003708	0.269685
410.93	3.42	0.25	0.004000	0.000292	0.003708	0.269716
411.06	3.42	0.25	0.004000	0.000292	0.003708	0.269716

Temp	T_2	T_2^*	$1/T_2^*$	$1/T_2$	$y=1/T_2^*-1/T_2$	$1/y$
411.07	3.41	0.25	0.004000	0.000293	0.003707	0.269778
411.20	3.41	0.25	0.004000	0.000293	0.003707	0.269778
411.21	3.40	0.25	0.004000	0.000294	0.003706	0.269841
411.35	3.40	0.25	0.004000	0.000295	0.003705	0.269873
411.49	3.39	0.24	0.004167	0.000295	0.003872	0.258286
411.63	3.38	0.24	0.004167	0.000296	0.003871	0.258324
411.77	3.37	0.24	0.004167	0.000297	0.003870	0.258403
411.91	3.36	0.24	0.004167	0.000298	0.003869	0.258462
411.92	3.35	0.24	0.004167	0.000299	0.003868	0.258521
412.06	3.34	0.24	0.004167	0.000299	0.003868	0.258561
412.07	3.33	0.24	0.004167	0.000300	0.003866	0.258641
412.21	3.33	0.24	0.004167	0.000300	0.003866	0.258641
412.35	3.32	0.23	0.004348	0.000302	0.004046	0.247147
412.49	3.31	0.23	0.004348	0.000302	0.004046	0.247175
412.50	3.30	0.23	0.004348	0.000303	0.004045	0.247231
412.64	3.29	0.23	0.004348	0.000304	0.004044	0.247288
412.65	3.28	0.23	0.004348	0.000305	0.004043	0.247344
412.79	3.28	0.23	0.004348	0.000305	0.004043	0.247344
412.93	3.27	0.23	0.004348	0.000306	0.004042	0.247430
413.07	3.25	0.23	0.004348	0.000308	0.004040	0.247517
413.21	3.25	0.23	0.004348	0.000308	0.004040	0.247517
413.22	3.24	0.23	0.004348	0.000309	0.004039	0.247575
413.35	3.24	0.23	0.004348	0.000309	0.004039	0.247575
413.36	3.23	0.23	0.004348	0.000310	0.004038	0.247653
413.50	3.22	0.23	0.004348	0.000311	0.004037	0.247692
413.64	3.22	0.23	0.004348	0.000311	0.004037	0.247722
413.78	3.21	0.23	0.004348	0.000312	0.004036	0.247752
413.92	3.20	0.23	0.004348	0.000313	0.004035	0.247811
413.93	3.19	0.23	0.004348	0.000313	0.004034	0.247872
414.06	3.19	0.23	0.004348	0.000313	0.004034	0.247872
414.07	3.18	0.23	0.004348	0.000314	0.004033	0.247932
414.21	3.17	0.23	0.004348	0.000315	0.004032	0.247993
414.22	3.17	0.23	0.004348	0.000315	0.004032	0.247993
414.36	3.16	0.23	0.004348	0.000317	0.004031	0.248085
414.50	3.15	0.23	0.004348	0.000317	0.004030	0.248116
414.64	3.15	0.22	0.004545	0.000318	0.004227	0.236547
414.65	3.13	0.22	0.004545	0.000320	0.004225	0.236661
414.93	3.12	0.22	0.004545	0.000321	0.004224	0.236718
415.07	3.10	0.22	0.004545	0.000323	0.004223	0.236806
415.21	3.10	0.22	0.004545	0.000323	0.004223	0.236806
415.35	3.09	0.22	0.004545	0.000324	0.004222	0.236864
415.36	3.09	0.22	0.004545	0.000324	0.004222	0.236864
415.50	3.08	0.22	0.004545	0.000325	0.004221	0.236923
415.64	3.07	0.22	0.004545	0.000326	0.004220	0.236982
415.78	3.07	0.21	0.004762	0.000326	0.004436	0.225420
415.92	3.06	0.21	0.004762	0.000327	0.004435	0.225501
416.06	3.05	0.21	0.004762	0.000328	0.004434	0.225528
416.07	3.04	0.21	0.004762	0.000329	0.004433	0.225583
416.21	3.04	0.21	0.004762	0.000329	0.004433	0.225583
416.35	3.03	0.21	0.004762	0.000330	0.004432	0.225638
416.49	3.03	0.21	0.004762	0.000331	0.004431	0.225666
416.63	3.02	0.21	0.004762	0.000332	0.004430	0.225722
416.64	3.00	0.21	0.004762	0.000333	0.004429	0.225806
416.91	3.00	0.21	0.004762	0.000333	0.004429	0.225806
417.05	2.99	0.21	0.004762	0.000334	0.004427	0.225863
417.19	2.99	0.21	0.004762	0.000335	0.004427	0.225892
417.20	2.98	0.21	0.004762	0.000336	0.004426	0.225921
417.34	2.97	0.21	0.004762	0.000337	0.004425	0.225978
417.48	2.96	0.21	0.004762	0.000338	0.004424	0.226036
417.48	2.97	0.21	0.004762	0.000337	0.004425	0.225978
417.62	2.96	0.21	0.004762	0.000338	0.004424	0.226036
417.63	2.95	0.21	0.004762	0.000339	0.004423	0.226095
417.77	2.94	0.20	0.005000	0.000340	0.004660	0.214599

Temp	T_2	T_2^*	$1/T_2^*$	$1/T_2$	$y=1/T_2^*-1/T_2$	$1/y$
417.91	2.93	0.20	0.005000	0.000341	0.004659	0.214652
418.05	2.92	0.20	0.005000	0.000342	0.004658	0.214706
418.06	2.92	0.20	0.005000	0.000342	0.004658	0.214706
418.20	2.91	0.20	0.005000	0.000344	0.004656	0.214760
418.21	2.90	0.20	0.005000	0.000345	0.004655	0.214833
418.35	2.89	0.20	0.005000	0.000346	0.004654	0.214870
418.36	2.88	0.20	0.005000	0.000348	0.004652	0.214953
418.50	2.87	0.20	0.005000	0.000348	0.004652	0.214981
418.51	2.86	0.20	0.005000	0.000350	0.004650	0.215038
418.65	2.85	0.20	0.005000	0.000351	0.004649	0.215094
418.66	2.84	0.20	0.005000	0.000352	0.004648	0.215152
418.81	2.82	0.20	0.005000	0.000354	0.004646	0.215248
418.96	2.81	0.20	0.005000	0.000357	0.004643	0.215355
419.10	2.79	0.19	0.005263	0.000358	0.004905	0.203885
419.11	2.79	0.19	0.005263	0.000358	0.004905	0.203885
419.25	2.78	0.19	0.005263	0.000360	0.004903	0.203965
419.40	2.77	0.19	0.005263	0.000361	0.004902	0.203992
419.54	2.76	0.19	0.005263	0.000363	0 0.0049	0.204074
419.55	2.75	0.19	0.005263	0.000364	0 0.0049	0.204102
419.69	2.74	0.19	0.005263	0.000365	0.004898	0.204157
419.83	2.73	0.19	0.005263	0.000366	0.004897	0.204213
419.97	2.72	0.19	0.005263	0.000368	0.004896	0.204269
419.98	2.72	0.19	0.005263	0.000368	0.004896	0.204269
420.12	2.71	0.19	0.005263	0.000369	0.004894	0.204325
420.13	2.70	0.19	0.005263	0.000370	0.004893	0.204382
420.27	2.70	0.19	0.005263	0.000370	0.004893	0.204382
420.41	2.69	0.19	0.005263	0.000372	0.004891	0.204469
420.55	2.68	0.19	0.005263	0.000373	0.004890	0.204498
420.56	2.67	0.19	0.005263	0.000375	0.004889	0.204556
420.70	2.67	0.19	0.005263	0.000375	0.004889	0.204556
420.84	2.66	0.18	0.005556	0.000376	0.005180	0.193065
420.98	2.65	0.18	0.005556	0.000377	0.005178	0.193117
420.99	2.65	0.18	0.005556	0.000377	0.005178	0.193117
421.13	2.64	0.18	0.005556	0.000380	0.005176	0.193198
421.14	2.62	0.18	0.005556	0.000382	0.005174	0.193279
421.28	2.62	0.18	0.005556	0.000382	0.005174	0.193279
421.42	2.61	0.18	0.005556	0.000383	0.005172	0.193333
421.56	2.60	0.18	0.005556	0.000385	0.005171	0.193388
421.57	2.60	0.18	0.005556	0.000385	0.005170	0.193416
421.58	2.58	0.18	0.005556	0.000388	0.005168	0.193500
421.72	2.58	0.18	0.005556	0.000388	0.005168	0.193500
421.73	2.57	0.18	0.005556	0.000389	0.005166	0.193556
421.87	2.56	0.18	0.005556	0.000391	0.005165	0.193613
421.88	2.55	0.18	0.005556	0.000392	0.005163	0.193671
422.02	2.54	0.18	0.005556	0.000394	0.005162	0.193729
422.16	2.54	0.18	0.005556	0.000394	0.005162	0.193729
422.17	2.53	0.18	0.005556	0.000395	0.005160	0.193787
422.18	2.52	0.18	0.005556	0.000397	0.005158	0.193866
422.19	2.51	0.18	0.005556	0.000398	0.005157	0.193906
422.33	2.50	0.17	0.005882	0.000400	0.005482	0.182403
422.34	2.49	0.17	0.005882	0.000402	0.005481	0.182457
422.35	2.49	0.17	0.005882	0.000402	0.005481	0.182457
422.48	2.48	0.17	0.005882	0.000403	0.005479	0.182511
422.49	2.47	0.17	0.005882	0.000404	0.005478	0.182547
422.50	2.46	0.17	0.005882	0.000406	0.005476	0.182602
422.51	2.46	0.17	0.005882	0.000407	0.005475	0.182648
422.52	2.45	0.17	0.005882	0.000408	0.005474	0.182675
422.65	2.44	0.17	0.005882	0.000410	0.005473	0.182731
422.66	2.44	0.17	0.005882	0.000410	0.005473	0.182731
422.67	2.43	0.17	0.005882	0.000412	0.005470	0.182806
422.68	2.42	0.17	0.005882	0.000413	0.005469	0.182844
422.82	2.41	0.17	0.005882	0.000415	0.005467	0.182902
422.83	2.40	0.17	0.005882	0.000417	0.005466	0.182960

Temp	T_2	T_2^*	$1/T_2^*$	$1/T_2$	$y=1/T_2^*-1/T_2$	$1/y$
422.97	2.40	0.17	0.005882	0.000418	0.005465	0.182989
422.98	2.39	0.17	0.005882	0.000418	0.005464	0.183018
423.12	2.38	0.17	0.005882	0.000420	0.005462	0.183077
423.13	2.37	0.17	0.005882	0.000422	0.005460	0.183136
423.14	2.36	0.17	0.005882	0.000424	0.005459	0.183196
423.15	2.35	0.17	0.005882	0.000426	0.005457	0.183257
423.29	2.35	0.17	0.005882	0.000426	0.005456	0.183287
423.30	2.34	0.17	0.005882	0.000428	0.005454	0.183349
423.31	2.33	0.17	0.005882	0.000430	0.005452	0.183411
423.45	2.32	0.17	0.005882	0.000431	0.005451	0.183442
423.46	2.31	0.17	0.005882	0.000433	0.005449	0.183505
423.60	2.30	0.17	0.005882	0.000435	0.005448	0.183568
423.61	2.29	0.17	0.005882	0.000436	0.005446	0.183611
423.75	2.29	0.17	0.005882	0.000437	0.005446	0.183632
423.76	2.28	0.17	0.005882	0.000439	0.005444	0.183697
423.90	2.27	0.17	0.005882	0.000441	0.005442	0.183762
423.91	2.27	0.17	0.005882	0.000442	0.005441	0.183795
424.05	2.26	0.17	0.005882	0.000442	0.005440	0.183828
424.06	2.25	0.17	0.005882	0.000444	0.005438	0.183894
424.20	2.24	0.17	0.005882	0.000446	0.005436	0.183961
424.34	2.24	0.17	0.005882	0.000446	0.005436	0.183961
424.35	2.23	0.17	0.005882	0.000448	0.005434	0.184029
424.49	2.23	0.16	0.006250	0.000448	0.005802	0.172367
424.50	2.22	0.16	0.006250	0.000450	0.005800	0.172427
424.64	2.21	0.16	0.006250	0.000452	0.005798	0.172488
424.78	2.21	0.16	0.006250	0.000454	0.005796	0.172518
424.79	2.20	0.16	0.006250	0.000455	0.005795	0.172549
424.92	2.20	0.16	0.006250	0.000455	0.005795	0.172549
424.93	2.19	0.16	0.006250	0.000457	0.005793	0.172611
425.07	2.19	0.16	0.006250	0.000458	0.005792	0.172642
425.08	2.18	0.16	0.006250	0.000459	0.005791	0.172673
425.22	2.17	0.16	0.006250	0.000461	0.005789	0.172736
425.23	2.17	0.16	0.006250	0.000462	0.005788	0.172768
425.24	2.15	0.16	0.006250	0.000464	0.005786	0.172843
425.38	2.14	0.16	0.006250	0.000467	0.005783	0.172929
425.39	2.14	0.16	0.006250	0.000468	0.005782	0.172962
425.40	2.13	0.16	0.006250	0.000470	0.005780	0.173017
425.41	2.12	0.16	0.006250	0.000472	0.005778	0.173061
425.42	2.11	0.16	0.006250	0.000474	0.005776	0.173128
425.43	2.11	0.16	0.006250	0.000475	0.005775	0.173162
425.44	2.09	0.16	0.006250	0.000478	0.005772	0.173264
425.45	2.09	0.16	0.006250	0.000480	0.005770	0.173299
425.46	2.08	0.16	0.006250	0.000482	0.005768	0.173368
425.47	2.07	0.16	0.006250	0.000483	0.005767	0.173403
425.48	2.06	0.16	0.006250	0.000487	0.005763	0.173509
425.49	2.05	0.16	0.006250	0.000489	0.005761	0.173581
425.50	2.04	0.16	0.006250	0.000490	0.005760	0.173617
425.51	2.03	0.16	0.006250	0.000493	0.005757	0.173690
425.64	2.03	0.16	0.006250	0.000493	0.005757	0.173690
425.65	2.03	0.16	0.006250	0.000493	0.005757	0.173690
425.66	2.02	0.16	0.006250	0.000495	0.005755	0.173763
425.67	2.01	0.16	0.006250	0.000498	0.005752	0.173838
425.68	2.00	0.16	0.006250	0.000500	0.005750	0.173913
425.69	1.99	0.16	0.006250	0.000503	0.005747	0.173989
425.70	1.98	0.16	0.006250	0.000505	0.005745	0.174066
425.84	1.97	0.15	0.006667	0.000508	0.006159	0.162363
425.85	1.97	0.15	0.006667	0.000508	0.006159	0.162363
425.86	1.96	0.15	0.006667	0.000510	0.006156	0.162431
426.00	1.96	0.15	0.006667	0.000512	0.006155	0.162465
426.01	1.95	0.15	0.006667	0.000514	0.006153	0.162535
426.02	1.94	0.15	0.006667	0.000515	0.006151	0.162570
426.03	1.93	0.15	0.006667	0.000518	0.006149	0.162640
426.04	1.92	0.15	0.006667	0.000521	0.006146	0.162712

Temp	T_2	T_2^*	$1/T_2^*$	$1/T_2$	$y=1/T_2^*-1/T_2$	$1/y$
426.05	1.92	0.15	0.006667	0.000521	0.006146	0.162712
426.19	1.91	0.15	0.006667	0.000524	0.006143	0.162784
426.20	1.90	0.15	0.006667	0.000526	0.006140	0.162857
426.21	1.89	0.15	0.006667	0.000529	0.006138	0.162931
426.35	1.89	0.15	0.006667	0.000529	0.006138	0.162931
426.36	1.88	0.15	0.006667	0.000532	0.006135	0.163006
426.37	1.87	0.15	0.006667	0.000535	0.006132	0.163081
426.38	1.86	0.15	0.006667	0.000537	0.006130	0.163132
426.39	1.86	0.15	0.006667	0.000539	0.006128	0.163196
426.53	1.85	0.15	0.006667	0.000541	0.006126	0.163235
426.54	1.84	0.15	0.006667	0.000542	0.006124	0.163287
426.55	1.84	0.15	0.006667	0.000543	0.006123	0.163314
426.69	1.83	0.15	0.006667	0.000546	0.006120	0.163393
426.70	1.82	0.15	0.006667	0.000549	0.006117	0.163473
426.84	1.82	0.15	0.006667	0.000549	0.006117	0.163473
426.85	1.81	0.15	0.006667	0.000552	0.006114	0.163554
426.99	1.81	0.15	0.006667	0.000554	0.006113	0.163595
427.00	1.80	0.15	0.006667	0.000556	0.006111	0.163636
427.01	1.79	0.15	0.006667	0.000559	0.006108	0.163720
427.02	1.79	0.15	0.006667	0.000560	0.006106	0.163761
427.03	1.78	0.15	0.006667	0.000563	0.006103	0.163846
427.04	1.77	0.15	0.006667	0.000567	0.006100	0.163932
427.08	1.64	0.15	0.006667	0.000610	0.006057	0.165101
427.09	1.63	0.15	0.006667	0.000613	0.006053	0.165203
427.10	1.62	0.15	0.006667	0.000616	0.006051	0.165271
427.11	1.62	0.15	0.006667	0.000617	0.006049	0.165306
427.12	1.61	0.15	0.006667	0.000621	0.006046	0.165411
427.13	1.61	0.15	0.006667	0.000623	0.006044	0.165464
427.14	1.60	0.15	0.006667	0.000624	0.006043	0.165482
427.18	1.59	0.15	0.006667	0.000629	0.006038	0.165625
427.19	1.58	0.15	0.006667	0.000633	0.006034	0.165734
427.31	1.58	0.15	0.006667	0.000633	0.006034	0.165734
427.32	1.57	0.15	0.006667	0.000638	0.006028	0.165882
427.32	1.57	0.15	0.006667	0.000638	0.006028	0.165882
427.33	1.56	0.15	0.006667	0.000641	0.006026	0.165957
427.34	1.55	0.15	0.006667	0.000645	0.006022	0.166071
427.34	1.55	0.15	0.006667	0.000645	0.006022	0.166071
427.35	1.54	0.15	0.006667	0.000648	0.006019	0.166148
427.36	1.54	0.15	0.006667	0.000649	0.006017	0.166187
427.37	1.53	0.15	0.006667	0.000654	0.006013	0.166304
427.51	1.53	0.15	0.006667	0.000654	0.006013	0.166304
427.52	1.52	0.15	0.006667	0.000658	0.006009	0.166423
427.53	1.51	0.15	0.006667	0.000662	0.006004	0.166544
427.54	1.51	0.15	0.006667	0.000664	0.006003	0.166585
427.55	1.50	0.15	0.006667	0.000667	0.006000	0.166667
427.69	1.50	0.15	0.006667	0.000667	0.006000	0.166667
427.70	1.49	0.15	0.006667	0.000671	0.005996	0.166791
427.71	1.48	0.15	0.006667	0.000676	0.005991	0.166917
427.85	1.48	0.14	0.007143	0.000676	0.006467	0.154627
427.86	1.47	0.14	0.007143	0.000680	0.006463	0.154737
427.87	1.46	0.14	0.007143	0.000685	0.006458	0.154848
427.88	1.45	0.14	0.007143	0.000690	0.006453	0.154962
427.88	1.45	0.14	0.007143	0.000690	0.006453	0.154962
427.89	1.44	0.14	0.007143	0.000694	0.006448	0.155077
427.89	1.44	0.14	0.007143	0.000694	0.006448	0.155077
427.90	1.42	0.14	0.007143	0.000704	0.006439	0.155313
427.90	1.42	0.14	0.007143	0.000704	0.006439	0.155313
427.91	1.41	0.14	0.007143	0.000709	0.006434	0.155433
427.91	1.41	0.14	0.007143	0.000709	0.006434	0.155433
427.92	1.40	0.14	0.007143	0.000714	0.006429	0.155556
427.92	1.40	0.14	0.007143	0.000714	0.006429	0.155556
427.93	1.39	0.14	0.007143	0.000719	0.006423	0.15568
427.93	1.39	0.14	0.007143	0.000719	0.006423	0.15568

Temp	T_2	T_2^*	$1/T_2^*$	$1/T_2$	$y=1/T_2^*-1/T_2$	$1/y$
427.94	1.38	0.14	0.007143	0.000725	0.006418	0.155806
427.94	1.38	0.14	0.007143	0.000725	0.006418	0.155806
427.95	1.37	0.14	0.007143	0.000730	0.006413	0.155935
427.95	1.37	0.14	0.007143	0.000730	0.006413	0.155935
427.96	1.36	0.14	0.007143	0.000735	0.006408	0.156066
427.96	1.36	0.14	0.007143	0.000735	0.006408	0.156066
427.97	1.35	0.14	0.007143	0.000741	0.006402	0.156198
427.97	1.35	0.14	0.007143	0.000741	0.006402	0.156198
427.98	1.33	0.14	0.007143	0.000752	0.006391	0.156471
427.98	1.33	0.14	0.007143	0.000752	0.006391	0.156471
427.99	1.32	0.14	0.007143	0.000758	0.006385	0.156610
427.99	1.32	0.14	0.007143	0.000758	0.006385	0.156610
427.99	1.32	0.14	0.007143	0.000758	0.006385	0.156610
428.00	1.31	0.14	0.007143	0.000763	0.006379	0.156752
428.00	1.31	0.14	0.007143	0.000763	0.006379	0.156752
428.01	1.30	0.14	0.007143	0.000767	0.006376	0.156848
428.02	1.30	0.14	0.007143	0.000771	0.006372	0.156945
428.03	1.29	0.14	0.007143	0.000775	0.006368	0.157043
428.17	1.29	0.14	0.007143	0.000775	0.006368	0.157043
428.18	1.28	0.14	0.007143	0.000781	0.006362	0.157193
428.19	1.28	0.14	0.007143	0.000781	0.006362	0.157193
428.20	1.27	0.14	0.007143	0.000787	0.006355	0.157345
428.21	1.27	0.14	0.007143	0.000791	0.006352	0.157422
428.35	1.26	0.14	0.007143	0.000794	0.006349	0.157500
428.36	1.26	0.14	0.007143	0.000794	0.006349	0.157500
428.37	1.25	0.14	0.007143	0.000800	0.006343	0.157658
428.38	1.25	0.14	0.007143	0.000800	0.006343	0.157658
428.39	1.24	0.14	0.007143	0.000806	0.006336	0.157818
428.40	1.24	0.14	0.007143	0.000810	0.006333	0.157900
428.41	1.23	0.14	0.007143	0.000813	0.006330	0.157982
428.42	1.23	0.14	0.007143	0.000815	0.006328	0.158037
428.43	1.22	0.14	0.007143	0.000820	0.006323	0.158148
428.44	1.21	0.14	0.007143	0.000826	0.006316	0.158318
428.45	1.21	0.14	0.007143	0.000826	0.006316	0.158318
428.46	1.20	0.14	0.007143	0.000831	0.006312	0.158433
428.47	1.20	0.14	0.007143	0.000833	0.006310	0.158491
428.48	1.19	0.14	0.007143	0.000840	0.006303	0.158667
428.49	1.19	0.14	0.007143	0.000840	0.006303	0.158667
428.50	1.18	0.14	0.007143	0.000847	0.006295	0.158846
428.51	1.18	0.14	0.007143	0.000847	0.006295	0.158846
428.52	1.17	0.14	0.007143	0.000855	0.006288	0.159029
428.53	1.17	0.14	0.007143	0.000855	0.006288	0.159029
428.54	1.16	0.14	0.007143	0.000862	0.006281	0.159216
428.55	1.16	0.14	0.007143	0.000862	0.006281	0.159216
428.69	1.15	0.14	0.007143	0.000870	0.006273	0.159406
428.70	1.15	0.14	0.007143	0.000870	0.006273	0.159406
428.71	1.14	0.14	0.007143	0.000877	0.006266	0.159600
428.72	1.14	0.14	0.007143	0.000877	0.006266	0.159600
428.73	1.13	0.14	0.007143	0.000882	0.006261	0.159732
428.74	1.13	0.14	0.007143	0.000885	0.006250	0.159798
428.88	1.13	0.13	0.007692	0.000888	0.006805	0.146957
428.89	1.12	0.13	0.007692	0.000893	0.006799	0.147071
428.90	1.12	0.13	0.007692	0.000893	0.006799	0.147071
428.91	1.11	0.13	0.007692	0.000901	0.006791	0.147245
429.19	1.11	0.13	0.007692	0.000901	0.006791	0.147245
429.20	1.10	0.13	0.007692	0.000909	0.006783	0.147423
429.21	1.10	0.13	0.007692	0.000909	0.006783	0.147423
429.35	1.09	0.13	0.007692	0.000917	0.006775	0.147604
429.50	1.09	0.13	0.007692	0.000917	0.006775	0.147604
429.51	1.08	0.13	0.007692	0.000926	0.006766	0.147789
429.65	1.08	0.13	0.007692	0.000926	0.006766	0.147789
429.66	1.07	0.13	0.007692	0.000932	0.006761	0.147915
429.81	1.07	0.13	0.007692	0.000935	0.006758	0.147979

Temp	T_2	T_2^*	$1/T_2^*$	$1/T_2$	$y=1/T_2^*-1/T_2$	$1/y$
429.82	1.06	0.13	0.007692	0.000943	0.006749	0.148172
429.97	1.06	0.13	0.007692	0.000946	0.006746	0.148237
430.11	1.05	0.13	0.007692	0.000952	0.006740	0.148370
430.12	1.05	0.13	0.007692	0.000952	0.006740	0.148370
430.26	1.04	0.13	0.007692	0.000958	0.006734	0.148504
430.28	1.04	0.13	0.007692	0.000962	0.006731	0.148571
430.42	1.03	0.13	0.007692	0.000968	0.006725	0.148708
430.57	1.03	0.13	0.007692	0.000974	0.006718	0.148848
430.58	1.02	0.13	0.007692	0.000980	0.006712	0.148989
430.59	1.02	0.12	0.008333	0.000980	0.007353	0.136000
430.73	1.01	0.12	0.008333	0.000990	0.007343	0.136180
430.88	1.01	0.12	0.008333	0.000990	0.007343	0.136180
430.89	1.00	0.12	0.008333	0.001000	0.007333	0.136364
431.18	1.00	0.12	0.008333	0.001003	0.007330	0.136426
431.32	0.99	0.12	0.008333	0.001010	0.007323	0.136552
431.33	0.99	0.12	0.008333	0.001010	0.007323	0.136552
431.34	0.98	0.12	0.008333	0.001020	0.007313	0.136744
431.48	0.98	0.11	0.009091	0.001020	0.008071	0.123908
431.49	0.98	0.11	0.009091	0.001020	0.008071	0.123908
431.63	0.97	0.11	0.009091	0.001031	0.008060	0.124070
431.78	0.97	0.11	0.009091	0.001031	0.008060	0.124070
431.79	0.96	0.11	0.009091	0.001042	0.008049	0.124235
431.94	0.96	0.11	0.009091	0.001042	0.008049	0.124235
431.95	0.95	0.11	0.009091	0.001053	0.008038	0.124405
432.10	0.95	0.11	0.009091	0.001058	0.008033	0.124491
432.11	0.94	0.11	0.009091	0.001064	0.008027	0.124578
432.26	0.94	0.11	0.009091	0.001070	0.008021	0.124667
432.27	0.93	0.11	0.009091	0.001075	0.008016	0.124756
432.28	0.93	0.11	0.009091	0.001075	0.008016	0.124756
432.29	0.92	0.11	0.009091	0.001087	0.008004	0.124938
432.30	0.92	0.11	0.009091	0.001087	0.008004	0.124938
432.31	0.91	0.11	0.009091	0.001095	0.007996	0.125062
432.33	0.91	0.11	0.009091	0.001099	0.007992	0.125125
432.34	0.90	0.11	0.009091	0.001111	0.007980	0.125316
432.35	0.90	0.11	0.009091	0.001111	0.007980	0.125316
432.36	0.89	0.11	0.009091	0.001119	0.007972	0.125447
432.38	0.89	0.11	0.009091	0.001128	0.007963	0.125579
432.39	0.88	0.11	0.009091	0.001136	0.007955	0.125714
432.54	0.88	0.11	0.009091	0.001136	0.007955	0.125714
432.55	0.87	0.11	0.009091	0.001149	0.007941	0.125921
432.56	0.87	0.11	0.009091	0.001149	0.007941	0.125921
432.57	0.86	0.11	0.009091	0.001163	0.007928	0.126133
432.73	0.86	0.11	0.009091	0.001163	0.007928	0.126133
432.74	0.85	0.11	0.009091	0.001176	0.007914	0.126351
432.75	0.85	0.11	0.009091	0.001176	0.007914	0.126351
432.89	0.84	0.10	0.010000	0.001190	0.008810	0.113514
433.05	0.84	0.10	0.010000	0.001190	0.008810	0.113514
433.06	0.83	0.10	0.010000	0.001205	0.008795	0.113699
433.21	0.83	0.10	0.010000	0.001210	0.008790	0.113761
433.22	0.82	0.10	0.010000	0.001220	0.008780	0.113889
433.37	0.82	0.10	0.010000	0.001220	0.008780	0.113889
433.38	0.81	0.10	0.010000	0.001235	0.008765	0.114085
433.40	0.81	0.10	0.010000	0.001235	0.008765	0.114085
433.54	0.80	0.10	0.010000	0.001250	0.008750	0.114286
433.56	0.80	0.10	0.010000	0.001250	0.008750	0.114286
433.57	0.79	0.10	0.010000	0.001266	0.008734	0.114493
433.73	0.79	0.10	0.010000	0.001266	0.008734	0.114493
433.86	0.78	0.10	0.010000	0.001282	0.008718	0.114706
434.02	0.78	0.10	0.010000	0.001282	0.008718	0.114706
434.03	0.77	0.10	0.010000	0.001299	0.008701	0.114925
434.32	0.77	0.10	0.010000	0.001307	0.008693	0.115038
434.33	0.76	0.10	0.010000	0.001316	0.008684	0.115152
434.35	0.76	0.09	0.011111	0.001316	0.009795	0.102090

Temp	T_2	T_2^*	$1/T_2^*$	$1/T_2$	$y=1/T_2^*-1/T_2$	$1/y$
434.36	0.75	0.09	0.011111	0.001333	0.009778	0.102273
434.51	0.75	0.09	0.011111	0.001333	0.009778	0.102273
434.52	0.74	0.09	0.011111	0.001345	0.009766	0.102398
434.68	0.74	0.09	0.011111	0.001357	0.009754	0.102526
434.69	0.73	0.09	0.011111	0.001370	0.009741	0.102656
434.71	0.73	0.09	0.011111	0.001370	0.009741	0.102656
434.72	0.72	0.09	0.011111	0.001389	0.009722	0.102857
434.74	0.72	0.09	0.011111	0.001395	0.009716	0.102926
434.75	0.71	0.09	0.011111	0.001408	0.009703	0.103065
434.77	0.71	0.09	0.011111	0.001408	0.009703	0.103065
434.78	0.70	0.09	0.011111	0.001429	0.009683	0.103279
434.80	0.70	0.09	0.011111	0.001429	0.009683	0.103279
434.81	0.69	0.09	0.011111	0.001442	0.009669	0.103425
434.84	0.69	0.09	0.011111	0.001456	0.009655	0.103575
434.98	0.68	0.09	0.011111	0.001471	0.009641	0.103729
435.14	0.68	0.09	0.011111	0.001478	0.009633	0.103807
435.15	0.67	0.09	0.011111	0.001493	0.009619	0.103966
435.17	0.67	0.09	0.011111	0.001493	0.009619	0.103966
435.18	0.66	0.09	0.011111	0.001515	0.009596	0.104211
435.45	0.66	0.09	0.011111	0.001515	0.009596	0.104211
435.47	0.70	0.09	0.011111	0.001429	0.009683	0.103279
435.48	0.69	0.09	0.011111	0.001449	0.009662	0.103500
435.49	0.69	0.09	0.011111	0.001449	0.009662	0.103500
435.49	0.69	0.09	0.011111	0.001449	0.009662	0.103500
435.50	0.69	0.09	0.011111	0.001449	0.009662	0.103500
435.51	0.68	0.09	0.011111	0.001463	0.009648	0.103652
435.51	0.69	0.09	0.011111	0.001449	0.009662	0.103500
435.52	0.68	0.09	0.011111	0.001471	0.009641	0.103729
435.58	0.66	0.09	0.011111	0.001508	0.009604	0.104128
435.59	0.70	0.09	0.011111	0.001429	0.009683	0.103279
435.60	0.70	0.09	0.011111	0.001429	0.009683	0.103279
435.65	0.68	0.09	0.011111	0.001471	0.009641	0.103729
435.66	0.68	0.09	0.011111	0.001471	0.009641	0.103729
435.70	0.67	0.09	0.011111	0.001493	0.009619	0.103966
435.71	0.67	0.09	0.011111	0.001493	0.009619	0.103966
435.80	0.68	0.09	0.011111	0.001471	0.009641	0.103729
435.81	0.68	0.09	0.011111	0.001471	0.009641	0.103729
435.82	0.67	0.09	0.011111	0.001493	0.009619	0.103966
435.82	0.67	0.09	0.011111	0.001493	0.009619	0.103966
435.83	0.67	0.09	0.011111	0.001493	0.009619	0.103966
435.83	0.71	0.09	0.011111	0.001408	0.009703	0.103065
435.84	0.70	0.09	0.011111	0.001435	0.009676	0.103352
435.85	0.70	0.09	0.011111	0.001429	0.009683	0.103279
435.94	0.72	0.10	0.010000	0.001389	0.008611	0.116129
435.95	0.72	0.10	0.010000	0.001399	0.008601	0.116260
435.96	0.71	0.10	0.010000	0.001408	0.008592	0.116393
436.05	0.72	0.10	0.010000	0.001389	0.008611	0.116129
436.06	0.72	0.10	0.010000	0.001389	0.008611	0.116129
436.07	0.72	0.10	0.010000	0.001389	0.008611	0.116129
436.15	0.74	0.10	0.010000	0.001351	0.008649	0.115625
436.16	0.73	0.10	0.010000	0.001370	0.008630	0.115873
436.16	0.73	0.10	0.010000	0.001370	0.008630	0.115873
436.17	0.73	0.10	0.010000	0.001370	0.008630	0.115873
436.18	0.73	0.10	0.010000	0.001370	0.008630	0.115873
436.26	0.74	0.10	0.010000	0.001351	0.008649	0.115625
436.27	0.74	0.10	0.010000	0.001351	0.008649	0.115625
436.28	0.74	0.11	0.009091	0.001351	0.007740	0.129206
436.39	0.75	0.11	0.009091	0.001333	0.007758	0.128906
436.40	0.74	0.11	0.009091	0.001351	0.007740	0.129206
436.50	0.75	0.11	0.009091	0.001333	0.007758	0.128906
436.51	0.75	0.11	0.009091	0.001333	0.007758	0.128906
436.52	0.75	0.11	0.009091	0.001333	0.007758	0.128906
436.57	0.78	0.11	0.009091	0.001290	0.007801	0.128195

Temp	T_2	T_2^*	$1/T_2^*$	$1/T_2$	$y=1/T_2^*-1/T_2$	$1/y$
436.58	0.77	0.11	0.009091	0.001299	0.007792	0.128333
436.59	0.77	0.11	0.009091	0.001299	0.007792	0.128333
436.60	0.77	0.11	0.009091	0.001304	0.007787	0.128426
436.61	0.76	0.11	0.009091	0.001316	0.007775	0.128615
436.62	0.76	0.11	0.009091	0.001316	0.007775	0.128615
436.63	0.76	0.11	0.009091	0.001325	0.007766	0.128760
436.69	0.78	0.11	0.009091	0.001282	0.007809	0.128060
436.70	0.78	0.11	0.009091	0.001282	0.007809	0.128060
436.82	0.78	0.11	0.009091	0.001282	0.007809	0.128060
436.94	0.79	0.11	0.009091	0.001266	0.007825	0.127794
436.95	0.78	0.11	0.009091	0.001282	0.007809	0.128060
437.04	0.80	0.11	0.009091	0.001250	0.007841	0.127536
437.05	0.80	0.11	0.009091	0.001258	0.007833	0.127664
437.06	0.79	0.11	0.009091	0.001266	0.007825	0.127794
437.14	0.81	0.11	0.009091	0.001235	0.007856	0.127286
437.15	0.81	0.11	0.009091	0.001235	0.007856	0.127286
437.16	0.80	0.11	0.009091	0.001245	0.007846	0.127452
437.24	0.82	0.11	0.009091	0.001220	0.007871	0.127042
437.25	0.82	0.11	0.009091	0.001220	0.007871	0.127042
437.26	0.82	0.11	0.009091	0.001227	0.007864	0.127163
437.27	0.81	0.11	0.009091	0.001235	0.007856	0.127286
437.30	0.82	0.11	0.009091	0.001219	0.007872	0.127029
437.31	0.82	0.12	0.008333	0.001213	0.007120	0.140452
437.32	0.83	0.12	0.008333	0.001208	0.007125	0.140350
437.33	0.83	0.12	0.008333	0.001203	0.007130	0.140249
437.37	0.82	0.12	0.008333	0.001220	0.007114	0.140571
437.40	0.86	0.12	0.008333	0.001169	0.007165	0.139571
437.41	0.86	0.12	0.008333	0.001164	0.007170	0.139477
437.42	0.86	0.12	0.008333	0.001159	0.007174	0.139385
437.43	0.87	0.12	0.008333	0.001154	0.007179	0.139294
437.47	0.88	0.12	0.008333	0.001136	0.007198	0.138936
437.48	0.88	0.12	0.008333	0.001131	0.007202	0.138849
437.49	0.91	0.12	0.008333	0.001099	0.007234	0.138228
437.50	0.88	0.12	0.008333	0.001132	0.007201	0.138865
437.50	0.89	0.12	0.008333	0.001122	0.007211	0.138676
437.51	0.89	0.12	0.008333	0.001118	0.007215	0.138592
437.53	0.90	0.12	0.008333	0.001109	0.007224	0.138424
437.62	0.93	0.12	0.008333	0.001071	0.007262	0.137706
437.65	0.94	0.12	0.008333	0.001059	0.007274	0.137479
437.66	0.95	0.12	0.008333	0.001056	0.007278	0.137404
437.67	0.97	0.12	0.008333	0.001031	0.007302	0.136941
437.74	0.98	0.12	0.008333	0.001025	0.007308	0.136831
437.75	0.98	0.12	0.008333	0.001021	0.007312	0.136762
437.77	0.99	0.12	0.008333	0.001014	0.007319	0.136626
437.78	0.99	0.12	0.008333	0.001010	0.007323	0.136558
437.81	0.97	0.12	0.008333	0.001031	0.007302	0.136941
437.82	0.97	0.12	0.008333	0.001031	0.007302	0.136941
437.83	1.01	0.12	0.008333	0.000993	0.007341	0.136230
437.85	1.01	0.12	0.008333	0.000986	0.007347	0.136102
437.86	1.02	0.12	0.008333	0.000982	0.007351	0.136038
437.88	1.02	0.12	0.008333	0.000976	0.007358	0.135914
437.89	1.03	0.12	0.008333	0.000972	0.007361	0.135852
437.90	1.03	0.12	0.008333	0.000969	0.007364	0.135791
437.91	1.04	0.12	0.008333	0.000966	0.007368	0.13573
437.96	1.05	0.12	0.008333	0.000950	0.007384	0.135433
437.98	1.06	0.12	0.008333	0.000943	0.007390	0.135317
437.99	1.06	0.12	0.008333	0.000940	0.007393	0.13526
438.00	1.07	0.12	0.008333	0.000937	0.007396	0.135203
438.01	1.07	0.12	0.008333	0.000934	0.007399	0.135147
438.02	1.07	0.12	0.008333	0.000931	0.007402	0.135091
438.02	1.06	0.12	0.008333	0.000943	0.007390	0.135319
438.03	1.08	0.12	0.008333	0.000928	0.007405	0.135036
438.04	1.08	0.12	0.008333	0.000925	0.007408	0.13498

Temp	T_2	T_2^*	$1/T_2^*$	$1/T_2$	$y=1/T_2^*-1/T_2$	$1/y$
438.05	1.08	0.12	0.008333	0.000922	0.007411	0.134926
438.05	1.08	0.12	0.008333	0.000922	0.007411	0.134926
438.06	1.09	0.12	0.008333	0.000919	0.007414	0.134871
438.07	1.10	0.12	0.008333	0.000909	0.007424	0.134694
438.08	1.10	0.12	0.008333	0.000913	0.007420	0.134764
438.08	1.10	0.12	0.008333	0.000913	0.007420	0.134764
438.09	1.10	0.12	0.008333	0.000910	0.007423	0.134711
438.09	1.10	0.12	0.008333	0.000910	0.007423	0.134711
438.09	1.09	0.12	0.008333	0.000917	0.007416	0.134845
438.10	1.10	0.12	0.008333	0.000907	0.007426	0.134658
438.10	1.09	0.12	0.008333	0.000917	0.007416	0.134845
438.11	1.11	0.12	0.008333	0.000904	0.007429	0.134606
438.11	1.08	0.12	0.008333	0.000926	0.007407	0.135000
438.12	1.11	0.12	0.008333	0.000901	0.007432	0.134554
438.13	1.11	0.12	0.008333	0.000899	0.007435	0.134502
438.15	1.12	0.12	0.008333	0.000893	0.007440	0.134400
438.16	1.12	0.12	0.008333	0.000893	0.007440	0.134400
438.26	1.14	0.12	0.008333	0.000877	0.007456	0.134118
438.27	1.13	0.12	0.008333	0.000885	0.007448	0.134257
438.28	1.13	0.12	0.008333	0.000885	0.007448	0.134257
438.38	1.15	0.12	0.008333	0.000873	0.007460	0.134049
438.39	1.14	0.12	0.008333	0.000877	0.007456	0.134118
438.49	1.16	0.12	0.008333	0.000862	0.007471	0.133846
438.50	1.15	0.12	0.008333	0.000870	0.007464	0.133981
438.51	1.15	0.13	0.007692	0.000870	0.006823	0.146569
438.61	1.16	0.12	0.008333	0.000862	0.007471	0.133846
438.62	1.16	0.12	0.008333	0.000862	0.007471	0.133846
438.73	1.17	0.13	0.007692	0.000855	0.006838	0.146250
438.74	1.17	0.13	0.007692	0.000855	0.006838	0.146250
438.85	1.18	0.13	0.007692	0.000847	0.006845	0.146095
438.86	1.18	0.13	0.007692	0.000850	0.006842	0.146146
438.98	1.18	0.13	0.007692	0.000847	0.006845	0.146095
439.10	1.19	0.13	0.007692	0.000840	0.006852	0.145943
439.11	1.18	0.13	0.007692	0.000845	0.006847	0.146044
439.23	1.19	0.13	0.007692	0.000840	0.006852	0.145943
439.35	1.20	0.13	0.007692	0.000833	0.006859	0.145794
439.36	1.19	0.13	0.007692	0.000838	0.006854	0.145893
439.48	1.20	0.13	0.007692	0.000833	0.006859	0.145794
439.49	1.20	0.13	0.007692	0.000833	0.006859	0.145794
439.61	1.20	0.13	0.007692	0.000833	0.006859	0.145794
439.75	1.20	0.13	0.007692	0.000833	0.006859	0.145794
439.88	1.20	0.14	0.007143	0.000833	0.006310	0.158491
440.01	1.20	0.14	0.007143	0.000833	0.006310	0.158491
440.15	1.20	0.14	0.007143	0.000833	0.006310	0.158491
440.28	1.20	0.14	0.007143	0.000833	0.006310	0.158491
440.42	1.20	0.14	0.007143	0.000833	0.006310	0.158491
440.55	1.20	0.14	0.007143	0.000833	0.006310	0.158491
440.69	1.20	0.15	0.006667	0.000833	0.005833	0.171429
440.82	1.20	0.15	0.006667	0.000833	0.005833	0.171429
440.96	1.20	0.15	0.006667	0.000833	0.005833	0.171429
441.09	1.20	0.15	0.006667	0.000833	0.005833	0.171429
441.23	1.20	0.15	0.006667	0.000833	0.005833	0.171429
441.36	1.20	0.15	0.006667	0.000833	0.005833	0.171429
441.50	1.20	0.15	0.006667	0.000833	0.005833	0.171429
441.77	1.20	0.15	0.006667	0.000833	0.005833	0.171429
442.04	1.20	0.15	0.006667	0.000833	0.005833	0.171429
442.31	1.20	0.15	0.006667	0.000833	0.005833	0.171429
442.58	1.20	0.15	0.006667	0.000833	0.005833	0.171429
442.71	1.20	0.15	0.006667	0.000833	0.005833	0.171429
442.85	1.20	0.16	0.006250	0.000833	0.005417	0.184615
443.12	1.20	0.16	0.006250	0.000833	0.005417	0.184615
443.26	1.19	0.16	0.006250	0.000840	0.005410	0.184854
443.39	1.19	0.16	0.006250	0.000840	0.005410	0.184854

Temp	T_2	T_2^*	$1/T_2^*$	$1/T_2$	$y=1/T_2^*-1/T_2$	$1/y$
443.40	1.19	0.16	0.006250	0.000840	0.005410	0.184854
443.53	1.19	0.16	0.006250	0.000840	0.005410	0.184854
443.67	1.19	0.16	0.006250	0.000840	0.005410	0.184854
443.81	1.19	0.16	0.006250	0.000840	0.005410	0.184854
444.08	1.19	0.16	0.006250	0.000840	0.005410	0.184854
444.22	1.18	0.16	0.006250	0.000847	0.005403	0.185098
444.36	1.18	0.16	0.006250	0.000847	0.005403	0.185098
444.63	1.18	0.16	0.006250	0.000847	0.005403	0.185098
444.91	1.17	0.16	0.006250	0.000855	0.005395	0.185347
445.05	1.17	0.16	0.006250	0.000855	0.005395	0.185347
445.32	1.17	0.16	0.006250	0.000855	0.005395	0.185347
445.47	1.16	0.16	0.006250	0.000862	0.005388	0.185600
445.87	1.16	0.16	0.006250	0.000862	0.005388	0.185600
445.88	1.16	0.16	0.006250	0.000862	0.005388	0.185600
446.15	1.15	0.16	0.006250	0.000870	0.005380	0.185859
446.43	1.15	0.16	0.006250	0.000870	0.005380	0.185859
446.71	1.14	0.16	0.006250	0.000877	0.005373	0.186122
446.98	1.14	0.16	0.006250	0.000877	0.005373	0.186122
447.12	1.14	0.16	0.006250	0.000877	0.005373	0.186122
447.27	1.13	0.16	0.006250	0.000885	0.005365	0.186392
447.54	1.13	0.16	0.006250	0.000885	0.005365	0.186392
447.68	1.13	0.16	0.006250	0.000885	0.005365	0.186392
447.96	1.13	0.16	0.006250	0.000885	0.005365	0.186392
448.10	1.12	0.16	0.006250	0.000893	0.005357	0.186667
448.24	1.12	0.16	0.006250	0.000893	0.005357	0.186667
448.38	1.12	0.16	0.006250	0.000893	0.005357	0.186667
448.52	1.11	0.16	0.006250	0.000901	0.005349	0.186947
448.66	1.11	0.16	0.006250	0.000901	0.005349	0.186947
448.80	1.11	0.16	0.006250	0.000901	0.005349	0.186947
448.94	1.11	0.16	0.006250	0.000901	0.005349	0.186947
449.08	1.10	0.16	0.006250	0.000909	0.005341	0.187234
449.21	1.10	0.16	0.006250	0.000909	0.005341	0.187234
449.36	1.10	0.16	0.006250	0.000913	0.005337	0.187380
449.50	1.09	0.16	0.006250	0.000917	0.005333	0.187527
449.64	1.09	0.16	0.006250	0.000917	0.005333	0.187527
449.78	1.08	0.16	0.006250	0.000926	0.005324	0.187826
449.92	1.08	0.16	0.006250	0.000926	0.005324	0.187826
449.93	1.08	0.16	0.006250	0.000926	0.005324	0.187826
450.07	1.08	0.16	0.006250	0.000930	0.005320	0.187978
450.21	1.07	0.16	0.006250	0.000935	0.005315	0.188132
450.35	1.07	0.16	0.006250	0.000935	0.005315	0.188132
450.49	1.07	0.16	0.006250	0.000935	0.005315	0.188132
450.63	1.06	0.16	0.006250	0.000943	0.005307	0.188444
450.64	1.06	0.16	0.006250	0.000943	0.005307	0.188444
450.78	1.05	0.15	0.006667	0.000952	0.005714	0.175000
450.92	1.05	0.15	0.006667	0.000952	0.005714	0.175000
450.93	1.05	0.15	0.006667	0.000952	0.005714	0.175000
451.08	1.04	0.15	0.006667	0.000962	0.005705	0.175281
451.21	1.04	0.15	0.006667	0.000962	0.005705	0.175281
451.22	1.04	0.15	0.006667	0.000962	0.005705	0.175281
451.37	1.03	0.15	0.006667	0.000971	0.005696	0.175568
451.38	1.03	0.15	0.006667	0.000976	0.005691	0.175714
451.52	1.02	0.15	0.006667	0.000980	0.005686	0.175862
451.53	1.02	0.15	0.006667	0.000980	0.005686	0.175862
451.67	1.02	0.15	0.006667	0.000985	0.005681	0.176012
451.81	1.01	0.15	0.006667	0.000990	0.005677	0.176163
451.82	1.01	0.15	0.006667	0.000990	0.005677	0.176163
451.83	1.00	0.15	0.006667	0.001000	0.005667	0.176471
451.84	1.00	0.15	0.006667	0.001000	0.005667	0.176471
451.85	1.00	0.15	0.006667	0.001005	0.005662	0.176627
451.86	0.99	0.15	0.006667	0.001010	0.005657	0.176786
451.87	0.99	0.15	0.006667	0.001015	0.005651	0.176946
452.01	0.98	0.15	0.006667	0.001020	0.005646	0.177108

Temp	T_2	T_2^*	$1/T_2^*$	$1/T_2$	$y=1/T_2^*-1/T_2$	$1/y$
452.02	0.98	0.15	0.006667	0.001020	0.005646	0.177108
452.16	0.98	0.15	0.006667	0.001026	0.005641	0.177273
452.31	0.97	0.15	0.006667	0.001031	0.005636	0.177439
452.45	0.97	0.15	0.006667	0.001031	0.005636	0.177439
452.59	0.96	0.15	0.006667	0.001042	0.005625	0.177778
452.73	0.96	0.15	0.006667	0.001042	0.005625	0.177778
452.87	0.96	0.15	0.006667	0.001042	0.005625	0.177778
453.01	0.95	0.15	0.006667	0.001053	0.005614	0.178125
453.15	0.95	0.15	0.006667	0.001053	0.005614	0.178125
453.29	0.95	0.15	0.006667	0.001053	0.005614	0.178125
453.43	0.95	0.15	0.006667	0.001053	0.005614	0.178125
453.57	0.95	0.15	0.006667	0.001053	0.005614	0.178125
453.71	0.94	0.15	0.006667	0.001064	0.005603	0.178481
453.85	0.94	0.15	0.006667	0.001064	0.005603	0.178481
453.99	0.94	0.15	0.006667	0.001064	0.005603	0.178481
454.13	0.94	0.15	0.006667	0.001064	0.005603	0.178481
454.27	0.93	0.15	0.006667	0.001075	0.005591	0.178846
454.41	0.93	0.15	0.006667	0.001075	0.005591	0.178846
454.55	0.93	0.15	0.006667	0.001075	0.005591	0.178846
454.69	0.93	0.14	0.007143	0.001081	0.006062	0.164968
454.83	0.92	0.14	0.007143	0.001087	0.006056	0.165128
454.97	0.92	0.14	0.007143	0.001087	0.006056	0.165128
455.11	0.92	0.14	0.007143	0.001087	0.006056	0.165128
455.25	0.92	0.14	0.007143	0.001087	0.006056	0.165128
455.39	0.91	0.14	0.007143	0.001099	0.006044	0.165455
455.53	0.91	0.14	0.007143	0.001099	0.006044	0.165455
455.67	0.91	0.14	0.007143	0.001099	0.006044	0.165455
455.80	0.91	0.14	0.007143	0.001099	0.006044	0.165455
455.94	0.91	0.14	0.007143	0.001099	0.006044	0.165455
456.08	0.90	0.14	0.007143	0.001111	0.006032	0.165789
456.22	0.90	0.14	0.007143	0.001111	0.006032	0.165789
456.36	0.90	0.14	0.007143	0.001111	0.006032	0.165789
456.50	0.90	0.14	0.007143	0.001111	0.006032	0.165789
456.64	0.89	0.14	0.007143	0.001124	0.006019	0.166133
456.78	0.89	0.14	0.007143	0.001124	0.006019	0.166133
457.05	0.89	0.14	0.007143	0.001124	0.006019	0.166133
457.06	0.89	0.14	0.007143	0.001124	0.006019	0.166133
457.20	0.89	0.14	0.007143	0.001124	0.006019	0.166133
457.33	0.88	0.14	0.007143	0.001136	0.006006	0.166486
457.48	0.88	0.14	0.007143	0.001136	0.006006	0.166486
457.75	0.88	0.14	0.007143	0.001136	0.006006	0.166486
457.89	0.88	0.14	0.007143	0.001136	0.006006	0.166486
457.90	0.87	0.14	0.007143	0.001149	0.005993	0.166849
458.04	0.87	0.14	0.007143	0.001149	0.005993	0.166849
458.17	0.87	0.14	0.007143	0.001149	0.005993	0.166849
458.31	0.87	0.14	0.007143	0.001149	0.005993	0.166849
458.45	0.87	0.14	0.007143	0.001149	0.005993	0.166849
458.59	0.86	0.14	0.007143	0.001163	0.005980	0.167222
458.73	0.86	0.14	0.007143	0.001163	0.005980	0.167222
458.87	0.86	0.14	0.007143	0.001163	0.005980	0.167222
459.01	0.86	0.14	0.007143	0.001163	0.005980	0.167222
459.14	0.86	0.14	0.007143	0.001163	0.005980	0.167222
459.28	0.86	0.14	0.007143	0.001163	0.005980	0.167222
459.56	0.85	0.14	0.007143	0.001176	0.005966	0.167606
459.70	0.85	0.13	0.007692	0.001176	0.006516	0.153472
459.84	0.85	0.13	0.007692	0.001176	0.006516	0.153472
460.11	0.85	0.13	0.007692	0.001176	0.006516	0.153472
460.25	0.84	0.13	0.007692	0.001190	0.006502	0.153803
460.52	0.84	0.13	0.007692	0.001190	0.006502	0.153803
460.66	0.84	0.13	0.007692	0.001190	0.006502	0.153803
460.80	0.84	0.13	0.007692	0.001190	0.006502	0.153803
461.07	0.84	0.13	0.007692	0.001190	0.006502	0.153803
461.21	0.84	0.13	0.007692	0.001190	0.006502	0.153803

Temp	T_2	T_2^*	$1/T_2^*$	$1/T_2$	$y=1/T_2^*-1/T_2$	$1/y$
461.35	0.83	0.13	0.007692	0.001205	0.006487	0.154143
461.49	0.83	0.13	0.007692	0.001205	0.006487	0.154143
461.63	0.83	0.13	0.007692	0.001205	0.006487	0.154143
461.77	0.83	0.13	0.007692	0.001205	0.006487	0.154143
461.90	0.83	0.13	0.007692	0.001205	0.006487	0.154143
462.18	0.82	0.13	0.007692	0.001220	0.006473	0.154493
462.31	0.82	0.13	0.007692	0.001220	0.006473	0.154493
462.45	0.82	0.13	0.007692	0.001220	0.006473	0.154493
462.59	0.82	0.13	0.007692	0.001220	0.006473	0.154493
462.86	0.82	0.13	0.007692	0.001220	0.006473	0.154493
463.01	0.82	0.13	0.007692	0.001220	0.006473	0.154493
463.28	0.81	0.13	0.007692	0.001235	0.006458	0.154853
464.10	0.81	0.13	0.007692	0.001235	0.006458	0.154853
464.38	0.80	0.13	0.007692	0.001250	0.006442	0.155224
465.34	0.80	0.13	0.007692	0.001258	0.006434	0.155414
465.61	0.79	0.13	0.007692	0.001266	0.006426	0.155606
466.59	0.79	0.13	0.007692	0.001266	0.006426	0.155606

Final Result

The final form of the data after smoothing and parameterization is given here.

As in the previous data record, $y = 1/T_2^* - 1/T_2$.

Temp (K)	$y(\nu_-)$ (ms)	error (ms)	$y(\nu_+)$ (ms)	error (ms)
77.00000	2.71953	0.08369	1.38910	1.35183
78.97487	2.71057	0.08379	1.39287	1.34382
80.94974	2.70167	0.08392	1.39649	1.33588
82.92461	2.69106	0.08406	1.40011	1.32643
84.89948	2.67531	0.08419	1.40376	1.31243
86.87434	2.66661	0.08432	1.40741	1.30476
88.84921	2.65796	0.08446	1.41108	1.29717
90.82409	2.64937	0.08442	1.41224	1.28963
92.79896	2.63934	0.08452	1.41524	1.28086
94.77383	2.62391	0.08466	1.41892	1.26739
96.74870	2.61551	0.08465	1.42002	1.26011
98.72356	2.60709	0.08475	1.42293	1.25290
100.69843	2.59750	0.08489	1.42665	1.24465
102.67331	2.58234	0.08487	1.42802	1.23160
104.64818	2.57417	0.08496	1.43085	1.22463
106.62305	2.56487	0.08497	1.43212	1.21676
108.59792	2.54990	0.08506	1.43489	1.20404
110.57278	2.54186	0.08507	1.43623	1.19730
112.54765	2.53293	0.08513	1.43911	1.18979
114.52252	2.51813	0.08515	1.44052	1.17739
116.49740	2.51030	0.08523	1.44317	1.17088
118.47227	2.50164	0.08523	1.44482	1.16371
120.44714	2.48704	0.08531	1.44741	1.15162
122.42200	2.47858	0.08534	1.44896	1.14470
124.39687	2.46412	0.08540	1.45165	1.13284
126.37174	2.45658	0.08543	1.45329	1.12669
128.34662	2.44844	0.08548	1.45591	1.12009

Temp	$y(\nu_-)$	error	$y(\nu_+)$	error
130.32149	2.43418	0.08552	1.45762	1.10851
132.29636	2.42621	0.08557	1.46018	1.10213
134.27122	2.41210	0.08559	1.46212	1.09077
136.24609	2.40434	0.08566	1.46446	1.08459
138.22096	2.39042	0.08569	1.46646	1.07345
140.19583	2.38288	0.08562	1.46696	1.06748
142.17070	2.36874	0.08567	1.46937	1.05627
144.14557	2.35507	0.08572	1.47134	1.04547
146.12044	2.34783	0.08576	1.47366	1.03982
148.09531	2.33427	0.08580	1.47585	1.02921
150.07018	2.32713	0.08584	1.47812	1.02374
152.04504	2.31352	0.08589	1.48039	1.01322
154.01993	2.30012	0.08582	1.48088	1.00294
155.99480	2.29315	0.08575	1.48137	0.99776
157.96967	2.27976	0.08569	1.48186	0.98763
159.94453	2.26647	0.08562	1.48235	0.97765
161.91940	2.25324	0.08546	1.48127	0.96783
163.89427	2.24009	0.08518	1.47825	0.95815
165.86914	2.22699	0.08490	1.47523	0.94861
167.84401	2.21397	0.08462	1.47223	0.93922
169.81888	2.20108	0.08425	1.46784	0.92997
171.79375	2.18826	0.08377	1.46142	0.92085
173.76862	2.17556	0.08329	1.45506	0.91187
175.74348	2.16300	0.08283	1.44861	0.90302
177.71835	2.15061	0.08230	1.44096	0.89429
179.69324	2.13835	0.08166	1.43126	0.88570
181.66811	2.12626	0.08103	1.42167	0.87722
183.64297	2.11433	0.08043	1.41207	0.86887
185.61784	2.09727	0.07982	1.40265	0.85680
187.59271	2.08532	0.07918	1.39226	0.84848
189.56758	2.06881	0.07848	1.38087	0.83687
191.54245	2.05214	0.07784	1.37103	0.82524
193.51732	2.03079	0.07708	1.35920	0.81040
195.49219	2.01418	0.07637	1.34846	0.79899
197.46706	1.99357	0.07572	1.33941	0.78489
199.44193	1.97291	0.07495	1.32845	0.77084
201.41679	1.95263	0.07417	1.31780	0.75716
203.39168	1.92841	0.07337	1.30756	0.74092
205.36655	1.90846	0.07256	1.29767	0.72767
207.34142	1.88954	0.07170	1.28828	0.71512
209.31628	1.87105	0.07083	1.27926	0.70289
211.29115	1.85303	0.06996	1.27050	0.69098
213.26602	1.83936	0.06907	1.26212	0.68185
215.24089	1.82655	0.06818	1.25393	0.67329
217.21576	1.81406	0.06732	1.24575	0.66488
219.19063	1.80182	0.06647	1.23773	0.65663
221.16550	1.78988	0.06567	1.23003	0.64853
223.14037	1.77817	0.06502	1.22441	0.64058
225.11523	1.77026	0.06440	1.21870	0.63494
227.09010	1.75973	0.06381	1.21328	0.62767
229.06499	1.75216	0.06334	1.21001	0.62217
231.03986	1.74211	0.06288	1.20670	0.61514
233.01472	1.73160	0.06243	1.20340	0.60779
234.98959	1.72129	0.06201	1.20022	0.60058
236.96446	1.71118	0.06169	1.19916	0.59349
238.93933	1.70132	0.06126	1.19582	0.58653
240.91420	1.69173	0.06084	1.19253	0.57970
242.88907	1.67926	0.06041	1.18931	0.57123
244.86394	1.66930	0.05999	1.18610	0.56418
246.83881	1.65456	0.05956	1.18297	0.55442
248.81367	1.64138	0.05912	1.17998	0.54559
250.78854	1.62928	0.05856	1.17482	0.53743
252.76341	1.61483	0.05800	1.16983	0.52795

Temp	$y(\nu_-)$	error	$y(\nu_+)$	error
254.73830	1.59725	0.05744	1.16493	0.51682
256.71317	1.58185	0.05676	1.15802	0.50698
258.68802	1.56518	0.05609	1.15125	0.49652
260.66290	1.54811	0.05541	1.14461	0.48595
262.63776	1.53141	0.05465	1.13607	0.47570
264.61264	1.51511	0.05389	1.12759	0.46578
266.58749	1.49704	0.05314	1.11929	0.45502
268.56238	1.48066	0.05240	1.11117	0.44531
270.53723	1.46342	0.05167	1.10322	0.43527
272.51212	1.44777	0.05096	1.09538	0.42616
274.48697	1.43322	0.05018	1.08591	0.41774
276.46185	1.41898	0.04948	1.07812	0.40957
278.43671	1.40495	0.04880	1.07068	0.40163
280.41159	1.39122	0.04807	1.06169	0.39393
282.38647	1.37768	0.04741	1.05418	0.38644
284.36133	1.36609	0.04685	1.04855	0.37998
286.33621	1.35544	0.04625	1.04174	0.37405
288.31107	1.34488	0.04571	1.03616	0.36826
290.28595	1.33446	0.04520	1.03088	0.36260
292.26080	1.32568	0.04471	1.02559	0.35780
294.23569	1.31926	0.04428	1.02173	0.35416
296.21054	1.31213	0.04388	1.01819	0.35026
298.18542	1.30713	0.04356	1.01587	0.34740
300.16028	1.30370	0.04326	1.01393	0.34531
302.13516	1.30022	0.04302	1.01317	0.34324
304.11002	1.29807	0.04281	1.01276	0.34184
306.08490	1.29809	0.04267	1.01347	0.34145
308.05978	1.29882	0.04261	1.01574	0.34145
310.03464	1.30222	0.04258	1.01839	0.34272
312.00952	1.30725	0.04262	1.02216	0.34478
313.98438	1.31219	0.04274	1.02747	0.34687
315.95926	1.31982	0.04295	1.03443	0.35025
317.93411	1.32926	0.04320	1.04202	0.35453
319.90900	1.34011	0.04345	1.04962	0.35955
321.88385	1.35196	0.04373	1.05718	0.36513
323.85873	1.36535	0.04401	1.06485	0.37153
325.83359	1.37991	0.04419	1.07033	0.37858
327.80847	1.39612	0.04431	1.07444	0.38655
329.78336	1.41221	0.04443	1.07864	0.39459
331.75821	1.42893	0.04459	1.08408	0.40305
333.73309	1.44864	0.04488	1.09266	0.41315
335.70795	1.46845	0.04530	1.10410	0.42346
337.68283	1.48740	0.04586	1.11887	0.43351
339.65768	1.50511	0.04659	1.13683	0.44310
341.63257	1.52342	0.04745	1.15730	0.45315
343.60742	1.54348	0.04840	1.17931	0.46429
345.58231	1.56233	0.04947	1.20307	0.47495
347.55716	1.58017	0.05067	1.22858	0.48517
349.53204	1.60020	0.05195	1.25490	0.49665
351.50690	1.62253	0.05332	1.28207	0.50944
353.48178	1.64743	0.05471	1.30887	0.52372
355.45667	1.67487	0.05611	1.33518	0.53959
357.43152	1.70119	0.05760	1.36229	0.55514
359.40640	1.72611	0.05917	1.39025	0.57027
361.38126	1.75156	0.06076	1.41784	0.58603
363.35614	1.77803	0.06234	1.44475	0.60245
365.33099	1.80973	0.06400	1.47247	0.62197
367.30588	1.84934	0.06576	1.50104	0.64647
369.28073	1.89324	0.06771	1.53170	0.67394
371.25562	1.94348	0.06990	1.56539	0.70603
373.23047	2.00133	0.07232	1.60177	0.74395
375.20535	2.06176	0.07506	1.64171	0.78502
377.18021	2.12269	0.07800	1.68306	0.82781

Temp	$y(\nu_-)$	error	$y(\nu_+)$	error
379.15509	2.18643	0.08139	1.72867	0.87381
381.12997	2.25460	0.08545	1.78134	0.92423
383.10483	2.32906	0.08999	1.83832	0.98078
385.07971	2.41275	0.09518	1.90174	1.04639
387.05457	2.50098	0.10103	1.97057	1.11804
389.02945	2.60314	0.10766	2.04514	1.20402
391.00430	2.71461	0.11451	2.11869	1.30142
392.97919	2.83381	0.12185	2.19418	1.40982
394.95404	2.96450	0.13023	2.27692	1.53394
396.92892	3.09554	0.13904	2.36022	1.66421
398.90378	3.23023	0.14879	2.44920	1.80446
400.87866	3.37044	0.15941	2.54219	1.95760
402.85352	3.49244	0.16979	2.63100	2.09699
404.82840	3.61452	0.17858	2.70448	2.23650
406.80328	3.79443	0.18672	2.77113	2.44515
408.77814	4.01106	0.19337	2.82388	2.70708
410.75302	4.26331	0.19941	2.87009	3.03007
412.72787	4.53597	0.20600	2.91873	3.40238
414.70276	4.80554	0.21456	2.97980	3.79558
416.67761	5.04787	0.22637	3.06137	4.17307
418.65250	5.22926	0.24166	3.16219	4.47708
420.62735	5.29354	0.26541	3.31357	4.60914
422.60223	5.28578	0.29802	3.50790	4.64241
424.57709	5.31163	0.34858	3.79148	4.76383
426.55197	5.30460	0.42912	4.20250	4.85756
428.52682	5.22367	0.53700	4.69689	4.87099
430.50171	5.42970	0.74236	5.66242	5.38637
432.47659	6.90695	1.54949	8.28763	8.50566
434.45145	8.59154	1.13574	6.79950	13.40893
436.42633	7.03196	0.95107	5.96991	10.08016
438.40118	6.85806	1.01048	6.43197	9.34710
440.37607	6.58980	0.78845	5.51359	8.55358
442.35092	6.22964	0.70402	5.14628	7.65463
444.32581	6.13478	0.64676	4.88276	7.43908
446.30066	5.63787	0.61840	4.70541	6.45051
448.27554	5.65882	0.64816	4.79434	6.51676
450.25040	5.75241	0.72497	5.08521	6.73374
452.22528	5.78912	0.80525	5.38815	6.87041
454.20013	5.88565	0.92126	5.82146	7.15564
456.17502	5.96927	1.02512	6.17718	7.40876
458.14990	6.00217	1.10161	6.41411	7.53802
460.12476	6.06735	1.16907	6.61097	7.72910
462.09964	6.10555	1.25948	6.87507	7.86571
464.07449	6.18175	1.36188	7.16536	8.09659
466.04938	6.25734	1.47744	7.48114	8.33779
468.02423	6.33087	1.60845	7.82544	8.58993
469.99911	6.39180	1.75797	8.20135	8.82610

Refer to Figs. 4-1, 4-2, 4-3, 4-4, 4-5, 4-6, 4-7, 4-8, 5-1 and 5-2 for graphs of these data.

APPENDIX D
HIGGINS' UREA-WATER DATA

A search of the laboratory records revealed five original data sets taken on urea-water by Higgins [1990]. The five data sets are labelled by this author as H307000 - urea-water standard, H311047 - 46.7 Gy, H312073 - 72.9 Gy, H313130 - 129.6 Gy and H306292 - 291.7 Gy. The labels are not random. The H3 stands for Higgins' third data disk. The second and third numbers are between one and twenty, inclusive, and are the record number on the disk. The last three numbers give the appproximate dose in Gy, as per Higgins' notes. The original FIDs are illustrated in the five graphs that follow.

The results of analyzing this data with nonlinear least squares methods is given graphically in Fig. 5-4. The following are the fit.o files for these data sets.

```
H307000.prn
 4.520591110488192E-002
   4674.239909083890000
     -3.225104101660158
 5.399570182234144E-004

CHISQ =    7.296774898809715E-003

          alpha                       covar
     146.787165795069800   2.517243557192191E-002
  6.516362263841919E-005       94.352010331398970
  3.936498396815731E-001  -6.658807383607045E-002
    9907.075260872778000  -2.700016238427062E-004
  7.785780193701891E-008   4.778276231816261E+007
  1.281891243273161E-004  -21257.353723120680000
  1.668509778349226E-003  -8.676029972964042E-001
  2.894812854049731E-001      12.936886850625870
      10.103737765177400   6.123782464525720E-004
  921734.651014549300000   3.981825679220425E-006
```

```
H311047.prn
 5.069683276839258E-002
   4687.731977405945000
      2.884462506267060
 3.002926345499809E-004

CHISQ =    4.012654724578882E-003

        alpha                       covar
     48.115494391086140   1.245087734669910E-001
 4.310751714507418E-005      1021.220061313626000
 2.500609583256638E-001  -4.894423787076335E-001
   8734.463070783528000  -5.624195766378685E-004
 1.518804559558481E-008   3.858812596282219E+008
 3.795413125974999E-005  -128815.583609613900000
 4.091679506429544E-003       -3.842152928110857
 1.149553489029661E-001       51.904826562938840
     24.235081101806370   1.845941897487347E-003
1919979.599118864000000   3.064312418700144E-006


H312073.prn
 5.053842655811746E-002
   4699.473904927140000
     -2.866502250698467
 5.705481424903584E-004

CHISQ =    2.464791871599152E-002

        alpha                       covar
    167.136703056491300   2.054934280612495E-002
 5.507563176143528E-005       55.291284639487930
 3.665936875997666E-001  -3.981329173546847E-002
  11374.597975212190000  -2.130184568169568E-004
 1.150638611224113E-007   3.149734927418510E+007
 1.812936829528240E-004   -14488.131990009210000
 1.295185634576994E-003  -4.980115967336476E-001
 3.952394687506329E-001        9.204892322412517
      8.550600436277502   3.584961797629789E-004
1096016.286527734000000   3.120919834416422E-006


H313130.prn
 6.260460293894482E-002
   4664.109456813673000
     -3.043055224530246
 4.383617853965778E-004

CHISQ =    1.594514558091109E-002

        alpha                       covar
    106.068560966220500   3.885627789911571E-002
 7.325821594274412E-005      147.394356494475700
 4.586220988714317E-001  -8.877664612283782E-002
  13115.693577743930000  -2.357109350534046E-004
 7.858503698313117E-008   5.334216151156351E+007
 1.526488013612077E-004   -20962.329070208780000
 3.724409024849346E-003  -7.569459792970354E-001
 3.908033927854068E-001       10.823069131036250
     23.866966819011910   4.565809055191926E-004
2155424.660233004000000   1.894491812929767E-006
```

```
H306292.prn
4.4836047809007590E-02
 4641.412374532357
-3.023119669483421
6.0036610242618829E-04

CHISQ =    1.4043250407697847E-02

     alpha                    covar
 176.6002022176529        1.9447844284283272E-02
5.8546275405065102E-05     58.04008103019307
0.3693125952999622       -4.3935827567207267E-02
 10098.64725639763       -2.3980095035310034E-04
1.0554274438526976E-07     33798719.04302709
1.5907995383223229E-04    -16154.74718594504
1.1467797037305404E-03   -0.6201352905429013
0.3338719731933741         10.73076849013346
 7.282730990020938        4.6955480568528532E-04
 817942.9873377983        4.1799450322602822E-06
```

It was mentioned in Appendix B that the frequency was the easiest NQR parameter to measure. Higgins made all of his measurements at the same applied frequency and the difference frequency varied from 4641 - 4699 Hz. This is well within the 0.05 kHz that the spectrometer was known to vary.

Data Set	Higgins' Results (μs)	Higgins' Errors (μs)	Updated Results (μs)	Updated Errors (μs)
H307000	607	180	540	2000
H311047	342	100	300	1800
H312073	480	140	570	1800
H313130	379	110	440	1400
H306292	215	65	600	2000

Table D-1 Comparison of Higgins' analysis and nonlinear least squares analysis.

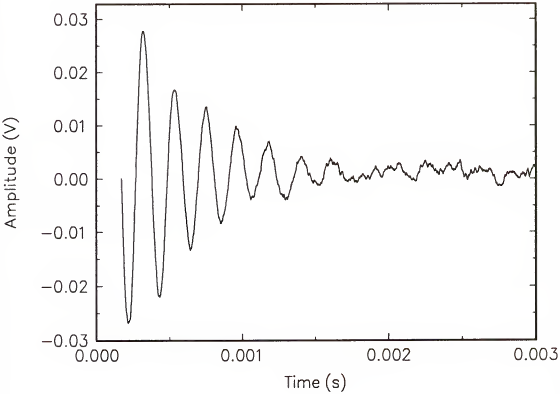

Figure D-1 Data set H307000.

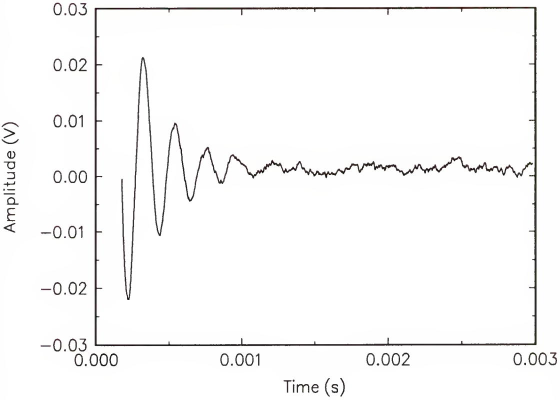

Figure D-2 Data set H311047.

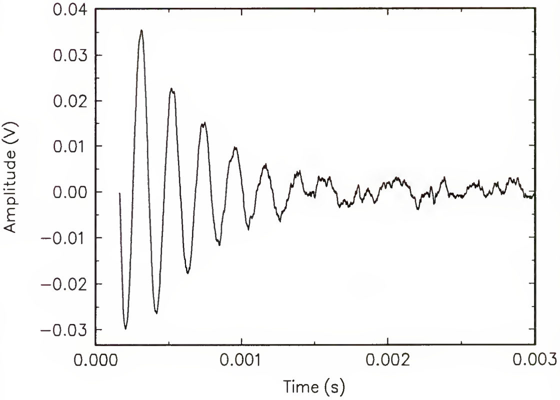

Figure D-3 Data set H312073.

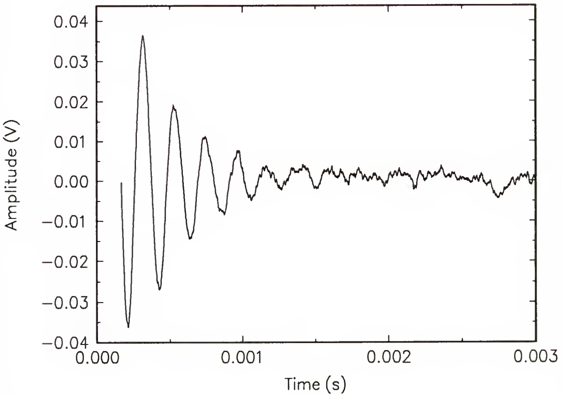

Figure D-4 Data set H313130.

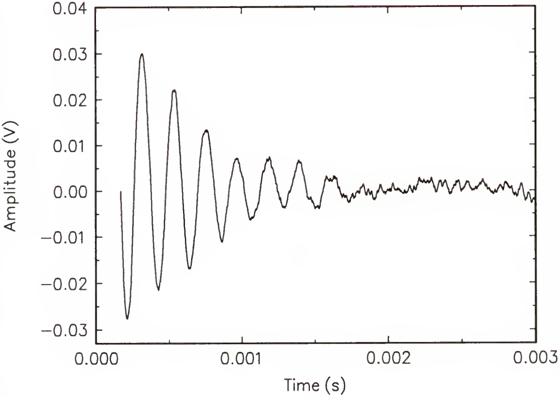

Figure D-5 Data set H306292.

REFERENCES

Barkhusian, H.; de Beer, R.; Bovée, W.M.M.J.; van Ormondt, D. Retrieval of frequencies, amplitudes, damping factors, and phases from time-domain signals using a linear least-squares procedure. J. Magn. Reson. 61:465-481; 1985.

Barkhusian, H.; de Beer, R.; van Ormondt, D. Improved algorithm for noniterative time-domain model fitting exponentially damped magnetic resonance signals. J. Magn. Reson. 73:553-557; 1987.

Blakeley, R.L.; Trestor, A.; Andrews, R.K.; Zerner, B. Nickel(II)-promoted ethanolysis and hydrolysis of N-(2-pyridylmethyl)urea. A model for urease. J. Am. Chem. Soc. 104:612-614; 1982.

Box, H.C. Radiation effects: ESR and ENDOR analysis. New York: Academic Press; 1977.

Buxton, G.V. Radiation chemistry of the liquid state: (1) water and homogeneous aqueous solutions. Farhataziz; Rodgers, M.A.J. Radiation chemistry: principles and applications. New York: VCH Publishers; 1987.

Caron, A.; Donohue, J. Three-Dimensional Refinement of Urea. Acta. Cryst. 17:544-546; 1964.

Chen, C.H.; Dodgen, H.W. Nuclear quadrupole resonance of nitrogen-14 in guanidine complexes, cyanoguanidine, and substituted ureas. J. Magn. Reson. 22:139-147; 1976.

Chiba, T.; Toyama, M.; Morino, Y. Nuclear quadrupole resonance spectra of N^{14} in urea crystal. J. Phys. Soc. Japan 14:379-380; 1959.

Cleveland, W.S.; Devlin, S.J. Locally weighted regression: An approach to regression analysis by local fitting. J. Am. Stat. Assn. 83:596-610;1988.

Conner, C.; Chang J.; Pines, A. Magnetic resonance spectrometer with a dc SQUID detector. Rev. Sci. Instrum. 61:1059-1063; 1990.

Cramér, H. Mathematical methods of statistics. Princeton, NJ: Princeton Univ. Press; 1946.

Darmois, G. Sur les limites de la dispersion de certaines estimations. Rev. Inst. Internat. Statist. 13:9-5; 1945. (in French)

Davies, M.; Whitting, I. J. A modified form of Levenberg's correction. Lootsma, F. A., Numerical methods for non-linear optimization. New York: Academic Press; 1972.

de Beer, R.; van Ormondt, D. Analysis of NMR data using time domain fitting procedures. Rudin, M. and Seelig, J. NMR 26 *In vivo* magnetic resonance spectroscopy. New York: Springer Verlag Berlin; 1992.

Dehmelt, H-G.; Krüger, H. Kernquadrupolfrequenzen in festen dichloräthylen. Naturwiss. 37:111-112; 1950. (in German)

Dinesh; Rogers, M.T. Nuclear quadrupole resonances in 1,3-dimethylurea and tetramethylurea. J. Chem. Phys. 57:3726-3728; 1972.

Duchesne, J.; Monfils, A.; Garson J. Nuclear quadrupole resonance of γ-irradiated *para*-dichlorobenze. J. Chem. Phys. 23:1969; 1955.

Duchesne, J.; Monfils, A.; Depireux, J. Résonance nucléaire. Compt. Rend. 243:259-261; 1956. (in French)

Ewing, D. Synergistic damage from H_2O_2 and OH radicals in irradiated cells. Radiat. Res. 94:171-189; 1983.

Farrar, T.C.; Becker, E.D. Pulse and fourier transform NMR: introduction to theory and methods. New York: Academic Press; 1971.

Fréchet, M. Sur l'extension de certains évaluations statistiques au cas des petites échantillons. Rev. Inst. Internat. Statist. 11:185-205; 1943.

Fritchie, C.J., Jr.; McMullan, R.K. Neutron diffraction study of the 1:1 urea:hydrogen peroxide complex at 81 K. Acta Cryst. B37:1086-1091; 1981.

Fukushima, E.; Roeder, S.B.W. Experimental pulse NMR: a nuts and bolts approach. Reading, MA: Addison-Wesley; 1981.

Guibé, L. Résonance magnétique nucléaire - sur la résonance quadrupolaire des noyaux d'azote dans l'uree. Compt. Rend. 250:1635-1636; 1960. (in French)

Hanrahan, R.J. A Co^{60} gamma irradiator for chemical research. Int. J. Appl. Rad. Isot. 13:254-255; 1962.

Heaton, N.J.; Vold, R.L.; Vold, R.R. Deuterium quadrupole echo study of urea motion in urea/n-alkane inclusion compounds. J. Am. Chem. Soc. 111:3211; 1989.

Higgins, G.A. Biochemical model dosimetry system based on nuclear quadrupole resonance of crystallized hydrated urea. Gainesville: Univ. of Florida; 1990. Unpublished M.S. Project.

Hintenlang, D.E.; Higgins, G.A. Radiation response of hydrated urea evaluated using ^{14}N nuclear quadrupole resonance. Nuc. Sci. Eng. 112:181-184; 1992.

Hintenlang, D.E.; Iselin, L.H.; Jamil, K. Biologically-equivalent dosimetry from nitrogen-14 nuclear quadrupole resonance. *IRPA8* The 8th Meeting of the International Radiation Protection Association, Montréal, Canada, July, 1992.

Hintenlang, D.E.; Jamil, K. Neutron damage studies of organic materials with NQR spectroscopy. American Nuclear Society Annual Meeting Abstracts, Boston, MA:169; 1992.

Hill, R.O., Jr. Elementary linear algebra. Orlando, FL: Academic Press; 1986.

Hunt, M.J.; Mackay, A.L. Deuterium and nitrogen pure quadrupole resonance in deuterated amino acids. J. Magn. Reson. 15:401-414; 1974.

Iselin, L.H. An analytical method for estimating the ^{14}N nuclear quadrupole resonance parameters of organic compounds with complex free induction decays for radiation effects studies. Gainesville: Univ. of Florida; 1992. M.Eng. Thesis.

Iselin, L.H.; Hintenlang, D.E. Feasibility of nuclear quadrupole resonance as a novel dosimetry tool. Health Physics Society Annual Meeting abstracts, Anaheim, CA, Health Phys. 60 Supplement 2:S97; June, 1990

Iselin, L.H.; Hintenlang, D.E. Potential biological dosimetry from the effects of ^{60}Co γ-rays on the nuclear quadrupole resonance spectral parameters of guanidine sulfate," Health Physics Society Annual Meeting Abstracts, Washington, DC, Health Phys. 60 Supplement 2:S83; July, 1991.

Iselin, L.H.; Hintenlang, D.E. Energy dependence of gamma-ray effects on hydrated urea using pulsed ^{14}N nuclear quadrupole resonance techniques. Health Physics Society Annual Meeting Abstracts, Columbus, OH, Health Phys. 62(6) Supplement:S33; June, 1992.

Jackson, J.D. Classical electrodynamics. 2nd ed. New York: Wiley; 1975.

Jamil, K. Effects of ionizing radiation on the environment of nitrogen-14 in organic compounds by nuclear quadrupole resonance. Gainesville: Univ. of Florida; 1992. Ph.D. Thesis.

Koizumi, M.; Tachibana, A.; Yamabe, T. Reaction ergodography for the hydrolysis of urea. THEOCHEM. 164:37-47; 1988.

Kung, S.Y.; Arun, K.S.; Bhaskar Rao, D.V. State-space and singular-value decomposition-based approximation methods for the harmonic retrieval problem. J. Opt. Soc. Am. 73:1799-1811; 1983.

Lawson, C.L.; Hanson, R.J. Solving least squares problems. Prentice-Hall series in automatic computation. Englewood Cliffs, NJ: Prentice-Hall; 1974.

Leppelmeier, G.W.; Hahn, E.L. Nuclear dipole field quenching of integer spins. Phys. Rev. 141:724-731; 1966.

Levenberg, K. A method for the solution of certain non-linear problems in least squares. Q. Appl. Math. 2:164-168; 1944.

Lu, C-S; Hughes, E.W.; Giguère, P.A. The Crystal Structure of the Urea-Hydrogen Peroxide Addition Compound $CO(NH_2)_2 \bullet H_2O_2$. J. Am. Chem. Soc. 63:1507-1513; 1941.

Marino R.A. A study of the bonding of nitrogen by nuclear quadrupole resonance. Providence, RI: Brown Univ.; 1969. Ph.D. Thesis.

Marquart, D. An algorithm for least-square estimation of nonlinear parameters. J. Soc. Ind. Appl. Math. 11:431-441; 1963.

Maybeck, P.S. Stochastic models estimation and control. New York: Academic Press; 1979.

Milia, F.K., Hadjoudis, E.K. Crystal structure effect in the γ radiation of p-dichlorobenzene. J. Chem. Phys. 72:4707-4708; 1968.

Minematsu, M. Nuclear quadrupole resonances of nitrogen in amino and amido compounds. J. Phys. Soc. Jpn. 14:1030-1038; 1959.

Murgich, J.; Santana R., M. Effect of the oxygen protonation on the electronic structure of urea in the solid state: A ^{14}N NQR Study. J. Chem. Phys. 74(7):3788-3790; 1981.

Negita, H.; Kubo, T.; Maekawa, M. ^{14}N nuclear quadrupole resonances of the molecular complexes of urea. Bull. Chem. Soc. Jpn. 50:2215-2216; 1977.

Negita, H.; Kubo, T.; Kato, H. ^{14}N nuclear quadrupole resonances of the molecular complexes of urea. Bull. Chem. Soc. Jpn. 54:391-393; 1981.

Norton J.P. An Introduction to identification. New York: Academic Press; 1986.

Oja, T. N^{14} NQR in quanidines. Bull. Amer. Phys. Soc. 14:31; 1969a.

Oja, T. ^{14}N nuclear quadrupole resonance in ferroelectric guanidines. Phys. Letters 30A:343; 1969b.

Oja, T. Nitrogen-14 nuclear quadrupole resonance study of the guanidinium ion. J. Chem. Phys. 59:2668-2675; 1973.

Oja, T.; Petersen, G. Pulsed nuclear quadrupole resonance instrumentation. 1973; 17 p. An application note AN-115. Available from: Matec, Inc., Warwick, RI.

O'Konski C.T.; Torizuka, K. Relaxation times and saturation of nuclear quadrupole resonance of ^{14}N in asymmetric field gradients. J. Chem. Phys. 51:461-463; 1969.

Panin, V.I. Study of kinetics of accumulation of products of γ radiolysis of aliphatic peptides by H NMR method. Khim. Vys. Energ. 19:14-19; 1985.

Panin, V.I.; Sidorov, P.S.; Usatyi, A.F. Analysis of gamma radiolysis products of aqueous solutions of esters of aliphatic amino acids by PMR method. Khim. Vys. Energ. 21:127-133; 1987.

Petersen, G. Pulsed nuclear quadrupole resonance instrumentation and study of the nitrogen-14 spectrum and relaxation in sodium-nitrite. Providence: Brown Univ.; 1975. Ph.D. Thesis.

Petersen, G. Bray, P.J. ^{14}N nuclear quadrupole resonance and relaxation measurements of sodium nitrite. J. Chem. Phys. 64:522-530; 1976.

Petersen, G.; Oja, T. A pulsed nuclear quadrupole resonance spectrometer. Smith, J. A. S. Advances in nuclear quadrupole resonance. Vol. 1. New York: Heyden & Sons; 1974: 179-184.

Pijnappel, W.W.F.; van den Boogaart, A.; de Beer, R.; van Ormondt, D. SVD-based quantification of magnetic resonance signals. J. Magn. Reson. 97:122-134; 1992.

Poole, C.P., Jr.; Farach, H.A. Theory of magnetic resonance. 2nd ed. New York: Wiley; 1987.

Press, W.H.; Flannery, B.P.; Teukolsky, S.A.; Vetterling, W.T. Numerical recipes: the art of scientific computing (Fortran version). New York: Cambridge Unversity Press; 1989.

Randall, J.L. Effects of Crystalline Defects on Pure Quadrupole Resonances. Birmingham: Univ. of Alabama; 1959. Ph.D. Thesis.

Rao, C.R. Information and accuracy obtainable in one estimation of a statistical parameter. Bull. Calcutta Math. Soc. 37:81-91; 1945.

Rao, C.R. Linear statistical inference and its applications. 2nd. ed. New York: John Wiley & Sons; 1973.

Rogers, M.T.; Kispert, L.D. Some effects of crystal structure on production of radicals in irradiated organic crystals. Hart, Edwin J. Radiation chemistry. Vol. II. Gases, solids, organic liquids. Advances in chemistry series 82. Washington, DC: American Chemical Society; 1968.

Sanctuary, B.C.; Krishnan, M.S. Theory of NQR pulses. Z. Naturforsh. 49a:71-79; 1994.

Sauer, E.G.; Bray, P.J. N-14 nuclear quadrupole resonance in compounds containing N-O bonds. II. hydroxyurea. J. Chem. Phys. 58:2662-2663; 1973.

Shannon, T.G. An annealing study of gamma-irradiated sodium chlorate using nuclear quadrupole resonance spectroscopy. Troy, NY: Rensselaer Polytechnic Institute; 1971. Ph.D. thesis.

Slichter, C.P. Principles of magnetic resonance with examples from solid state physics. 2nd ed. Seitz, E. Harper's physics series. New York: Harper and Row; 1990.

Smith, F.L., editor. The radiotron designer's handbook. 3rd ed. Sydney, Australia: The Wireless Press; 1941.

Smith, D.H.; Cotts, R.M. Nuclear electric quadrupole and proton magnetic resonances in thiourea. J. Chem. Phys. 41:2403-2416; 1964.

Subbarao, S.N. Nitrogen-14 nuclear quadrupole resonance study of organic molecular crystals. Providence, RI: Brown Univ.; 1978. Ph.D. Thesis.

Swallow, A.J. Radiation chemistry of organic compounds. Charlesby, A. International series of monographs on radiation effects in materials. Vol. 2. New York: Pergamon Press; 1960.

Swaminathan, S.; Craven, B.M. The crystal structure and molecular thermal motion of urea at 12, 60 and 123 K from neutron diffraction. Acta Cryst. B40:300-306; 1984.

Taylor, J.R. An introduction to error analysis. Mill Valley, CA: University Science Books; 1982.

Thomasson, D.M. Development and initial characterization of a nuclear magnetic resonance dosimetry system. Madison: Univ. of Wisconsin; 1990. Ph.D. Thesis.

Tolkachev, V.A. On free radical decay in γ-irradiated organic crystals. Dobó, J.; Hedvig, P. Proceedings of the Third Tihany Symposium on Radiation Chemistry. Budapest: Akadémiai Kiadó; 1972.

Townes, C.H. Electrostatic field strengths in molecules and nuclear quadrupole moments. Phys. Rev. 2nd Ser. 71:909-910; 1948.

Townes, C.H.; Daily, B.P. Determination of electronic structure of molecules from nuclear quadrupole effects. J. Chem. Phys. 17:782-796; 1949.

Vargas, H.; Pelzl, J.; Dimitropoulos, C. ^{35}Cl NQR studies of irradiation defects in chlorates. J. Magn. Reson. 30:423-429; 1978.

Watkins, G.D.; Pound, P.V. Phys. Rev. 85:1062; 1952.

Wheeler, H.A. Simple inductance formulas for radio coils. Proc. IRE 16:1398-1400; 1928.

Widman, R.H. Shifts of the nuclear quadrupole resonance spectra of ^{14}N in urea, cyanuric acid, and melamine. J. Chem. Phys. 40:2922-2923; 1963.

Wong, S. Introductory nuclear physics. Englewood Cliffs, NJ: Prentice-Hall; 1990.

Willard, J.E. The radiation chemistry of organic solids. Farhataziz; Rodgers, M.A.J. Radiation chemistry: principles and applications. New York: VCH Publishers; 1987.

Zussman, A. Effect of molecular reorientation in urea on the ^{14}N PNQR linewidth and relaxation time. J. Chem. Phys. 58:1514-1519; 1973.

BIOGRAPHICAL SKETCH

Louis Henry Iselin was born 8 February 1966, in Casa Grande, Arizona, the son of William Albin Iselin and Mary Corine (Trinkaus) Iselin. In May, 1984, he was an *honor graduate of distinction* from Jonesboro Senior High School in Jonesboro, Arkansas. Louis attended The University of Tulsa in Tulsa, Oklahoma, starting August 1984, as a National Merit Scholar and University Honors Scholar. After his freshman year, Louis was awarded the LaFortune Engineering Scholarship, as well. He graduated from The University of Tulsa on 7 May 1988, with a Bachelor of Science in Engineering Physics (*cum laude*). He was awarded membership in Sigma Pi Sigma National Physics Honorary Society and Tau Beta Pi National Engineering Honor Society (OK B) while at Tulsa. He is a registered Engineer Intern in the State of Oklahoma.

Louis Iselin was offered both of the Department of Energy Nuclear Science and Engineering Fellowships: Nuclear Engineering and Health Physics. He accepted the DOE Health Physics Fellowship and attended graduate school at the University of Florida starting in August 1988. He was elected to membership in the Alpha Nu Sigma National Nuclear Science and Engineering Honor Society in 1989 and served as the President of the Florida Alpha chapter in the 1993-1994 school year.

In May, 1989, Louis married the former Huong Vuong of Tulsa, Oklahoma. On their honeymoon, the newlyweds spent the summer in New Mexico at Los Alamos National Laboratory's Clinton P. Anderson Meson Physics Facility (LAMPF) where Louis spent his fellowship practicum working with the Accelerator Health Protection Group (then HSE-11).

Louis H. Iselin was awarded the degree of Master of Engineering from the Nuclear Engineering Sciences Department at the University of Florida on 11 May 1992 with a concentration in health physics and engineering physics and a minor in engineering science (applied mathematics). He continued his graduate work at the University of Florida for the Ph.D. On 2 December 1993, Huong gave birth to their first child, Megan Rochelle, at Shands Hospital at the University of Florida. On 27 January 1995, the faculty of the Department of Nuclear Engineering Sciences recognized Louis by naming him as the department's outstanding graduate student for 1995 and bestowing the James E. Swander Memorial Scholarship. Both Huong and Megan are relieved that Louis will be awarded the degree of Doctor of Philosophy on 16 December 1995. After graduation, Dr. Louis H. Iselin will join the physics faculty at Bloomsburg University of Pennsylvania as Assistant Professor.

I certify that I have read this study and that in my opinion it conforms to acceptable standards of scholarly presentation and is fully adequate, in scope and quality, as a dissertation for the degree of Doctor of Philosophy.

David E. Hintenlang, Chairman
Associate Professor of Nuclear Engineering Sciences

I certify that I have read this study and that in my opinion it conforms to acceptable standards of scholarly presentation and is fully adequate, in scope and quality, as a dissertation for the degree of Doctor of Philosophy.

Samim Anghaie
Professor of Nuclear Engineering Sciences

I certify that I have read this study and that in my opinion it conforms to acceptable standards of scholarly presentation and is fully adequate, in scope and quality, as a dissertation for the degree of Doctor of Philosophy.

E. Raymond Andrew
Graduate Research Professor of Physics and Nuclear Engineering Sciences

I certify that I have read this study and that in my opinion it conforms to acceptable standards of scholarly presentation and is fully adequate, in scope and quality, as a dissertation for the degree of Doctor of Philosophy.

Ulrich Kurzweg

Ulrich H. Kurzweg
Professor of Aerospace Engineering, Mechanics, and Engineering Science

I certify that I have read this study and that in my opinion it conforms to acceptable standards of scholarly presentation and is fully adequate, in scope and quality, as a dissertation for the degree of Doctor of Philosophy.

Michael T. Olexa
Professor of Food and Resource Economics

I certify that I have read this study and that in my opinion it conforms to acceptable standards of scholarly presentation and is fully adequate, in scope and quality, as a dissertation for the degree of Doctor of Philosophy.

Robert A. Marino
Professor and Chairman of Physics and Astronomy
Hunter College
City University of New York

This dissertation was submitted to the Graduate Faculty of the College of Engineering and to the Graduate School and was accepted as partial fulfillment of the requirements for the degree of Doctor of Philosophy.

December, 1995

Winfred M. Phillips
Dean, College of Engineering

Karen A. Holbrook
Dean, Graduate School